



THE HONG KONG  
POLYTECHNIC UNIVERSITY

香港理工大學

Pao Yue-kong Library

包玉剛圖書館

---

## Copyright Undertaking

This thesis is protected by copyright, with all rights reserved.

**By reading and using the thesis, the reader understands and agrees to the following terms:**

1. The reader will abide by the rules and legal ordinances governing copyright regarding the use of the thesis.
2. The reader will use the thesis for the purpose of research or private study only and not for distribution or further reproduction or any other purpose.
3. The reader agrees to indemnify and hold the University harmless from and against any loss, damage, cost, liability or expenses arising from copyright infringement or unauthorized usage.

### IMPORTANT

If you have reasons to believe that any materials in this thesis are deemed not suitable to be distributed in this form, or a copyright owner having difficulty with the material being included in our database, please contact [lbsys@polyu.edu.hk](mailto:lbsys@polyu.edu.hk) providing details. The Library will look into your claim and consider taking remedial action upon receipt of the written requests.

**FUNCTIONAL MATERIALS FOR THERMO-  
REGULATING TEXTILES**

**JAHID MD ANWAR**

**PhD**

**The Hong Kong Polytechnic University**

**2020**

**The Hong Kong Polytechnic University**

**Institute of Textiles and Clothing**

**FUNCTIONAL MATERIALS FOR THERMO-  
REGULATING TEXTILES**

**JAHID MD ANWAR**

**A thesis submitted in partial fulfillment of the  
requirements for the degree of Doctor of Philosophy**

**January 2020**

# CERTIFICATE OF ORIGINALITY

I hereby declare that this thesis is my own work and that, to the best of my knowledge and belief, it reproduces no material previously published or written, nor material that has been accepted for the award of any other degree or diploma, except where due acknowledgement has been made in the text.

---

(Signed)

JAHID MD ANWAR

---

(Name of student)

# Abstract

To provide thermo-physiological comfort to the wearer textile materials should have some functional properties such as highly water vapor transmittable, water resistant, air permeable, IR transmittable and temperature sensitive gating textile to allow body heat to escape. Recently, the high consumption of energy directly leading to excessive emissions of greenhouse gas becomes an extremely wide attention due to extreme weather and global warming. To reduce the energy consumptions in space cooling and heating, thermo-regulating textiles would play a vital role by reducing air conditioning. In this study, functional materials have been developed to make thermo-regulating textiles to fulfill such requirements. This PhD project is mainly focused on four main parts.

Firstly, a series of shape memory polyurethanes (SMPUs) was synthesized to coat on to the textile surface to make highly water vapor transmittable and water droplet resistant textile. The synthesized polymeric material can evaporate sweat (water vapor transmission approximate-  $6500 \text{ g m}^{-2} \text{ d}^{-1}$  at  $40^\circ\text{C}$ ) and transmit it from the body surface to the environment even in extreme weather conditions that require wind and rain proof (contact angle approximate-  $115^\circ$ ). The coated fabrics could provide thermal insulation with lower permeability at low temperature or low relative humidity (RH), and high permeability at room temperature or above, or high relative humidity with its water-resistance property.

Furthermore, polyurethane/silica aerogel composite membrane was prepared, which showed super evaporative and Radiative effects (can transmit approximate 98% of human body radiation) and which can facilitate the convection process of the human body. I also fabricated the sensitive membrane-based textile which can cool down the human body by releasing body heat. The developed material possessed robust mechanical properties (breaking strength approximate 26MPa) for the longevity of the material, high water evaporative (water vapor transmission approximate  $1800 \text{ g m}^{-2} \text{ d}^{-1}$  at  $40^\circ\text{C}$ ) ability and air permeability to provide comfort to the wearer. The developed textile can release most of our body heat.

In addition, segmented polyurethanes (PUs) were synthesized using a two-step polymerization method and additional highly porous PU membranes were produced by the leaching technique, using highly water-soluble silica particles. A crucial discovery during this work was reducing the particle leaching time. To make a porous structure the particles were leached out from the PU matrix over five minutes through sonication. An investigation was conducted into the surface morphology of the porous PU (PPU) membrane using a scanning electron microscopy (SEM). The effects of different silica particle percentage ratios were

investigated. Porous polyurethanes membranes have particular significance for various uses, e.g. laminated textiles, cell seeding, bio-materials, tissue engineering, etc.

The fourth study was to synthesize liquid crystal elastomers (LCEs) and fabricated a plain weave structure by using a different composition of low-temperature LCEs filaments and radial shaped three dimensional printed films (diameter 2cm). The plain weave structure showed very interesting results like closing its pores at 32°C (RM82/RM257 (80:20)) and 39°C (RM82/RM257 (80:20)) and returning back to its original position at room temperature (23°C). The radial shaped films were incorporated into textile to see the flip open/close mechanism when temperature applied. This pore closing fabric and flip opening/closing textile would be used to thermal comfort to the wearer when surrounding temperature increased.

Finally, the synthesized polyurethanes/polyurethane composite was unique to be applied for thermo-regulating textile applications due to its high water vapor transmitting ability including others body heat escaping ability. The time saving way of making porous polymer membrane by particulate leaching technique also very crucial, which is high water vapor transmittable and rain drop resistant membrane. Furthermore, LCEs filaments and film was prepared to make temperature responsive gating textile.

# Publications Arising from the Thesis

## Journal Publications:

1. **Jahid MA**, Hu JL, Wong KH, Wu Y, Zhu Y, Luo HHS and Zhongmin D, Fabric coated with shape memory polyurethane and its properties, *Polymers*, 2018, 10, 681.
2. Thakur S, **Jahid MA** and Hu JL, Mechanically strong shape memory polyurethane for water vapour permeable membranes, *Polymer International*, 2018, 67, 1386-1392. (equal contribution).
3. **Jahid MA** and Hu JL, Water vapor transmission and water resistant: opposite but may coexist, *Materials Today: Proceedings*, 2019, 16, 1485–1490.
4. **Jahid MA**, Hu JL and Thakur S, Novel approach of making porous polyurethane membrane and its properties for apparel application, *Journal of Applied Polymer Science*, 2020, 137, 48566.
5. **Jahid MA**, Hu JL and Thakur S, Mechanically robust, responsive composite membrane for thermo-regulating textile, *ACS Omega*, 2020, 5, 8, 3899-3907.
6. **Jahid MA**, Taylor HW and Hu JL, Open/close mechanism in a textile as a function of temperature. Ready to submit.

## **Conference Proceedings:**

1. **Jahid MA** and Hu JL, Water Vapor Permeability and Mechanical Properties of Fabric Coated with Stimuli-responsive Shape Memory Polyurethane. Fiber Society, UGA, USA, 2017.
2. **Jahid MA** and Hu JL, Water vapor transmission and water resistant: opposite but may coexist. Smart, The HK PolyU, HK, 2018.
3. **Jahid MA** and Hu JL, Nanocomposite membrane for human thermoregulation. AAAFM, UCLA, USA, 2019.
4. **Jahid MA** and Hu JL, Mechanically Strong, Shape Memory Polyurethane Membrane for Thermo-regulating Textile. Fiber Society's Fall 2019 Technical Meeting and Conference, UT Austin, USA, 2019.

## **Book Chapters:**

1. **Jahid MA**, Hu JL and Zhou H, Smart Textile Coatings and Laminates Chap6:155-173(2018)
2. Jinlian Hu, **Jahid MA**, HarishKumar N and Harun V, Fundamentals of the Fibrous Materials, Chap1 (Accepted for publication from Woodhead publisher).



# Acknowledgements

First of all, I would like to express my sincere gratitude to my chief supervisor, Prof. Hu Jinlian for her supervision, inspiration and encourage throughout the past three years' study. Without her patients and substantial help it would have been impossible for me to accomplish my study. Professional integrity of Prof. Hu always inspiring and encourages me during my PhD study. She sets an ideal example of persistence and attitude toward work, which helps me a lot during my PhD study.

I would like to acknowledge the support from group mates (Prof. Hu's group) during last three years. Special thanks to Dr Zhu Yong, Mr Han Jianping, Dr Suman, Ms Susanna Li, Dr Pathrick, Ms Sun. I would like to thank Zhongshan Breathtex Speciality Material Co., Ltd, China for their support to use their facility to make samples. I also would like to acknowledge the support from Dr Ware and his group (Assistant professor, University of Texas at Dallas) during my exchange programs at the University of Texas at Dallas.

Special thanks to colleagues, technician and other of members from the Institute of Textiles of Clothing, The Hong Kong Polytechnic University for their support during my time here.

Last but not least, I would like to deliver my deepest gratitude to my parents and beloved family for their encouragements, supports and understandings throughout all the time of my study. I am proud of having my beloved family.

# List of Symbols

Symbol	Definition	Unit
$T_g$	Glass transition temperature	°C
$T_m$	Melting transition temperature	°C
WVT	Water vapor Transmission	gm-2d-1
RH	Relative Humidity	%
LCE	Liquid Crystal Elastomer	
CA	Contact Angle	°
	Percentage	%
$\varepsilon_p$	Residual Strain	%
$\varepsilon_m$	maximum strain	%
$\varepsilon_u$	fixed strain	%
P	Porosity	%
D	Density	

# Table of Contents

CERTIFICATE OF ORIGINALITY.....	I
Abstract .....	II
Publications Arising from the Thesis .....	IV
Acknowledgements .....	VI
List of Symbols .....	VII
List of Abbreviations .....	XI
List of Figures .....	XII
List of Tables .....	XV
Chapter1. Introduction .....	1
1.1. Background.....	1
1.1.1. Thermo-regulating textiles.....	1
1.2. Limitations of the current research .....	9
1.3. Objectives and significance of the research .....	11
1.4. Thesis outline .....	13
Reference.....	16
Chapter2. Literature review .....	18
2.1. Thermo-regulating polymeric materials .....	18
2.2. Shape memory polyurethanes .....	22
2.3. Polymeric composite materials .....	28
2.3.1. Silica Aerogel .....	34
2.3.2. Limitations of existing composite for permeable membrane .....	40
2.4. Porous polymeric materials .....	40
2.4.1. Particulate leaching .....	42
2.4.2. Thermally-induced phase separation (TIPS).....	43
2.4.3. Gas foaming.....	45
2.4.4. Emulsion freeze-drying .....	47
2.4.5. Limitations of current porous membrane fabrication method .....	48
2.5. Liquid crystal elastomers. ....	49
2.6. Laminated/coated and responsive textiles.....	51
2.7. Summery.....	56
Reference.....	58
Chapter3. Experimental .....	67
3.1. Materials and equipment.....	67
3.2. Preparation of functional polymers .....	69
3.2.1. Synthesis of polyurethane .....	69

3.2.2. Preparation of composite materials and membrane .....	70
3.2.3. Preparation of porous polyurethane membrane.....	72
3.2.4. Synthesis and coating details.....	73
3.2.6. Fiber preparation.....	78
3.3. Characterization .....	79
3.3.1. Water vapor transmission.....	79
3.3.2. Water resistant/Contact angle.....	80
3.3.3. Mechanical property .....	80
3.3.4. SEM.....	80
3.3.5. FTIR.....	81
3.3.6. XRD.....	81
3.3.7. TGA.....	81
3.3.8. DSC .....	81
3.3.9. Absorbency.....	82
3.3.10. Wicking distance .....	82
3.3.11. Abrasion resistance .....	82
3.3.12. Porosity.....	82
3.3.13. Hydrostatic pressure .....	83
3.3.14. Air permeability.....	83
3.3.15. Shape memory property.....	83
3.3.16. IR transmittance .....	84
Chapter4. Water vapor transmittable and resistant textile .....	85
4.1. Introduction .....	85
4.2. Results and discussion .....	88
4.2.1. Water Resistance/Contact Angle.....	88
4.2.2. Water Vapor Transmission of Coated Fabric.....	90
4.2.3. Mechanism of Water Transmittance and Resistance Property of the Coated Fabric..	94
4.2.4. Thermo-Mechanical Properties.....	96
4.2.5. Mechanical Properties .....	100
4.2.6. Scanning Electron Microscopy (SEM) .....	102
4.3. Summery.....	103
Reference.....	105
Chapter5. Composite membrane for thermo-regulative textile. ....	107
5.1. Introduction .....	107
5.2. Results and discussion .....	112
5.2.1. Water vapor transmission mechanism of composite membranes .....	112

5.2.2. Water vapor transmission.....	115
5.2.3. Air permeability, mechanical property, absorbency of membranes. ....	120
5.2.4. Wicking height and mechanical property of membranes. ....	124
5.2.5. Radiative property of membranes.....	126
5.2.6. SEM and DSC of samples .....	128
5.3. Summery.....	129
Reference.....	130
Chapter6. Porous membrane for smart textile application.....	133
6.1. Introduction .....	133
6.2. Results and discussion .....	137
6.2.1. Water vapour transmission property of porous membranes .....	137
6.2.2. Water droplet resistant property of membranes .....	141
6.2.3. Water vapor transmission and resistant mechanism, SEM and porosity of membranes .....	143
6.2.4. Mechanical property, TGA, DSC and XRD of membranes .....	147
6.2.5. Abrasion resistant property of laminated fabric .....	151
6.7. Summery.....	152
Reference.....	154
Chapter7. Temperature sensitive gating textile .....	156
7.1. Introduction .....	156
7.2. Results and discussion .....	161
7.2.1. Molecular mechanism of LCEs .....	161
7.2.2. Pores are closing as a function of temperature.....	162
7.2.3. Contraction of single filament .....	164
7.2.4. DSC of Liquid crystal elastomers.....	165
7.2.5. Mechanical property of filaments .....	167
7.2.6. Flip opening/closing in a textile as a function of temperature.....	168
7.3. Summery.....	171
Reference.....	172
Chapter8. Conclusion & suggestions for future work.....	174
8.1. Conclusion.....	174
8.2. Suggestions for future work .....	177

# List of Abbreviations

3D	Three-dimensional
WVT	Water vapor Transmission
SMPU	Shape memory polyurethane
PU	Polyurethane
PEG	Polyethylene Glycol
PCL	Poly-caprolactone
PTMG	Polytetramethylene Glycol
MDI	Methylene Diphenyl Isocyanate
BDO	1,4-Butanediol
DMAC	N, N-dimethylacetamide
LCE	Liquid Crystal Elastomer
LC	Liquid Crystal
XRD	Wide angle X-ray diffraction
SEM	Scanning Electron Microscopy
DSC	Differential scanning Calorimetry
RM82	1, 4-Bis-[4-(6-acryloyloxyhexyloxy)-benzoyloxy]-2-methylbenzene
RM257	1,4-bis-[4-(3-acryloyloxypropypropyloxy) benzoyloxy]-2-methylbenzene
TATATO	1, 3, 5-triallyl-1, 3, 5-triazine-2, 4, 6(1H, 3H,5H)trione
TEA	Triethylamine
BHT	2,6-Di- <i>tert</i> -butyl-4-methylphenol
I-369	2-Benzyl-2-dimethylamino-1-(4-morpholinophenyl)-butanone-1
GDMP	Ethylene glycol bis-mercaptoacetate
TEM	Transmission Electron Microscopy
FTIR	Fourier Transform Infrared Spectroscopy
UF	Uncoated fabric
CFPEG	Fabric coated with PEG
CFPTMG	Fabric coated with PTMG
CFPCL	Fabric coated with PCL
DIW	Direct Ink Writing
IR	Infrared radiation

# List of Figures

**Figure 1.1.** The functional polyurethane membranes for thermo-regulating textiles.

**Figure 1.2.** General molecular mechanism of shape memory effect.

**Figure 1.3.** Water proof and permeable laminated textile of GORE-TEX

**Figure 1.4.** (a) woven textile using LCE fibers to develop pores upon heating. (b) LCE fibers sewn into a cotton shirt creating pores upon heating. (c) Demonstration of the LCE smart shirt demonstrating pores for improved heat transfers and sweats evaporation during exercise.

**Figure 2.1.** ‘Galaxy’ of nanostructured stimuli-responsive polymer materials.

**Figure 2.2.** Molecular structures of SMPs. A stable network and a reversible switching transition are the prerequisites for the SMPs to show SME.

**Figure 2.3.** Classification of polymeric shape memory effect.

**Figure 2.4.** General structure of segmented polyurethane.

**Figure 2.5.** Classification of composites.

**Figure 2.6.** Schematic diagram of the formation of the polyurethane– Al<sub>2</sub>O<sub>3</sub> anion-exchange fibrous composite.

**Figure 2.7.** Fabrication diagram of the polyacrylate/hollow silica composite film.

**Figure 2.8.** Effect of shell thickness of hollow silica spheres on water vapor permeability of composite film.

**Figure 2.9.** Effect of the content of hollow silica spheres on water vapor permeability of composite film.

**Figure 2.10.** The schematic illustration of water vapor molecules transporting through hollow silica spheres.

**Figure 2.11.** Pliable scaffolds with structural hierarchy can be synthesized using long-chain block copolymers.

**Figure 2.12.** Scaffold preparation using solvent casting combined with the salt leaching technique.

**Figure 2.13.** Phase diagram of a ternary system polymer-solvent- non/solvent.

**Figure 2.14.** Scaffold preparation using thermally induced phase separation technique.

**Figure 2.15.** Schematic representation of polymeric scaffolds prepared by gas foaming/salt leaching method.

**Figure 2.16.** Schematic representation of the emulsion freeze drying process.

**Figure 2.17.** Global polymer chain conformations for main-chain LCEs.

**Figure 2.18.** Knit textile achieving effective diameter shrinkage upon heating.

**Figure 2.19.** Personnel thermal management strategy by utilizing self- adaptive, temperature or humidity-responsive shape-memory material.

**Figure 2.20.** Schematic of dual-mode textile.

**Figure 2.21.** Back of a Nike ‘Sphere React Shirt’ with a smart vent structure

**Figure 3.1.** The fabrication process of PU and composite membranes.

**Figure 3.2.** Silica aerogel particle, composite membrane, laminated fabric.

**Figure 3.3.** (a) synthesis of segmented PU, (b) fabrication of PPU membrane, and (c) schematic of water vapor transmission and water droplet resistance property of the porous membrane.

**Figure 3.4.** Synthesis procedure of polyurethane

**Figure 3.5.** Theoretical approach of fabric coating and water vapor transmission.

**Figure 3.6.** Chemical structures of different components of liquid crystal elastomer.

**Figure 3.7.** Preparation of fiber and radial shaped flip by 3D printing.

**Figure 3.8.** The apparatus for measuring WVT.

**Figure 4.1.** Contact Angle of coated and uncoated fabric.

**Figure 4.2.** The contact angle of CFPTMG, CFPCL, CFPEG and uncoated with time variation.

**Figure 4.3.** WVT of UF (control), CFPEG, CFPTMG, and CFPCL

**Figure 4.4.** WVT of UF (control), CFPEG, CFPTMG, and CFPCL

**Figure 4.5.** Molecular structure design of responsive polyurethane.

**Figure 4.6.** Water resistance of coated fabric

**Figure 4.7.** DSC of different polyurethane

**Figure 4.8.** Thermogravimetric curves of three different polyurethane

**Figure 4.9.** Surface morphology and cross section.

**Figure 5.1.** Thermal management of human body.

**Figure 5.2.** **A)** TEM image of silica aerogel particle (scale 2 $\mu$ m, 50nm), **B)** Structure of silica aerogel, **C)** Schematic of hollow silica aerogel and water vapor passing channel, **D)** The fabrication process laminated fabric.

**Figure 5.3.** Mechanism of evaporation of perspiration.



**Figure 5.4.** A) Testing mechanism of water vapor transmission, and B) Temperature and relative humidity controlled climate chamber where water vapor transmission testing took place.

**Figure 5.5.** The relationship between water vapor transmission, temperature, and relative humidity.

**Figure 5.6.** A) Air convection of laminated fabric, B) Air permeability result of laminated fabric (PU, Composite 0.5% and 1%) and control (fabric), C) Mechanical properties of laminated fabric D) Water absorbency of laminated fabric.

**Figure 5.7.** A) Wicking properties of laminated fabric (warp direction), B) Wicking properties of laminated fabric (weft direction), C) Abrasion resistance property of laminated fabric.

**Figure 5.8.** A) Stress strain profile, B) Tensile modulus and C) Toughness of PU, composite 0.5% and composite 1% membranes.

**Figure 5.9.** A) The behavior of ERCF with solar radiation and IR radiation, B) IR transmittance percentage of Cotton fabric, PU, Composite 1% and Composite 0.5% (range 3-18 $\mu$ m), C) IR transmittance percentage of Cotton fabric, PU, Composite 1% and Composite 0.5% (range 7-14 $\mu$ m).

**Figure 5.10.** Scanning Electron Microscopy (SEM) images.

**Figure 5.11.** DSC of PU, composite 0.5% and composite 1% membranes.

**Figure 6.1.** Water vapor transmission of different membranes.

**Figure 6.2.** (a) Cup for water vapor transmission test, and (b) Temperature and relative humidity controlled climate chamber where water vapor transmission testing took place.

**Figure 6.3** The relationship between the water vapor transmission, temperature and relative humidity of PU membrane.

**Figure 6.4.** The relationship between the water vapor transmission, temperature and relative humidity of PPU1 membrane.

**Figure 6.5.** The relationship between the water vapor transmission, temperature and relative humidity of PPU2 membrane.

**Figure 6.6.** (a) water contact angle of membranes and (b) hydrostatic pressure of membranes.

**Figure 6.7.** Schematic of the mechanism of (a) water vapor transmission, (b) water resistant.

**Figure 6.8.** Surface roughness of (a) PU, (b) PPU1 and (c) PPU2 which were obtained by processing SEM image through ImageJ software.

**Figure 6.9.** (a) Mechanical property, (b) TGA curve, (c) DSC curve, (d) XRD patterns of PU, PPU1 and PPU2.

**Figure 6.10.** Lamination technique of fabric.

**Figure 6.11.** Abrasion resistant property of laminated fabric.

**Figure 6.12.** Fabricated membrane, fabric and prepared laminated fabric.

**Figure 7.1.** Mechanism of body heating and open/close in a textile as function of temperature.

**Figure 7.2.** Molecular mechanism of liquid crystal elastomers.

**Figure 7.3.** A) Open/close mechanism in weaved fabric, B) Pore actuation as a function of temperature and C) Contraction of filaments along with thickness changes.

**Figure 7.3.** Contraction of filaments as a function of temperature.

**Figure 7.4.** DSC of LCEs.

**Figure 7.5.** Transition temperature of LCEs.

**Figure 7.6.** Mechanical properties of LCEs.

**Figure 7.7.** A) Flip open/close mechanism in weaved fabric, B) Bending angle of flip as a function of temperature and C) bending height of flip as a function of temperature.

**Figure 7.8.** Flip open/close in woven fabric as a function of temperature.

## List of Tables

**Table 2.1.** Techniques and systems used to fabricate porosity.

**Table 3.1.** Raw materials used in this study.

**Table 3.2.** The main equipment used in this study.

**Table 3.3.** Synthesis details of samples.

**Table 3.4.** Concentration details of polyurethane synthesis.

**Table 3.5.** Coding and thickness of uncoated and different coated fabric

**Table 4.1.** The shape memory properties of different polyurethanes

**Table 4.2.** Tensile strength and elongation of uncoated and coated fabric.

# **Chapter1. Introduction**

This chapter will introduce the background of the study, shape memory polymers for thermo-regulating textiles, composite membranes for apparel applications, preparation of porous membrane, fabric coated with shape memory polyurethane and liquid crystal elastomers for apparel applications. This chapter will also introduce the limitations of the current research, Significance and objectives of the research, Findings and outcome and thesis outline.

## **1.1. Background**

### **1.1.1. Thermo-regulating textiles**

There are several definitions of thermo-regulating textiles; according to Xing-xiang et al., Thermo-regulating textile is a textile which helps to regulate the inner temperature of apparel by releasing or absorbing heat energy as the ambient temperature changes [1]. Babu et al., stated that the thermo-regulating is combination of cooling and heating [2]. The definition given by Fabien is the textile maintaining the thermal balance between the heat produced by the human body and that transfer to the outside environment [3]. Grazyna et al., stated that the feature of textiles which support the thermo-regulation process of their wearers to heat exchange with the surrounding environment, leading to a quick rise in the relative humidity and temperature in the microclimate of underclothing [4].

In fact, thermal-regulating textile a material that optimizes the heat exchanges process of a human body with its environment to achieve comfort/satisfaction.

When situation lead to a significant rise/drop in temperature and wetting of underclothing microclimate to cause dissatisfaction of a human body, thermal-regulating textiles are normally demanded. These situations include human activities such as sports and ambient conditions such as temperature, relative humidity, sunshine and raindrops in their environment. Our focus in this study is to develop thermo-regulating textiles intended to improve the thermal comfort of its user by releasing the excess heat of the human body to the environment. The features of fabrics that support the thermo-regulation techniques of their users allow them to be used during extreme working conditions, including water vapor transmittable, rain resistant, convective and human body IR transmittable textile. Such kind of thermo-regulating textile would help the human body to keep the core temperature constant by releasing body heat. **Figure 1.1** is showing the functional membrane is able to transmit water vapor molecule while it's resisting water droplet. There are various materials are being used to make thermo-regulating textile such as shape memory polyurethanes, polymer composite, porous polymeric membranes, liquid crystal elastomers and phase change materials.

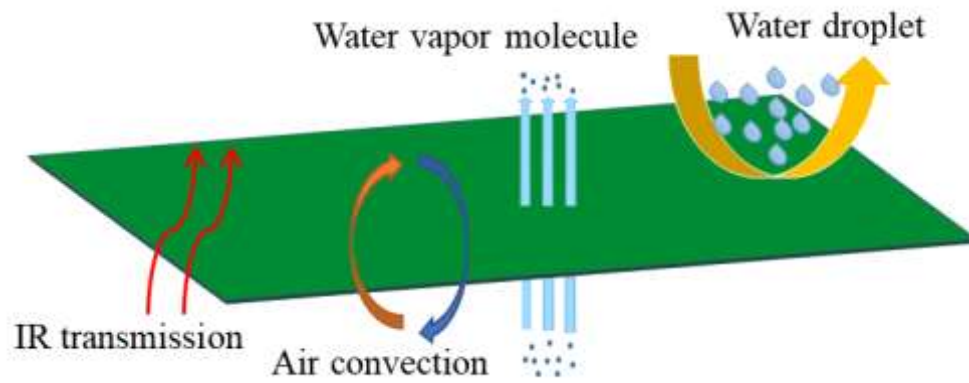


**Figure 1.1.** The functional polyurethane membranes for thermo-regulating textiles.

#### **1.1.1.1. Shape memory polyurethanes**

Shape memory polymeric material was initially produced by the Japanese Nippon Zeon Company in 1984, this is polynorbornene-based and has process ability limitations, with a  $T_g$  value ranging from 35 to 40°C [5]. Recently, many different shape memory polymers have been developed which have numerous applications depending on the stimulus, e.g. temperature, relative humidity, light, UV, etc. Thermo-moisture responsive materials are a class of polymeric material which can respond/react to specific changes in their surroundings (relative humidity (RH) and temperature) by altering their shape according to their shape memory behaviour [6].

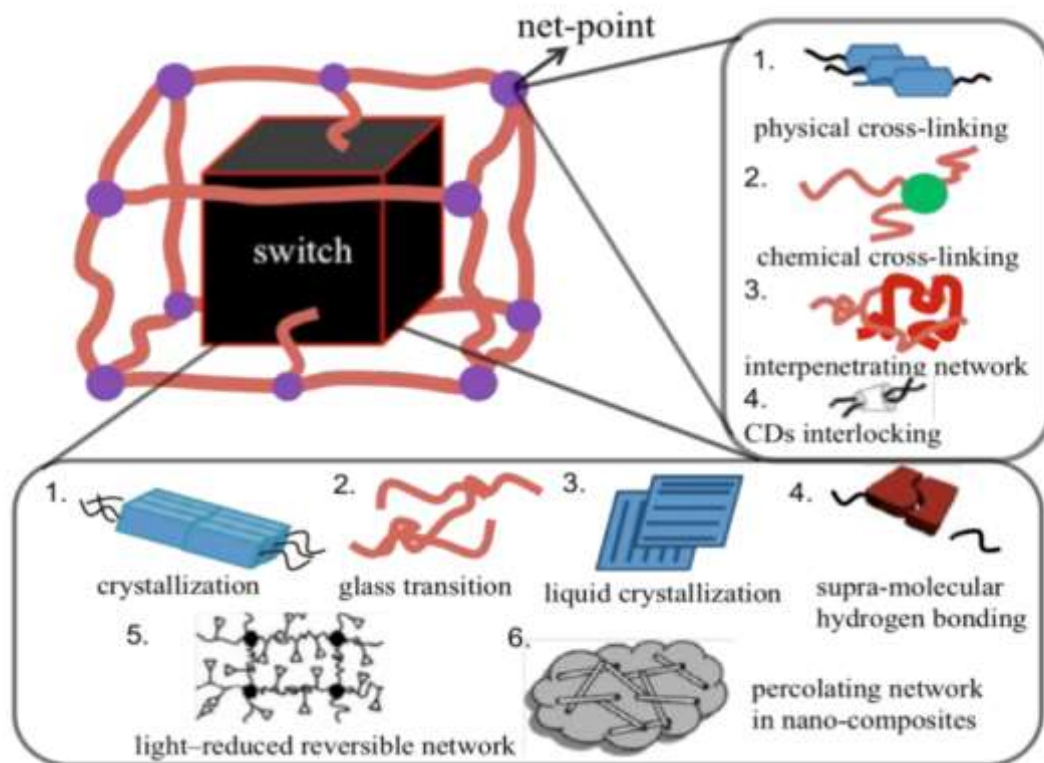


**Figure 1.2.** General molecular mechanism of shape memory effect [7, 8]

**Figure 1.2** shows the molecular structure of responsive polymers, indicating that the shape memory polymer is composed of net points and switches, net points can be physically cross-linking, chemically cross-linking, CDs interlocking or interpenetrated networks. The responsiveness includes a crystallization soft phase, light reduced reversible network, amorphous soft phase, liquid crystalline phase, percolating network in nano-composite and supramolecular switches [8,9]. Additional SMP functions have drawn the interest of the researcher, the functions include - thermal induced, light induced, RH induced, pH sensitive, luminescent, electronic sensitive, water sensitive, solvent sensitive, etc. Thermo-moisture responsive materials have many uses, the membranes are used for separation, coating and laminating, packaging, etc. They need to high permeability to certain classes of molecule [6].

### **1.1.1.2. Polyurethane composite**

A composite material is comprised of a minimum of two materials with completely different chemical or physical properties that, in combination, produce materials with characteristics which vary from the individual component [10]. The individual component stays distinct and separate in the final structures. A composite can be classified according to the fabrication manufacturing process; they are produced through the combination of different materials to form completely different structures with properties differing from the individual components. Thermo-regulating polymer composites can be defined as thermo-regulating polymers which are combined with completely different materials and which differ both physically and chemically [11]. Thermo-regulating polymers can react with temperature and moisture, whereby the responsive polymer surface makes contact with temperature or moisture, and then the soft part of the polymer begins to switch its state. The polymeric membranes are water vapour permeable materials, to make them more permeable, we studied different materials which make thermo-regulating polymers more water vapour permeable and found that silica aerogel is a kind of material which contains plenty of the –OH group, as we know the –OH group can attract and diffuse water molecules. Silica aerogel is a particle which is internally 95-96 % void, has a high specific surface area, is lightweight, and more importantly has better water vapour permeability compared with thermo-regulating polymers. Regardless of the composite material, reinforcement usually adds rigidity to the material [12]. Silica aerogel has been considered for different applications because of its unique chemical, thermal stability, and strong mechanical properties.

### **1.1.1.3. Porous polymeric materials**

The production of low-density polymeric and porous materials which possess mechanical properties have attracted increased attention in recent years because of the potentially important real-life applications of the porous material [13]. Porous polymeric materials have garnered increased interest as they are lightweight and have a high specific surface area, which makes them ideal for many applications. Porous polymeric materials have a broad variety of uses, including as tissue scaffolds, catalyst support, coating and laminating and membrane filters [14]. Preparing porous polymers includes methods such as phase separation [15], gas foaming [16], high internal phase emulsion [17], particle leaching, etc. These materials provide cooperation between transport properties, mechanical properties, and surface area. Particulate leaching is a widely used process to manufacture porous polymeric membranes, since this salt is one of the more widely used particles. However, the salt particle leaching out process is too long as it takes approximately 4-5 days [18,19]. Various processes have been used to prepare porous polymeric membranes for different applications, for example breathable and highly permeable membranes, tissue engineering [18], etc. Highly water soluble silica particles can be used to make porous polyurethane membranes through a particulate leaching technique.

### **1.1.1.4. Polymeric membranes for laminated textile.**

Textiles with good permeability (water vapour and air) have become indispensable as they are droplet resistant and have IR transmission properties. They provide protection from wind, snow, and rain, but also permit water vapour (perspiration) to penetrate. This ensures increased levels of comfort, particularly



when worn during physical exertions in sport and in the workplace [20]. A number of textile items offer a waterproofing ability, but only some provide “breathability”. Conversely, a standard fabric is “breathable”, yet is not waterproof. A breathable textile can be categorised into 4 primary types [21]: closely woven fabrics which have been treated with water repellents, microporous film coatings and laminates, hydrophilic film coatings and laminates, and combined microporous coatings with hydrophilic topcoats. Generally, the twin functions of high breathability, permeability and waterproofness is only possible because the barrier layers can distinguish between an individual water molecule and a larger water droplet. **Figure 1.3** is showing the water proof and permeable laminated textile of GORE-TEX.



**Figure 1.3.** Water proof and permeable laminated textile of GORE-TEX

### **1.1.1.5. Liquid crystal elastomer for textile applications.**

Liquid crystal elastomers (LCEs) are materials in a unique class combining liquid crystalline anisotropy with rubber elasticity for the production of outstanding optical and physical properties, for example birefringence, soft elasticity, and actuation. The fields of liquid-crystal elastomers (LCEs) and liquid crystals are very wide, complicated, and thrilling. Such materials are found in everyone's lives, from the natural organisation of biological material to advances in electronic display development. LCEs are challenging the standard material classification. The term 'liquid-crystal' presents something of a paradox, since the majority of researchers have explained that liquids are amorphous and crystals fit into the category of rigid solids. When they are covalently bonded into flexible polymer networks, liquid crystals display amazing features, for example soft elasticity, reversible actuation, and anisotropic responses (optical and mechanical) in elastomeric materials. Consequently, LCEs are occasionally known as a new matter state [22-24]. Such LCEs are excellent candidates for an apparel application because of their lower temperature actuations; these low temperatures actuated materials can be utilised for the manufacture of thermo-regulating textiles. **Figure 1.4** is showing the textile applications of LCEs.

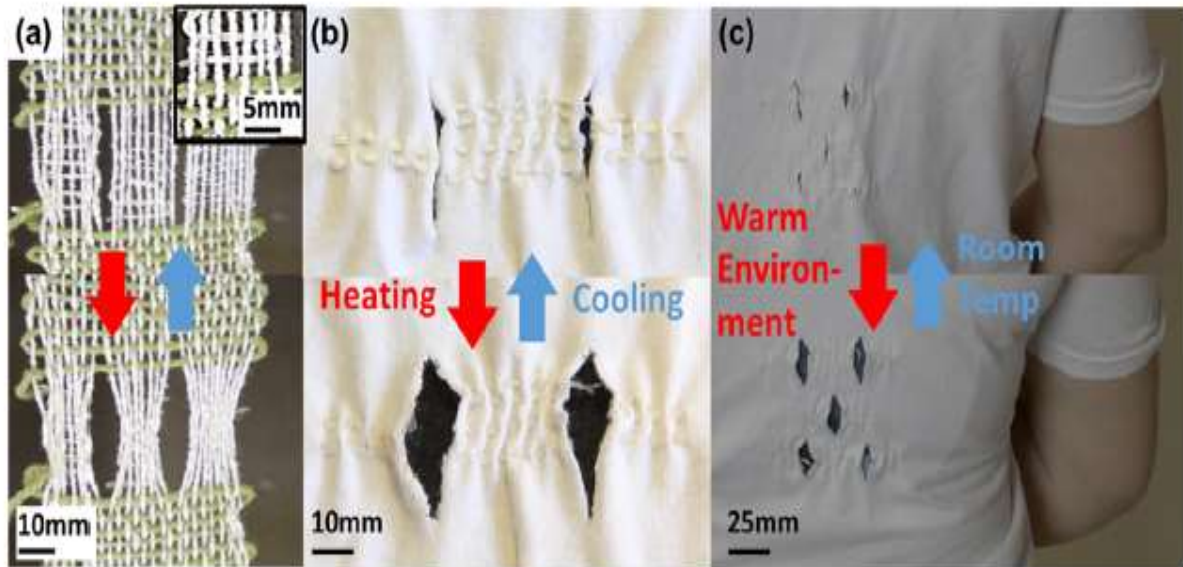


**Figure 1.4.** (a) woven textile using LCE fibers to develop pores upon heating. (b) LCE fibers sewn into a cotton shirt creating pores upon heating. (c) Demonstration of the LCE smart shirt demonstrating pores for improved heat transfers and sweats evaporation during exercise [25].

## 1.2. Limitations of the current research

Considerable work has been done over the last few decades to develop the permeable (water vapor and air), water droplet resistant and IR transmittable membranes for thermo-regulating textiles. Polymeric membranes laminated/coated to textile are widely used for waterproof breathable and water vapor transmittable textile. The current polymeric membranes cannot fulfill the requirement of high water vapor transmittable, water resistance and IR transmittance property of textiles. Therefore, the current polymeric membranes cannot be regarded as highly water vapor transmittable and responsive to temperature and humidity. Recently, Prof. Yi Cui and his group from Stanford University, proposed the nanoporous polyethylene for human body cooling with

good radiative property but the air and water vapor permeability of nanoporous polyethylene is not high enough compared with other polymeric membranes and the mechanical property of nanoporous polyethylene is not good enough compared with normal polyethylene, this kind of nanoporous polyethylene textile cannot fulfill the requirement of the user. Professor Hiroshi Ishii and his team from MIT, proposed a sandwich-structured biohybrid film for producing wet responsive wearables, and showed a textile prototype before sport activity with flat flaps (F) for ventilation and after sport activity with ventilation flaps in curved structure. In order to fabricate the biohybrid film they have used the very common class of Escherichia coli cells. But limitation of this invention is the lifetime of Escherichia coli cells. Authors only discussed about the moisture sensitiveness of Escherichia coli cells, but they did not discuss about temperature sensitiveness of this kind of material and longevity of this kind of material. Furthermore, current research cannot fulfil the water vapor transmit ability, air permeability, and IR transmission requirement of the wearers; we need to improve the above properties in order to get thermo-regulating textiles. Conventional polymeric membranes are not highly water vapor transmit able and cannot transmit human body IR efficiently. Furthermore, Traditional particulate leaching technique of making porous polymeric membranes is time consuming, which takes 2-3 days particulate to be leached out and conventional polymeric membranes and are not highly water vapor transmittable and water droplet resistant. Liquid crystal elastomers are excellent materials to be applied for apparel applications, the limitations of these materials is large scale productions

and low actuation temperature (near body temperature).

### **1.3. Objectives and significance of the research**

Polyurethanes are a class of materials for their various applications in the industry to provide inspiration to create smart materials with actuation structure and in response to moisture, thermal and other stimulation. Responsive polymer with smart properties such as quick responsive, thermo-regulating effect, near body temperature melting/glass transition can have more potential applications not only in thermo-regulating textile areas but other areas like scaffolding materials, wound dressing, and so on. Low water vapor transmit ability at lower temperature and significant increase of the water vapor transmitting with increasing temperature is required for breathable textiles. When the temperature within the textile is low, the membrane would act to reduce water vapor transmission which will prevent the escape of body heat to escaping through the material. This will help to maintain body heat on the skin which would increase the body temperature. However, there is less systematic study on micro structure and water vapor transmission of thermo-moisture responsive polymer for breathable textile applications and the current breathable laminated textile cannot fulfil the water vapor transmission, water droplet and IR transmission requirements of the wearer. To fulfil such requirement, we have synthesized a series of segmented polyurethane, prepared polyurethane composite with silica aerogel in order to get high water vapor transmitting ability, air permeable and IR transmittable. Quick soluble porous polyurethane membrane and coated synthesized polyurethane with textile in order to get thermo-regulating textiles,

also worked with liquid crystal elastomers to make temperature responsive textile (open/close mechanism temperature applied). The main aim of this project is to obtain polymer/polymer composite to produce robust thin film with thermo-regulating property (high water-vapor permeable, IR transmit able) for commercial apparel applications. Another objective of this study is to make highly water vapor transmittable and water resistant porous polyurethane membrane. The resulted high water vapor transmit able and water resistant laminated/coated textiles can be used for extreme conditions where we need both water vapor transmit able under high working intensity and water resistance so that body sweat can escape and be transmitted from body surface to environment and wind and rain proof are also required. Furthermore, I also fabricated temperature responsive (open/close mechanism in a textile as a function of temperature) weaved fabric.

The major objectives of these studies are as follows-

- To design and synthesise of thermo-regulating polymer by two-step polymerization technique with variation in hard to soft segment and molecular weight of macro glycol. The effect of soft segment and molecular weight of macroglycol on the thermo-mechanical properties, thermo regulating textile (water vapor transmit able, water resistance and IR transmit able) and other properties of synthesized thermo-regulating membrane were investigated to achieve a good thermo regulating textile.
- To design and synthesis of polyurethane composite in order to produce the re-enforced highly water vapor and IR transmittable membrane, to

fabricate and optimize thin membranes for laminating with textiles by various methods.

- To design and fabricate a quick particulate leaching technique to make porous membrane. Fabricated membrane would be used to make water vapor transmit able and water resistant textile by laminating technique, and to design and fabricate coated textile.
- To design and fabricate temperature responsive (open/close mechanism in a textile as a function of temperature) woven fabric.
- To investigate the structure, thermal, chemical and mechanical properties of the films by FTIR, DSC, TEM, SEM, XRD, and DMA.
- To establish relationships between structures, properties, performance and the responsiveness of the materials and fabrics.

## **1.4. Thesis outline**

This thesis will discuss the multiple functional polymer for thermo-regulating textiles. The structure of this thesis is designed as follows-

**Chapter 1**, the general background of the entire thesis, limitations of current research, significance and objectives. In the background part, shape memory polymers for responsive textile, composite membranes for apparel applications, preparation of porous membrane, fabric coated with shape memory polyurethane, liquid crystal elastomer for textile applications has been discussed.

After analyzing the background part, the limitations of current research and objective of this study are stated.

**Chapter 2**, comprehensive literature review related to this study and progress of current research in this area has been studied. In this chapter, mainly talk about shape memory polyurethane, composite membrane, porous membrane, laminating/coating techniques, and liquid crystal elastomer.

**Chapter 3**, this chapter will briefly describe all the materials we used in this study, sample preparation methods, equipment's used, and characterization techniques.

**Chapter 4**, this chapter will discuss about the preparation of composite membrane for thermo-regulating textile. The influence of silica aerogel on conventional polyurethane's transmittable and mechanical property. Detailed characterization of composite membrane has been done by using DSC, TEM, SEM, FTIR, WVT, IR transmittance and so on. The structure and property relationship also discussed.

**Chapter 5**, this chapter will discuss about the preparation of porous membrane, a time saving particulate leaching technique has been introduced in this chapter. Normally, it takes few days to make porous membrane by using particulate leaching technique, here; we reported a time saving technique to make porous



polyurethane membrane. To know further details of the prepared porous membrane, SEM, XRD, DSC, TGA, water vapor transmission, water resistance, porosity and so on. The structure and property relationship for apparel application also discussed.

**Chapter 6**, this chapter will discuss about the coated fabric. In this part of work we made coated fabric using different tapes polyurethanes and study the surface property of coated fabric. To understand better about the performance of the coated fabric, SEM, WVT, shape memory, TGA, contact angle has been performed.

**Chapter 7**, this chapter will introduce the textile applications of liquid crystal elastomers filaments. Here, we will be talking about the 3D printing techniques to make LCEs filament to make temperature responsive weaved fabric and radial shaped flip. Furthermore, open/close mechanism in a textile as a function of temperature also will be discussed.

**Chapter 8**, this chapter will conclude the entire study, the major contribution and limitations of this work. Furthermore, the suggestions for the future work to make thermo-regulating textile also will be provided.

## Reference

1. Zhang et al., structures and properties of thermo-regulating knitted fabrics. *Indian j. of fiber and Text. Rese.*, 2005. 30: p. 377-383.
2. Babu et al., Thermo regulated clothing with phase change materials. *J Text. Eng. Fashion Technol.*, 2018. 4(5): p. 344–347.
3. Fabien et al., Phase Change Materials for Textile Application. *Phase Change Materials for Textile Application*. DOI:<http://dx.doi.org/10.5772/intechopen.85028>
4. Grażyna et al. Assessment of the Thermoregulation Properties of Textiles with Fibres Containing Phase Change Materials on the Basis of Laboratory Experiments. *Fib. & Text. in East. Euro.*, 2012. 20: p. 47-52.
5. Liang C., et al., Investigation of shape memory polymers and their hybrid composites. *J. of Intel. Mater. Syst. and Struc.*, 1997, 8.
6. Huang W.M., thermos-moisture responsive polyurethane shape memory polymer and composite: a review. *J. of Mater. Chem.*, 2010. 20: p. 3367-3381.
7. Wu Y., Studies of shape memory polymers with novel functions. PhD thesis, the Hong Kong polytechnic university, 2015.
8. Hu et al., A review of actively moving polymers in textile applications. *J. of Mater. Chem.*, 2010. 20: p. 3346–3355.
9. Hu et al., Recent advances in shape–memory polymers: Structure, mechanism, functionality, modeling and applications. *Prog. in Polym. Sci.*, 2012. 37: p. 1720–1763.
10. [https://en.wikipedia.org/wiki/Composite\\_material](https://en.wikipedia.org/wiki/Composite_material).
11. Josmin et al., *Advances in Polymer Composites: Macro- and Micro composites – State of the Art, New Challenges, and Opportunities*. *Polym. Comp.*, 2012. 1 (first edition).
12. Zahra et al., The effect of the nano-structured aerogel powder on the structural parameters, water repellency, and water vapor/air permeability of a fibrous polyester material. *Mater. Chem. and Phy.*, 2016. 177: p. 99-111.
13. Xiangli et al., Facile preparation of porous polymeric composite monoliths with superior performances in oil–water separation – a low-molecular mass gelators-based gel emulsion approach. *J. of Mater. Chem. A*, 2014. 2: p. 10081–10089.
14. Mu et al., Porous polymeric materials by 3D printing of photo curable resin. *Mater. Horiz.*, 2017. 4: p.442-449.
15. Lo et al., Fabrication of controlled release biodegradable foams by phase separation. *Tissue Eng.*, 1995. 1(1): p. 15-28.
16. Nam et al., A novel fabrication method of macro porous biodegradable polymer scaffolds using gas foaming salt as a porogen additive. *Biomed. Mater. Res.*, 2000. 53(1): p.1–7.
17. Li et al., Porous heterogeneous organic photocatalyst prepared by HIPE polymerization for oxidation of sulfides under visible light. *J. of Mater. Chem.*, 2012. 22: p. 17445–17448.
18. Qingpu H., Porous polymeric structures for tissue engineering prepared by a coagulation, compression moulding and salt leaching technique. *Biomaterials*, 2003. 24: p. 1937–1947.
19. Joel et al., Preparation of interconnected poly(3-caprolactone) porous scaffolds by a combination of polymer and salt particulate leaching. *Polymer*, 2006. 47: p. 4703-4717.
20. Kubin I, Functional and fashion coating for apparel, *Melliand Inter*, 2001. P. 134-138.
21. Sen et al., *Coated Textiles Principle and Applications*, Tech Ed Damewood J, Technomic Publishing Co., USA, 2001. p.133-154.
22. Oxtoby DW. *Liquid crystals: the fourth state of matter* (Saeva, Franklin D.). New York (NY): ACS Publications, 1981.
23. Warner M, Terentjev EM. Nematic elastomers—A new state of matter? *Prog Polym*

- Sci., 1996. 21(5): p. 853–891.
24. Sabina et al., Liquid crystal elastomers: an introduction and review of emerging technologies. *Liq. Crys. Revi.*, 2018. 6: p. 78–107.
  25. Devin et al., Long Liquid Crystal Elastomer Fibers with Large Reversible Actuation Strains for Smart Textiles and Artificial. *ACS Appl. Mater. Interfaces*, 2019. 11: p. 19514–19521.

## **Chapter2. Literature review**

In chapter 2, there will be a comprehensive study about thermo-regulating polymeric materials for textile applications. In this chapter, I will discuss details about the self-adaptive, thermo-moisture responsive and highly water vapor permeable composite membranes, porous membranes, coatings and laminating's and liquid crystal elastomers for smart textiles. Furthermore, will discuss about the limitations of previous research and structure-property relationship of polymer for improving the thermo-regulating and other mechanical property. In addition, the detail study will expose the obvious gap of the previous research and development of responsive and self-adaptive polymer.

### **2.1. Thermo-regulating polymeric materials**

A stimuli-responsive shape memory polymer is a class of responsive polymeric material which can respond to particular alterations in the surroundings (e.g. relative humidity (RH), temperature, pH and light) by obtaining a particular shape, according to their sensitive behaviour, they are defined as a shape memory polymer (SMP) and a thermally induced material. A shape memory polymer (SMP) can quickly change their shapes from permanent shapes to temporary shapes and can return to their original shape given the correct stimulus such as temperature, light, RH, pH. SMPs can maintain two or three shapes and the shape change between those is happened by external stimulus [1-4]. Polyurethane (PU), a unique class of smart material, studied in depth since they were discovered in 1988 by Mitsubishi, this has recently attracted much attention because of their individual properties like the broad variety of shape recovery

temperatures, good processing ability, excellent biocompatibility and high shape recoverability [5-7]. Compared to shape memory alloys (SMAs), polyurethanes (PUs) are lightweight and low cost. The SMPUs are composed of 2 phases, the permanent phase and the reversible phase. A hard segment will form through crystallization and hydrogen bonding, which act as frozen phases when under melting temperatures. The soft segment's reversible phase transformation has responsibility for shape memory effects. Such effects can be controlled through the soft segments of the polymer, the molar ratio of the different segment (soft and hard segments), and the process of polymerization [8, 9].

A responsive polymer material is able to change according to the surrounding environment, regulate molecule an ion transport, alter adhesion and wettability of various part on external stimuli, converting biochemical and chemical function (signals) into mechanical, thermal, optical signals and electrical, and vice versa. The materials have a crucial role in various applications, e.g. tissue engineering diagnostics, 'smart' optical systems, and drug delivery, in addition to micro-electromechanical systems, biosensors, textiles and coatings [10-13]. Stimuli-responsive macromolecular nanostructures can perform chemical and conformational changes on receiving external signals. Such changes have various accompaniments in the polymer's physical properties. The signals derive from alterations in the materials environment, like changes in temperature, or applied mechanical pressure, or chemical component, or that which is exogenously triggered by being irradiated with light or being exposed to magnetic or electrical fields [14, 15]. **Figure 2.1** is showing the stimuli responsive polymeric materials.

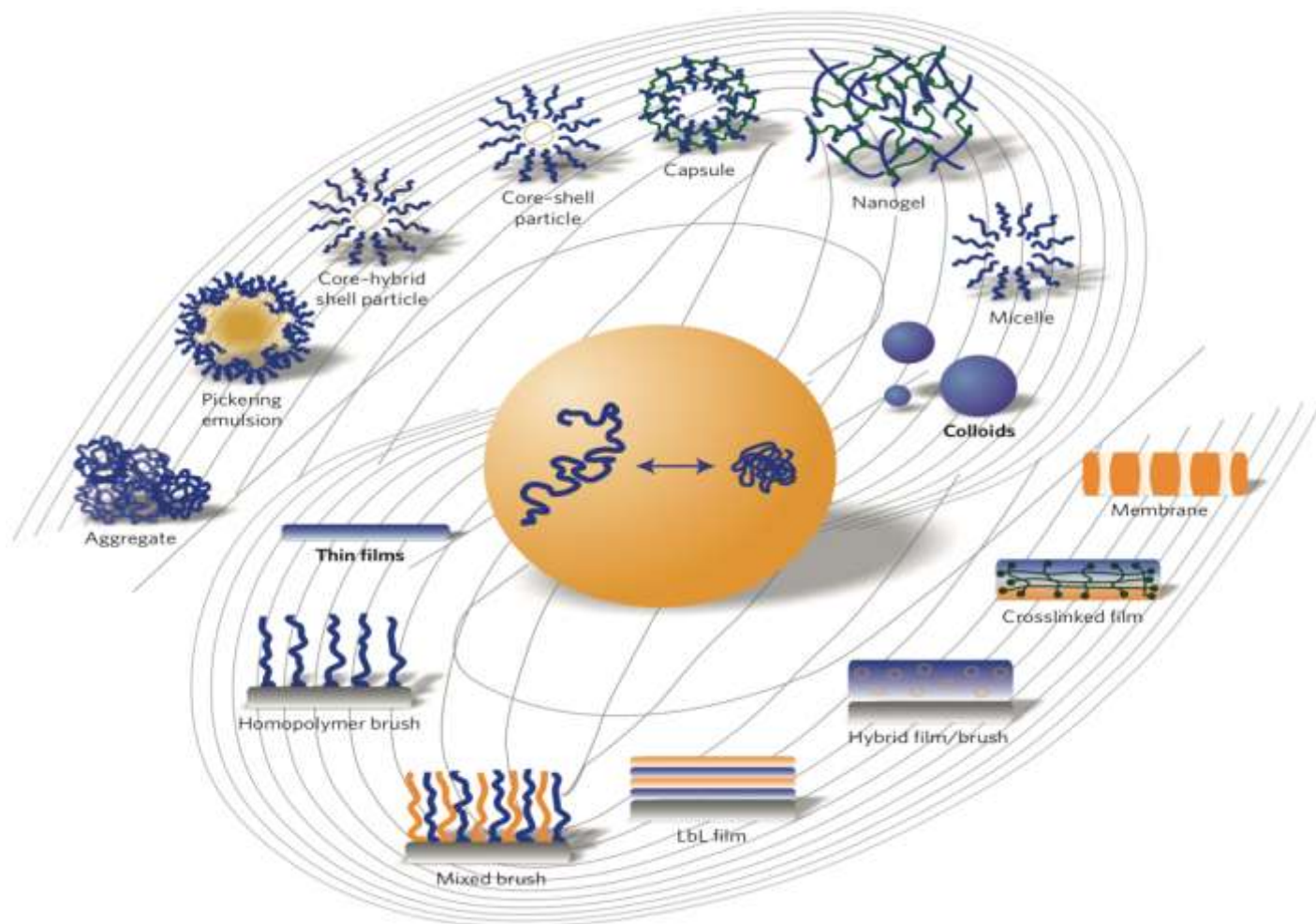


**Figure 2.1.** ‘Galaxy’ of nanostructured stimuli-responsive polymer materials. [4].

Shape memory is where materials can recall their actual shapes, the polymers change shape into temporary shapes and can return to their original shapes via an external stimulus. The first materials with these properties were developed in the 1960s and are known as shape memory alloys (SMAs).

SMPs are a shape memory material, the definition of which is a polymeric material which can sense and respond to an external stimulus in a pre-set shape, first developed in France and commercialised in 1984 by the Japanese. Polymers

like polynorbornenes, trans-polyisoprenes, styrene-butadiene copolymers, crystalline polyethylenes, few block copolymers, and ethylene-vinyl acetate copolymers, and the segmented polyurethanes are known to have shape memory effects. Compared to shape memory alloys, SMPs possess an improved potential for clothing and textiles, and associated products: regarding SMAs, mechanical properties are only adjustable in a short range and the highest change is approximately 8%. [15]. Conversely, shape memory polymers (SMPs) are easily shaped, controllable transition temperatures and have good shape stability. SMPUs are a type of polyurethanes which differ from conventional polyurethanes, given that they have segment structures and a big range of transition temperature. When an SMPUs are cooled down from the higher temperature then  $T_g$  to the temperatures under  $T_g$ , when mechanical loads are present, and after load removal, a substantial deformation can occur in the area of 10-200 percentage and become fixed into the polymer [16].

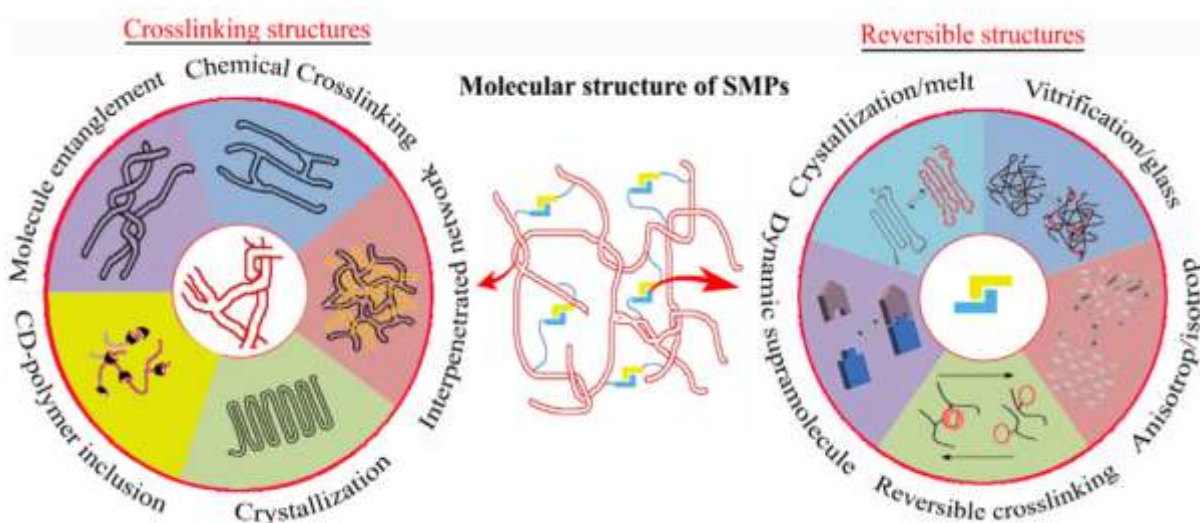


**Figure 2.2.** Molecular structures of SMPs. A stable network and a reversible switching transition are the prerequisites for the SMPs to show SME [17].



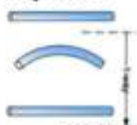
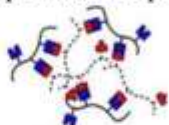








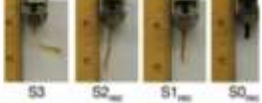
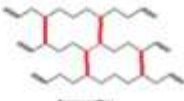


## 2.2. Shape memory polyurethanes

SMPUs are usually referred to as the polymer with the greatest versatility. This material diversity is used for synthesizing PUs that provide them with this flexibility. Consequently, polyurethanes are beneficial in four different major product types: foams, fibres, elastomers, and laminations/coatings [17, 18]. Polyurethanes are the reactor materials of polyols and polyisocyanates. These belong to a heterogeneous polymer family and feature the urethane linkage (-NH-CO-), which is similar to carbamate group which present in the organic chemistry in the chains of the polymer [19]. Urethane groups are not always forming most of the functional groups in the polyurethanes. It can incorporate alternative of the functional groups into the backbone of the polymer, contributing to the variety of properties shown by polyurethane [20]. Therefore, the properties PUs extend from rigidly hard materials (thermosetting) to soft elastomers. In general, thermoplastic polyurethanes possess better tensile strength, robustness, and are resistant to degradation and abrasion. The PU domain structure and the potential for structural diversity lead to many uses for such materials.

Segmented polyurethanes display shape-memory abilities. Shape memory PUs have 3 essential initial materials- I) long chain polyester or polyether polyols, II) diisocyanate, and III) chain extender diamine or glycol. Chain extender and diisocyanates are act as hard segmented, whereas long chain polyols are soft segmented. Such polymers are characterised by segmented structures and morphology of the polymer is dependent on the chemical details and segment



(block) size (length). Shape memory polyurethanes have micro phase separated structures because of not being compatible thermodynamically. A hard segment is able to bind itself through crystallization and hydrogen bonding, causing the PUs to be very strong below  $T_m$  (melting temperatures). Soft segment reversible shape change is thought to be the reason for shape memory effects. Shape memory effects are controllable through soft segment molecular weight, ratio of moles between different segments (hard and soft), and the polymerisation processes. The usual textile uses of SMPs are as textile fibres and coatings etc. Shape memory effects of ordinary polyurethanes are unable to wholly restore their residual inelastic deformation when heated. Contrastingly, SMPUs can recover any residual plastic deformations until 400 percent via a micro-Brownian movement caused by it being heated 10-20 degree Celsius above their  $T_g$  (glass transition temperature) [21-23].

Polymerization & Crosslink	Composition & structure	Stimulus	Shape memory function
Polyaddition •Urea/urethane •Acrylate/acrylic	Block-copolymer 	Temperature 	One way SME 
Polycondensation •esterification	Supramolecular polymer 	Electricity  Magnetic 	Two way SME 
Free-radical polymerization	Polymer blend / composite 	Water sensitive 	Triple shape SME 
Photochemical polymerization	Polymer IPN/semi IPN 	Light/radiation 	Multi shape SME 
Radiation crosslink	Crosslinked Homopolymer 	Oxidation-reduction 	Multi functionality 

**Figure 2.3.** Classification of polymeric shape memory effect. [9]

Traditional polyurethanes properties (e.g., from 1,6-hexane di-isocyanate and 1,4-butane diol) have similarities with that of polyamides. This is made of 2 initial materials -(I) di-isocyanate, and (II) short-chain glycols or long-chain of polyethers or polyester glycols [19]. The polyurethanes produced from short-chain glycols and the diisocyanates has several bonding of hydrogens between -OC- and -NH- groups, higher strength and hardness, and low solubility. Conversely, PUs gained by reactions of non-crystalline, long chain, unbranched, OH-functional polyesters or polyethers with stoichiometric quantities of di-isocyanates are composed of approximately a 4–7% urethane group [17, 18]. The

intermolecular force for polyesters and polyethers in polyurethanes are weak van der Waals forces; consequently, strength hardness is lower and the product displays rubber-like properties. Each product has a one phase, and not a segmented structure. The technical criticality of traditional PUs is in crosslinked strong products (non-textile coatings, PU foams).

Conversely, segmented PUs are reversible block copolymers composed of rigid hard segments, and flexible soft segments [24–26]. Segmented PUs are comprised of 3 essential initial materials, (I) long chain polyester or polyether polyols, (II) diisocyanates and (III) glycol chain extenders. The hard blocks form because of reactions of diisocyanates with lower-molecular-weight glycols (chain extenders), usually semi crystalline and imparting reinforcement to the polymers. Hard blocks normally constitute 30–50% by weight of entire volume. The micro phase of soft-segment-rich, made by polyols, are accountable because of the PUs elastic behaviour, and is typically in the range of below glass transition temperature it is amorphous. The micro phase separations of blocks produce areas of the hard block concentrations acting as crosslinking points for the soft blocks, therefore producing the rubbery texture of such polymers. These types of segmented structure display shape memory effects dependent upon the composition. The micro-phase separated structure in the segmented polyurethanes because of soft and hard segments are thermodynamically incompatibility. Hard phase can bind through crystallization and bonding (hydrogen), causing the polyurethanes to be very hard below  $T_m$  (melting temperatures). Soft segment alternative phase transformation is responsible for

shape memory effects. These are controlled through the soft segments molecular weight, mole ratio between soft and hard segments, and polymerisation processes [53].

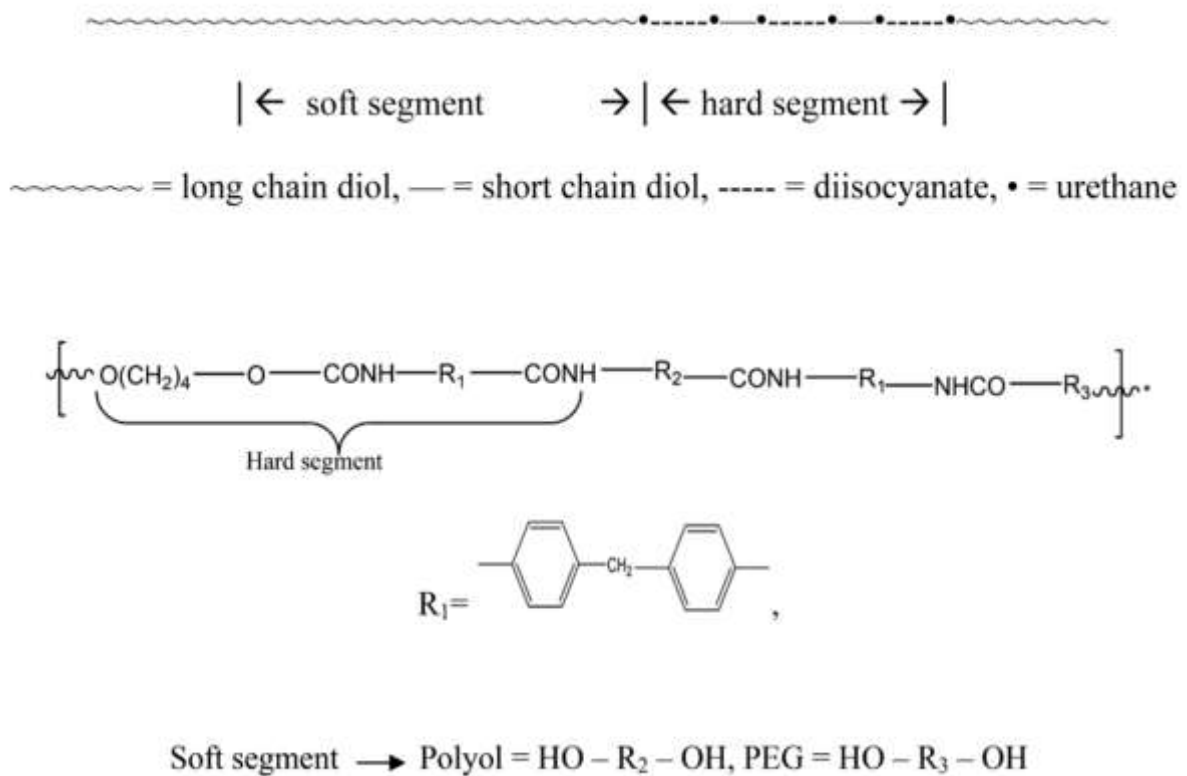


**Figure 2.4.** General structure of segmented polyurethane [23, 24]

The segmented PU structure is prepared with 1 mol long-chain linear polyol, 1 mol polyethylene glycol (PEG), 2 mol diisocyanate (MDI) and 1 mol chain extender (1,4-butane diol) in **Fig2.4**. Soft segments have some mobility and usually coiled shapes, and hard segment, alternately. The morphology of polyurethanes blocks copolymers depending on composition and the contents of the soft and hard segments. Because of the extreme contrariety in the physical property between their parts, co-polymers are thought to phase separation in domain and solution structures in their different (solid) state [28–32]. The phase

separation occurs in PUs because of soft and hard segments are thermodynamically incompatible. The phase separation has an influence on PUs physical properties, in addition to their functional properties, for instance permeability. The microphase separating of segmented polyurethane and their influences upon PU properties are subsequently discussed.

The PUs are block copolymers [20] with the structures of  $A_nB_m$ . In general, the soft and hard PU segments have a positive mixing heat and are therefore not compatible. Therefore, there tends to be a skew towards the two components phase separation; yet, the block co-polymer molecule topology restricts segregation, causing micro-domain formations [28]. Consequently, a phase separation (segregation) happens and micro-phase structures of covalently-linked are formed. The matrix (coherent), consisting of soft segments (flexible), resulting in deformability (high) of the resultant materials. Contrastingly, in the segment domain (hard), physical interactions help the molecules to be fixed. As a result of coupling of covalent bond to the soft segments, it restricts the PU chain plastic flow. Hard domains (segments) are functional spacious crosslinked areas. When phase segregation is larger, there is lower the flexible segments polarity. Thus, segregations are emphasised few in polyester urethanes by comparison to polyether urethanes and is mostly seen in urethanes of polybutadiene. The formation of bonds (hydrogen), hard segment crystallization, folding of chains, free volume effects, and kinetic arguments are all potential explanations for the phase separation behaviour of the segmented polyurethanes. Because of the very high polarity differences of soft and hard segments, 3D hydrogen (bonding)

network structures will form. The micro-phase separation of these two chemical compounds provides useful functional, physical, and mechanical properties of the segmented PUs [2].

### **2.3. Polymeric composite materials**

The composite materials are formed of two/ more materials, frequently those with extremely different properties. These different materials combine to provide the unique properties to the composite materials. Yet, in the composite materials are different materials are easy to tell apart because they would not blend or dissolve into among them.

The natural composites are found in both the animals and plants. Wood is one of composite – composed of very long fibres (cellulose) bonded together by substances (weaker) called lignin. Cellulose can additionally be found in cotton, yet without the lignin as a binder it is not as strong. The two substances (weak) – cellulose and lignin – construct a more powerful one. The bones in the body (human) are a composite material too. Composites have been made for many of years. For instance, mud bricks. Mud is dried into brick shapes to be used as construction materials. It is stronger if you attempt squashing it (it possesses excellent compressive strength) but is easily broken if bent (poor tensile strength). Straw appears strong, if you attempt to stretch this, and yet it can be easily crumpled. By combining this two (straw and mud), it is possible to manufacture bricks which are normally resistant to tearing and squeezing, and make very good building materials. The first modern composite material is fibre

glass, which is used in sports equipment, building panels, car bodies, and boat hulls.

A few advanced composite materials are manufactured using the carbon fibres rather than glass. These materials normally are stronger and lighter than fibreglass but their production is more costly, and these materials are applied in more expensive equipment (sports) like golf clubs, and in aircraft structures. Carbon nanotubes also been successfully applied to form different composite materials. They are very lighter and very stronger than traditional composites composed of traditional carbon fibres, but remain very expensive. Yet, they do provide the possibility to make lighter aircraft and cars (using less fuel than current heavier vehicles).

One main point of latest composite materials is that they are very strong yet light. By selecting the correct combination of two materials (matrix and reinforcement), new materials can be prepared which exactly meet a particular application's requirements. Additionally, composites offer different design flexibility, and they are capable of moulded into complicated shapes, although this is costly. Even though the resultant product has greater efficiency, the raw materials are frequently quite costly [34].

Based on the matrix phase, composites are classified into polymer matrix composites (PMCs), ceramic matrix composites (CMCs), and metal matrix composites (MMCs) (see figure 14). [61]. The classifications are accorded by reinforcement type, and are laminate composites (composed of laminates, fibrous

composites (composed of fibres), and particulate composites (composed of particles). Fibrous composites are then subdivided based on or synthetic fibres or natural/biofibres. Biofibres encompass composites known as biofibre composites. They are divided again based on the matrix, the biodegradable matrix and the nonbiodegradable matrix [36]. Bio-based composites are composed of natural/biofibres and biodegradable polymers are known as green composites. These are able to be subdivided again as textile composites and hybrid composites. Hybrid composites are formed by combining at least two fibre types.

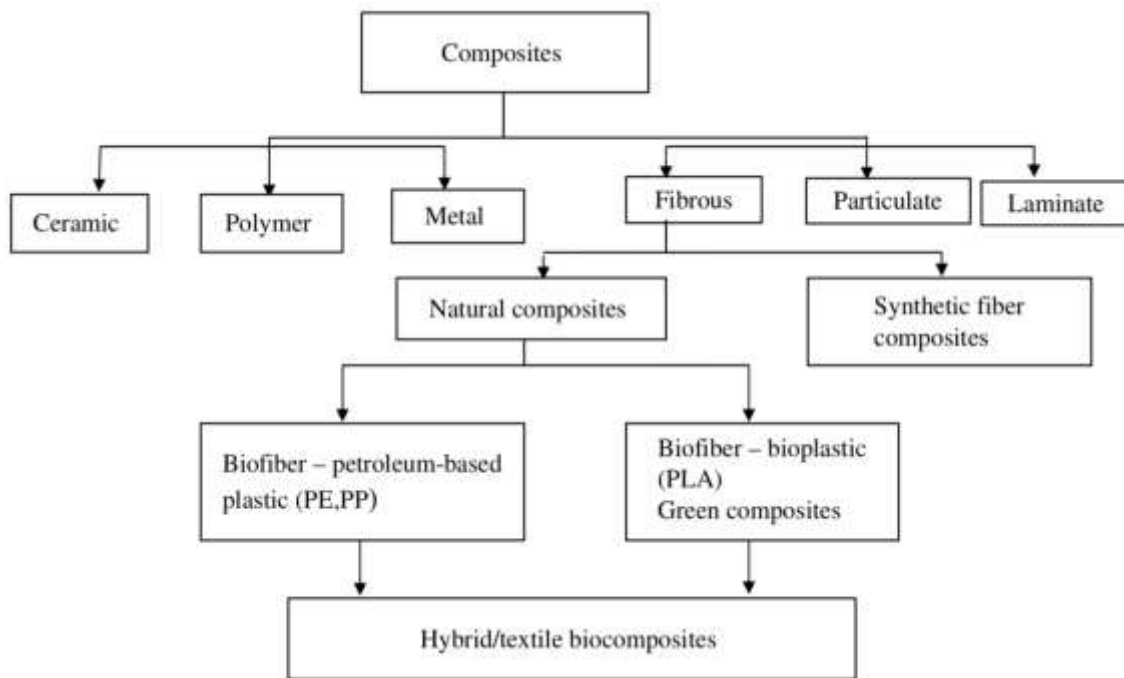


**Figure 2.5.** Classification of composites [37]

Composites are materials which made of two/more than two physically and chemically different phases separate distinct interfaces. These processes are together to be more meaningful functional or structural properties unobtainable by any one of the above constituents. Composites have become a vital



component of modern materials because of advantages like faster assembly, high strength (fatigue), resistance of corrosion, and low weight. These are in wide use to make electronic packaging for medical equipment, aircraft structures, homebuilding, and space vehicles [37]. The main differences between composites and blends are that the two primary constituents of the composites are still recognisable whilst these might not be recognisable in blends. Furthermore, the main materials applied in our everyday lives are ceramics, concrete, wood, etc. It is a surprise that the more vital polymeric materials (composites) are discovered in the nature, and are termed natural composite materials. Mammalian connective tissue is an advanced polymer composite where collagen, fibrous protein, provides reinforcement in the materials. It serves as both hard and soft connective tissue. Composite is a material combined with another in differing combinations, whereby individual constituents keep their own individual identity. The separate constituents combine to provide the required mechanical stiffness or strength to composite material parts. The composites are comprised of at least two very distinct phases (dispersed phase and matrix phase) and have many properties which largely differ from their constituents. The matrix has greater ductility and is a less hard part. It holds the dispersed part (phase) and shares its load. The reinforced dispersed part (phase) is discontinuously entrenched into the matrix. The secondary part (phase) is termed the dispersed part (phase). The dispersed part (phase) is normally stronger compare with matrix, thus, it is often termed the reinforcing the phases [38, 39].

Membrane technology has become popular in many types of separation, including gas and water, over recent decades. Because of the advantageous features using membrane separation, e.g. not much need for chemicals, easy to scale-up, and have little relatively low energy, membrane separation is used in many industries, including water desalination. Desalination removes salt from saline water and provided fresh water suitable for human consumption in addition to agricultural and industrial purposes, and is considered an effective and reliable approach to help the worldwide water crisis [40]. Amongst various membrane-based desalination processes so far developed, the reverse osmosis (RO) membrane process has a primary role in the desalination industry because of the advantage of combined capital cost and energy consumption [41-44].

Polymer science has recently gathered increased attention in the separation technology field. The various chemical structures and polymer properties help to create different membranes for applications like gas separation and water purification [45,46]. Various gases with differing polarity degrees and molecular sizes have particular properties, so separation is attempted. The main issue with polymeric membranes is the trade-off relationship between selectivity and permeability [47-49]. Some studies have reported the direct relationship between selectivity and permeability [50,51]. One main procedure for increasing the performance of polymeric membranes, by using nanoparticles for gas separation, these possess vital influence on the properties of polymer [52–54]. Some nanoparticles with differing properties can better the performance of the polymeric membrane [53–56]. Nanoparticle effects on the gas permeation of

membranes are dependent on their shape, weight fraction, and size in addition to their interactions with the polymers. A nanoparticle has a bigger ratio of the surface area to the volume than a bigger particle [52]. Additionally, their matrix mixture is complex especially at higher concentrations.

Fibre reinforced polymers are a fast growing class of materials popularly used as high-performance materials. [57, 58]. In such a material, the polymer matrix has received interest because of the broad range of applications in which they can be used in the petroleum chemical industrial, aeronautical, automotive parts and architectural fields [57]. In a fibre reinforced composite, the polymers are normally the matrix (continuous phase) whilst the fibre is the discontinuous phase [59]. The properties (mechanical) of fibres (short) strong composites are administered by orientation, fibre content and fibre-matrix adhesion [59-61].

The reinforcement property and the interface matrix can take various and complicated structures which differ from the matrix and the fibre phases [62, 63]. Because of the interface area appearance, the role of polymers and fibre has independence but these are not separated [63]. Fibre's particular surface area is so large that it permits improved transferring of load between polymers and fibres which causes it to maintain strength. [64, 65]. The interface differs from the matrix; such sites are crucial for designing composites.

Because fibre-polymer interfaces can lower the composites' water durability conditions [61, 67-69], here we attempted to use these particular interface (trait) in the gas separation technology. First, we selected a polymer and fibre for

creating a favourable interface. Polymer needs to have good gas transmitting ability behaviour [70-74].

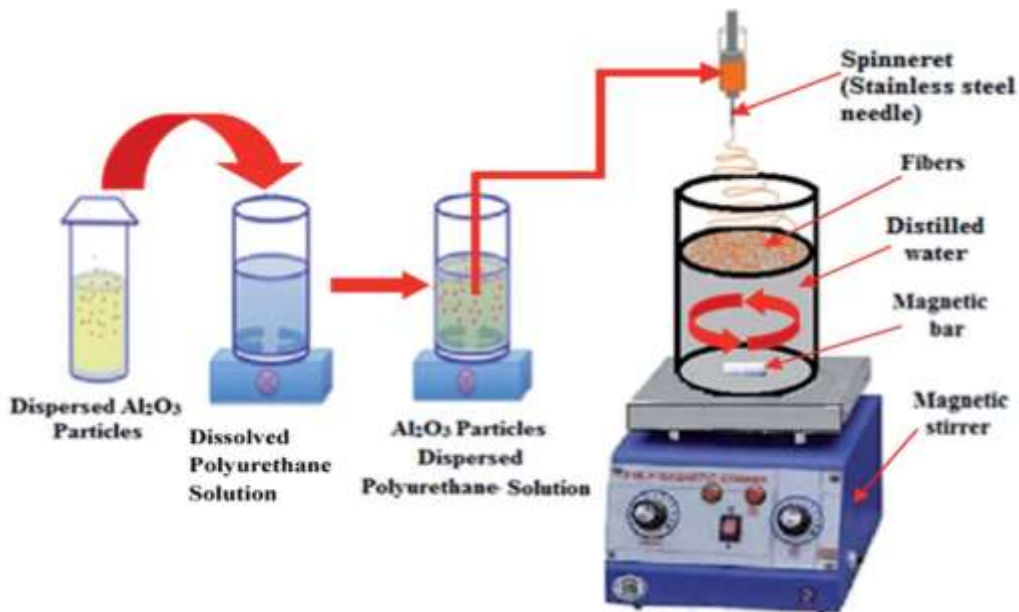


**Figure 2.6.** Schematic diagram of the formation of the polyurethane– Al<sub>2</sub>O<sub>3</sub> anion-exchange fibrous composite [75].

### 2.3.1. Silica Aerogel

Aerogel is an ultra-light, synthetic porous material which derives from a gel, whereby the gel's liquid components have been replaced with gases [76]. This results in a solid with low conductivity (thermal) and low density [77]. Aerogels can be produced from various chemical compounds [78]. Aerogel was first created in 1931 by Samuel Stephen Kistler.

Aerogels are normally produced by extraction of gel liquid components by supercritical (drying). The aerogels (first) were made from the silica gels. Later, Kistler worked on aerogels based on tin dioxide, chromia, and alumina. Carbon aerogels were initially developed in the late 1980s [79-83].

In spite of the name aerogels are originally rigid, solid, and is not actually resemble gels in their property (physical), the name simply indicates that they are made from gels. Softly pressing on aerogels usually will not leave any mark, pressing very firmly leaves the permanent depression. The pressing very firmly would break down the structure (sparse), meaning It will smash like glass (this property is called friability), although newer variations will not have this property. Although it can shatter, it is structurally extremely strong.

The aerogels are 99.8% air. They are composed of a porous solid network containing air pockets, which take up most of the space in the materials [84]. Lack of solid materials permits aerogels to have nearly no weight at all. The aerogels are very good thermal insulators, because they nearly nullify two out of 3 techniques of heat transfer – convection (the microstructure prevents net gas movement), and conduction (nearly entirely comprised of insulating gas). They are excellent conductive insulators as they are made nearly completely out of gas, which do not conduct heat very well. Silica aerogel is a particularly excellent insulator reason of silica has poor heat conductivity; carbon or metallic aerogels have less efficacy. They are an ideal convective inhibitor as air is unable to circulate through the lattice. Those who handle aerogels for longer periods should use gloves for preventing dry brittle space showing to the skin. This gives an appearance of yellowish against bright backgrounds and smoky blue against dark backgrounds. Aerogels are hydrophilic, but treating them chemically can cause them to be hydrophobic. When they absorb moisture they will undergo structural changes, for instance deteriorate, and contraction, but prevention of

degradation can be achieved by ensuring they are hydrophobic. The aerogels with a hydrophobic interior are less likely to degrade than the aerogels with only outside hydrophobic layers, even if cracks penetrate their surface. Silica aerogels are a common aerogel type, and are the most used and studied [85-88].

The silica solidifies into 3D, interconnected clusters making up just 3% by volume. Conduction via the solid is thus extremely low. The other volume of 97% is comprised of air in tiny Nano pores. The air does not have much room for manoeuvre, which inhibits both gas-phase conduction and convection [89]. Additionally, a silica aerogel has a low refractive index of  $\sim 1.05$  and a high optical transmission of  $\sim 99\%$  [90]. It has extraordinary properties of thermal insulation, with very low conductivity (thermal). Silica aerogel once had fifteen entries in the Guinness Book of for material properties (World record), including lowest-density solid and best insulator, although it was ousted from the former title by aero graphite in 2012 and then aerographene in 2013 [91-93].

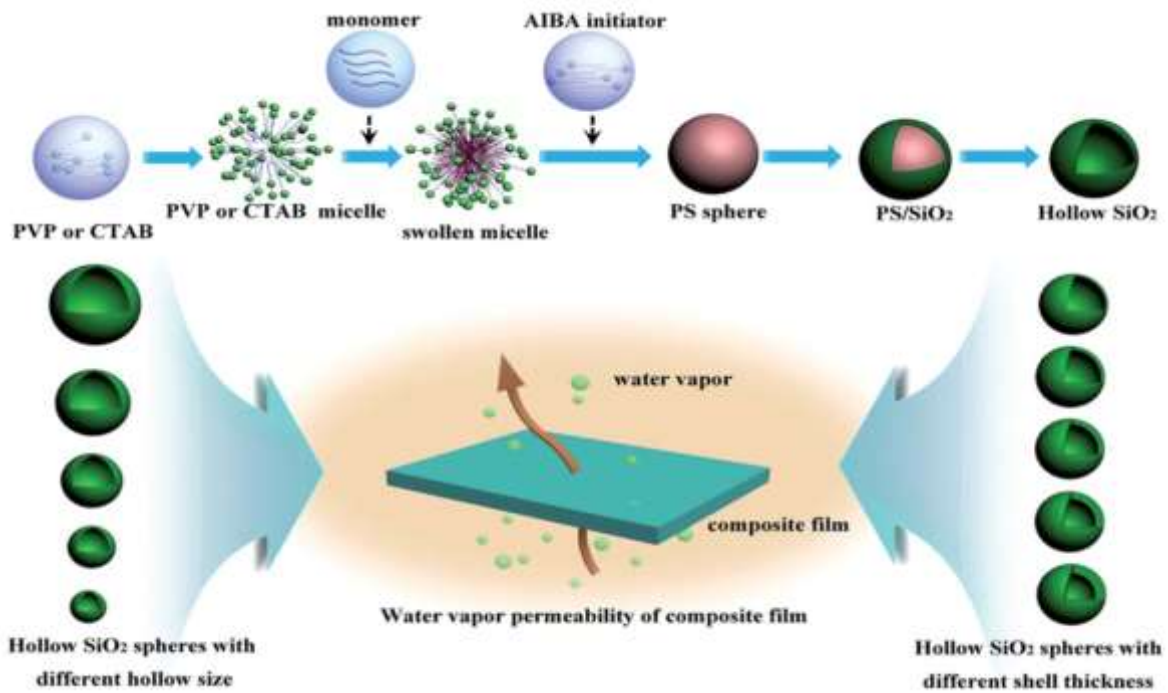


**Figure 2.7.** Fabrication diagram of the polyacrylate/hollow silica composite film [94].

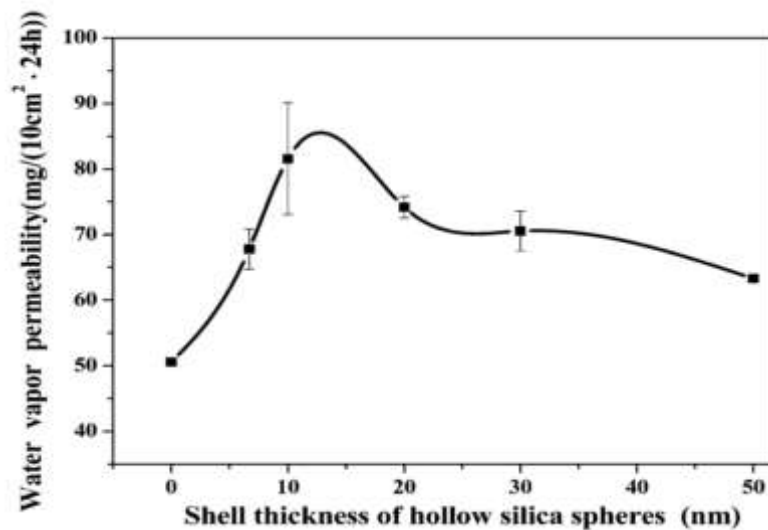


**Figure 2.8.** Effect of shell thickness of hollow silica spheres on water vapor permeability of composite film [94].

Hollow silica spheres' shell thickness is one of the other factors influencing water vapour transmutability of composite film. Hollow silica materials (spheres)

with varying shell thicknesses were completed by adjusting the quantity of TEOS with 150 nm PS spheres as a template. The shell thicknesses of silica (spheres) on water vapour transmission of composite films can be seen in Figure. Permeability of composite membranes is usually of a parabola shape with increases in the shell thickness of hollow silica spheres. Composite film has better water vapour transmission when shell thickness of the hollow silica sphere is 10 nm. Water vapour molecular process across silica spheres are because of the phase (crystalline) and distribution of pore size of the shell of the silica sphere.

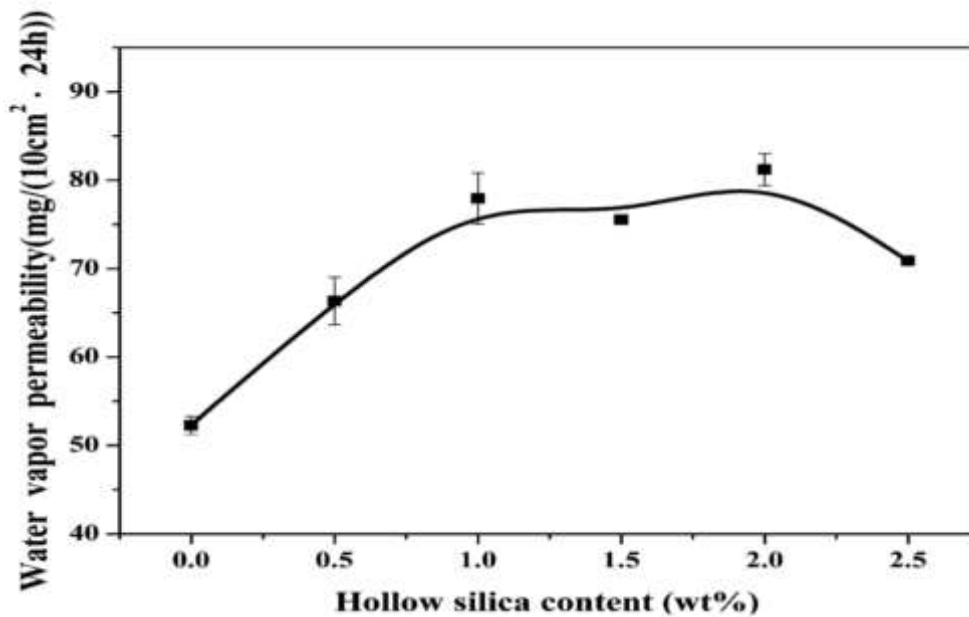


**Figure 2.9.** Effect of the content of hollow silica spheres on water vapor permeability of composite film [94].

The content of a silica sphere is crucial in the influence of water vapour transmutability of the composite film. The influence of the amount of silica (spheres) on water vapour transmission of composite membrane. This increases



along with increases of the content the silica (spheres), when the fewer than 2.0 wt%, because introducing silica ((hollow spheres) increases the volume (free) in composite membrane and interfacial regions between polymer chains and silica (hollow spheres). Consequently, water vapour transmission of the composite membrane was improved. Yet, the contents of silica (hollow spheres) were greater than 2 (wt%), the water vapour transmission of the composite film was marginally lower. Agglomerating silica (hollow spheres) is the main reason for the result. Because of high specific energy (surface).

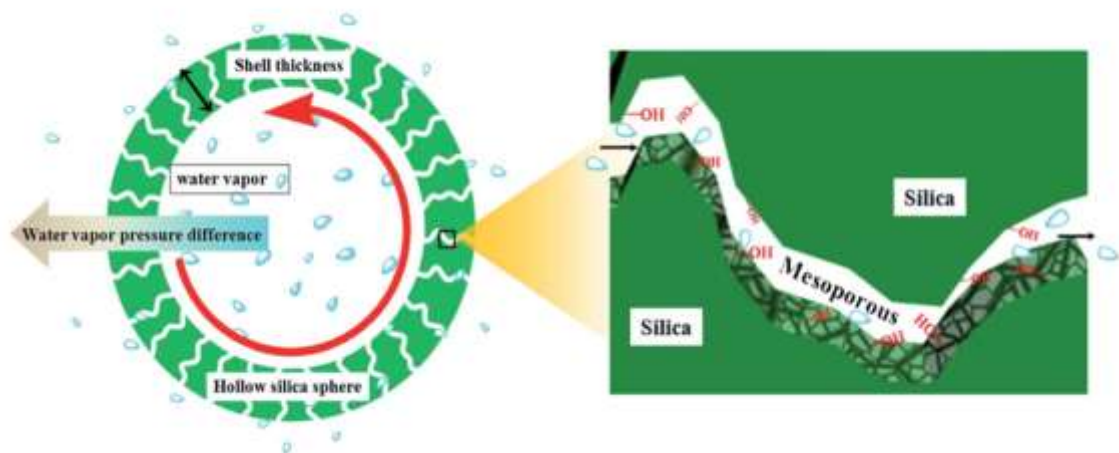


**Figure 2.10.** The schematic illustration of water vapor molecules transporting through hollow silica spheres [94].

The volume (free) is the required condition for the water vapour transmission of the composite film. Introducing the silica (hollow spheres) increases the volume (free) in the composite film. The illustrations (schematic) of a water vapor molecule transported through the silica spheres. Because of the numerous hydroxyl groups and mesoporous in the shells of silica (hollow spheres), water vapour molecules can transport into the hollow core through the shell. When the

amount of water vapour (molecules) in the silica core is big enough. The cores (hollow) of the silica spheres (hollow) acts as the shortcut and storage station for water vapour molecules to improve the water vapour transmission of the composite film [94].

### **2.3.2. Limitations of existing composite for permeable membrane**

Current polyurethane composite film cannot fulfil the requirements of high permeability, and other properties such as tensile strength, thermo-mechanical properties, thermo-moisture responsiveness. Yan B. et al., produced polyacrylate film composite with silica aerogel in order to get high permeability, reported that water vapor permeability of polymer composite depends on different things like shell thickness, percentage of silica aerogel, temperature, humidity, but the permeability they have reported in their paper is not satisfactory and the mechanical property. Thus, to fulfil such requirements of permeability and mechanical property we have proposed polyurethane composite, which can be re-enforced the polyurethane and enhance the water vapor transmitting ability, can be applied for the propose of thermo-regulating textile.

## **2.4. Porous polymeric materials**

Synthesis, utilization and design of advanced polymeric material with a porous architecture in the microscale range is always an important thing in many scientific fields [95]. Versatile application can be proposed for Porous polymeric material including, filtration, tissue scaffolds, permeable membrane, laminated/coated on textile surface and so on [96]. There are several methods to

fabricate porous polymeric film, mostly used process are leaching of particles, thermal induced melt moulding, phase separation, emulsion freeze drying, gas foaming, etc [97]. The micro-structure and properties of 3D polymeric scaffolds are of diverse importance for their application in different filed. The morphology and the property of the resultant porous film largely depends on the manufacturing process of those scaffolds.

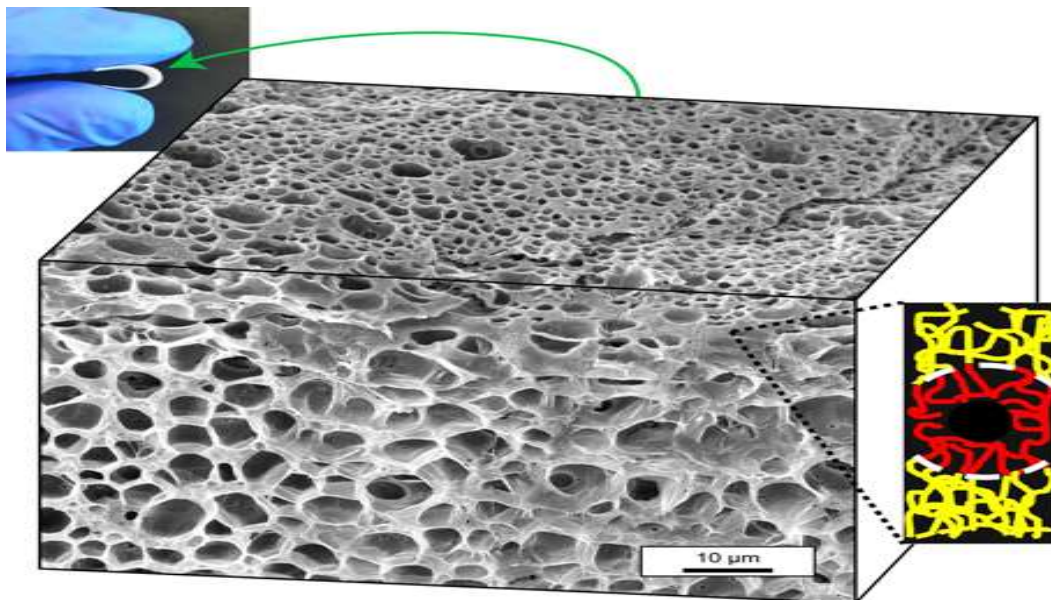


**Figure 2.11.** Pliable scaffolds with structural hierarchy can be synthesized using long-chain block copolymers [98].

**Table 2.1.** Techniques and systems used to fabricate porosity. [97]

Technique	No.	PU system	Solvent	PU concentration [%]	Porosity [%]	Pore size [ $\mu\text{m}$ ]
SC/PL	1	Zytar® Z1A1 (thermoplastic polyether-urethane)	DMF/THF	15	>91	~250
	2	PCL/HMDI/EG	1-Methylo-2-pyrrolidone	20	>70	100-400
	3	PCL/HMDI/isosorbide diol	DMF	-	90	200 $\pm$ 16
TIPS	4	PHB-PCL/TMDI	1,4-Dioxane	5	-	100-150
	5	PCL-PEG/BDI/Putrescyna	DMSO	10	94	76-387
	6	PCL/BDI/BDO	DMSO	10	>80	36-203
TIPS/PL	7	PCL/BDI/BDO	1,4-Dioxane	17	-	150-300
	8	PCL/BDI/BDO	DMSO	35	80	Different
	9	PCL/HDI/isosorbide diol	DMF/THF	9,5	90	200 $\pm$ 45
	10	Poly(ethylene adipate) diol/IPDI/hexamethylene diamine	-	-	87	50-400
Freeze-drying	11	PCL/BDI	1,4-Dioxane/water	-	>80%	150-300
	12	PCL-PEG/IPDI/BDO/L-lysine	Water	16	-	10-172
	13	PCL-PEBA-PLA/IPDI	-	5	97%	-
Melt moulding	14	Texin (thermoplastic polyether-urethane)	-	-	64	30-450
	15	PCL-PEG/HDI/benzoic acid	-	-	88	153 $\pm$ 70
Gas foaming	16	PEG-PPG/TDI	-	-	85	300-800
	17	POP/TDI	-	-	-	95 $\pm$ 40
	18	PCL-PEG/HMDI	-	-	>75	50-2000

### 2.4.1. Particulate leaching

A number of methods are used for fabricating the porous polymeric film, particulate leaching is one of the widely used technique. Particulate leaching/solvent casting can be characterised by its easy operation and properly controlling the pore size by choosing the amount and size of salt Particle. The salt particle dispersion is always not uniform and perfect in the solution of polymer, the viscosity of the solution of the polymer, and the solid salt particle differ and the range of contact between the polymer solutions and the salt particles are not well controlled [99,100]. The advantage of this process is the simple to fabricate without any specialized equipment. Salt particles are widely used for Particulate leaching/solvent casting method but the sugar, sucrose, ammonium chloride, starch particles and gelatin, microspheres paraffin can be used [102,103]. There are many factors to be considered during this method including, the size of the particulate, amount, distribution and so no. If the

quantity of added salt is too high, an inadequate structure of polymer will form with lots of void due to close geometric packing [103]. The mechanical property of the scaffolds mostly depends on pore size; the effect of pore size should also be into count [104].

The disadvantage of this process is, it's difficult to choose adequate amount particle required for high porosity and the main disadvantage of this method is time consuming process, it needs 2-3 days to leach out the particle [99], which cannot be accepted for industrial purpose. To avoid this time consuming process, we have proposed water soluble silicone for making porous scaffold.

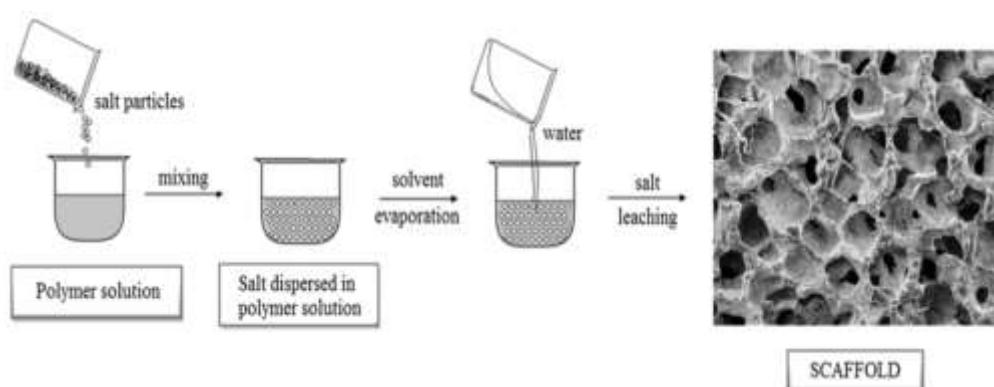


**Figure 2.12.** Scaffold preparation using solvent casting combined with the salt leaching technique [97].

### **2.4.2. Thermally-induced phase separation (TIPS)**

The Royal Society of Chemistry states that “A method for preparing a polymer membrane by mixing the polymer with a substance that acts as a solvent a high temperature and casting the solution into a film. When the solution is cooled, solidification occurs”.

Among the different porous film fabricating methods, TIPS is the more flexible methods among all other method for producing porous polymeric film and is widely utilised for its ability in producing highly porous and interconnected scaffolds. In this technique, de-mixing happened of a homogeneous solution (polymer) by change in induced temperature, thus fabricate multi-phase systems. While the mixing of the polymer solution happens, the polymer solution (homogeneous) starts to separate into the polymer-rich phase and the polymer poor phase. Rich phase of polymer solidifies, when the poor phase of polymers crystalline, when the formed of the crystals has been removed, then it's a leaving highly porous polymeric structure. this kind of de-mixing can be solid-liquid (normally for binary polymer-solvent mixtures) or liquid-liquid (normally for ternary polymer/non-solvent mixtures/solvent) [105-107].

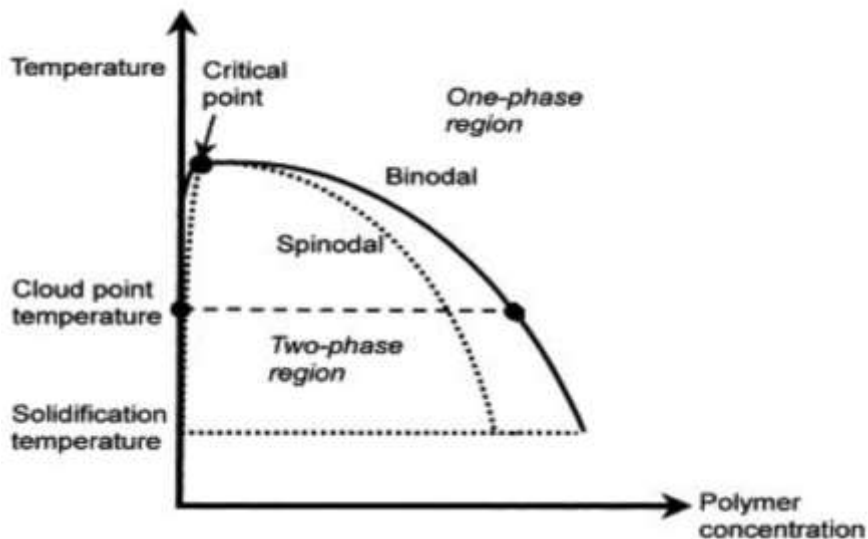


**Figure 2.13.** Phase diagram of a ternary system polymer-solvent- non/solvent [105].

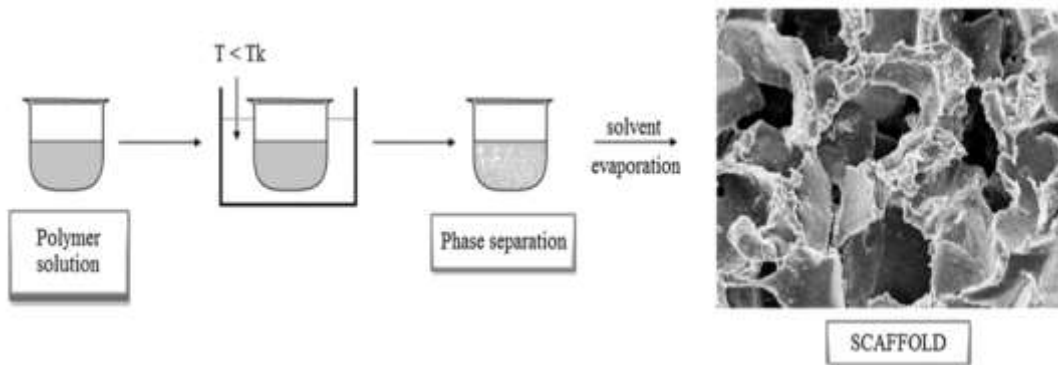


**Figure 2.14.** Scaffold preparation using thermally induced phase separation technique [97].

The obtained scaffold structure is mainly dependent on the concentrations of polymer solution, the adequate rate and temperature [108]. The rate and temperature also affect the process of solvent crystallization. On the other hand, it's also possible that the pore shape can be controlled by modifying the TIPS method. The disadvantage of this process is the toxicity of the solvents used during film fabrication. Because of this environmental concerns, many researchers are trying to replace this toxic solvent by using environmental friendly solvent [109].

### 2.4.3. Gas foaming

Polymer gas foaming is a widely used process in the industry for preparing a porous scaffold. Gas-foaming can be fabricated by releasing the gas or reacting the components which are ingredients of the gas-foaming agent's thermal degradation. The fabrication of polyurethane foams is one of the examples. Water, added to polymer solution mixture, which reacts with the isocyanate group to form a derivative of the carbamic acid, can be transformed into the carbon dioxide later decarboxylation. Fabrication process is commonly applied

for the preparation of porous scaffolds. On the other hand, it is difficult to control the pore area and average of pore area is too big [111,112]. However, the scaffolds of polymer formed by this process are used for different purposes like - bone regeneration, permeably membrane and so on [113,114]. In addition, there is a process of foaming polymer, which is the introduction of gas to the polymer solution. The solution of polymer is produce at very high pressure to gases like- fluoform, nitrogen, and carbon dioxide [115,116].

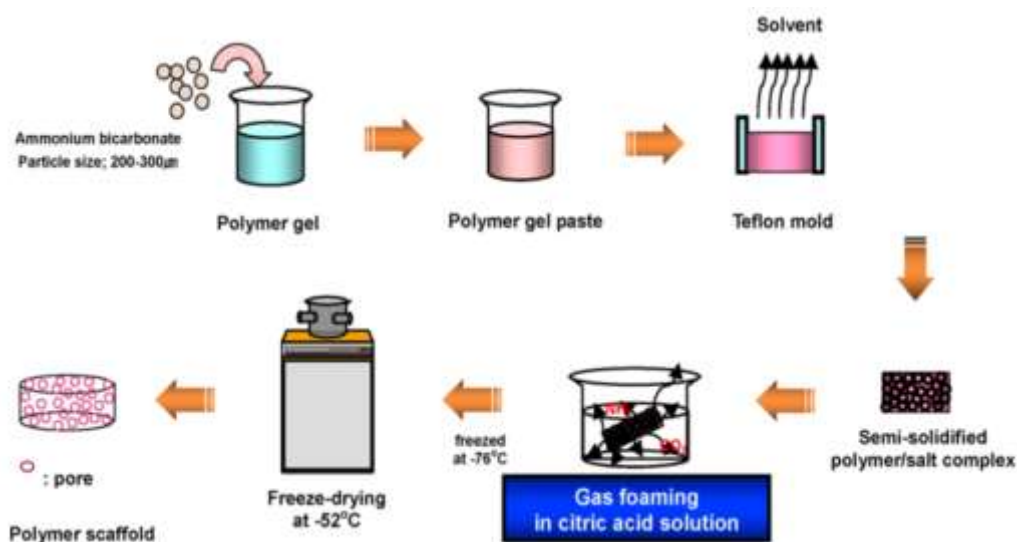


**Figure 2.15.** Schematic representation of polymeric scaffolds prepared by gas foaming/salt leaching method [110].

Uses of the organic solvents are unnecessary for gas foaming process, which is the biggest advantage of this process. The difficulty of the control of pore size is the main disadvantage of this method and pore interconnections. The large and closed pores of it can be produced into the structure of polymers, while the process of gas-foaming [117].



#### **2.4.4. Emulsion freeze-drying**

The Emulsion freeze-drying is the process to make porous scaffold within a pore size from 20-200  $\mu\text{m}$ . This process required the emulsion prepared by homogenisation of two phases which is immiscible. From the obtained scaffold structure by the freeze-drying of emulsions, two different categories of the pores can be achieved, macro and micro pores. by removing the liquid solvent micro pores are created, while macro pores are created by coming together of micro pores during process of homogenisation [119] The viscosity and concentration of the polymer solutions affects porosity and pore size, and the quantity of liquid phase dispersal in the process. The volume and amount of the liquid phase into the solution can effects of the size of the pore; the decrease of water amount, the average pore size will be decreased [120]. Constant rate of cooling technique can produce more uniform porous scaffolds. The technique of emulsion freeze-drying is widely applied for the creation of the scaffolds of soft tissue [122,123]. The main benefits of this process are the minimize the toxic solvent used and elimination drying time and leach out processes. The instability of solution of this process is the biggest problem, which appears to the fabrication of scaffolds process, and it needed the addition of suitable surfactants [121], WBPU (waterborne polyurethane) can be option for solving this issue [124].

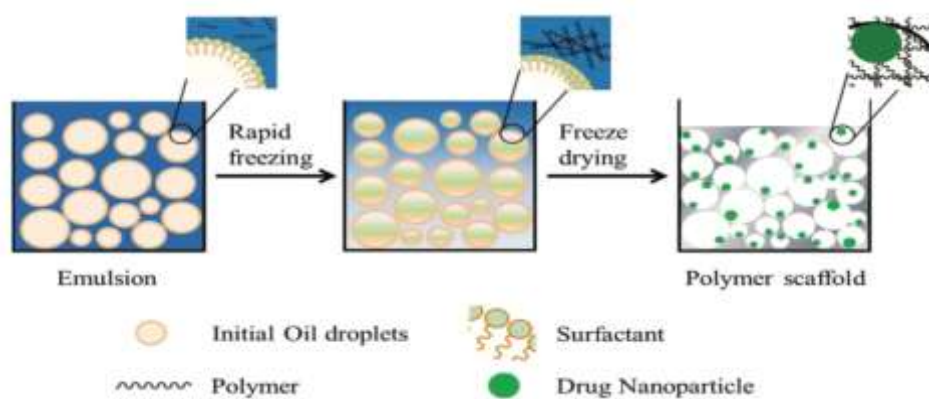


**Figure 2.16.** Schematic representation of the emulsion freeze drying process

[128].

### **2.4.5. Limitations of current porous membrane fabrication method**

Several methods are used for fabricating the porous polymeric films, such as particulate leaching, TIPS, Emulsion freeze-drying, and gas foaming, and so on. Particulate leaching is one of the widely used techniques. The particulate leaching/solvent casting can be characterized by its easy operation and proper control of size of pore by choosing the amount and size of salt Particle. The salt particle dispersion is always not uniform and perfect in the solution of polymer, the viscosity of the solid salt particle and the polymer solution are different, and the range of contact of the polymer solution and the particles (salt) is not well controlled. The advantage of this process is the simple to fabricate without any specialized equipment. Salt particles are widely used for Particulate leaching/solvent casting method but the sugar, sucrose, ammonium chloride, starch particles and gelatin, microspheres paraffin can be used. There are many factors to be considered during this method including, the size of the particulate, amount, distribution and so no. The mechanical property of the scaffolds mostly

depends on pore size; the effect of pore size should also be into count. The main disadvantage of this process is the leaching out time, normally for salt particle it needs 2-3 days to leach out the particle [99], which cannot be accepted for industrial purpose. To avoid this time consuming process, I have proposed a quick water soluble silica particle for making the porous scaffold, which is quick water soluble compare to salt particle leaching technique.

## **2.5. Liquid crystal elastomers.**

The first reported two ways shape memory polymers are LCEs, this turn LCs units into the network of polymeric crosslinking. Their reversible strain and soft elasticity actuation makes an LCE an excellent actuator and artificial muscle. Two-way shape-memory effects are integral to LCEs and stem from their polymer-chain (anisotropic). Crossing the transition (clearing) from the LCs phase into the rubber phase (isotropic), each polymer chain will randomly contract from the prolate to the spherical configuration. Opposite happens when cooling. Regarding LCEs (monodomain), the microscopic deformation accumulates into the macroscopic one into the direction of the LC director. In comparison with a two-way SMA, LCEs can be bigger recoverable strains, up to 300%. In 2001, as a result of the hydrosilation reaction in between poly(methyl-hydrogensiloxane), and vinyl functionalised LC mesogen, and the cross-linker, a type of mono-domain nematic LCEs has been prepared by the Finkelmann's group. Using a small preloading stress (6kPa), the recoverable strain (as high as 300%) was seen in the nematic LCE isotropic transition (TNI). Additionally,

over 90 percentage of the entire strain quickly come back in a short temperature range of  $0.95 < T_{red} < 1$ , (where,  $T_{red}$  is defined as the  $T/TNI$ ). These rapid transitions, the amount of shape change (recovery/deformation) are determined mainly by the thermal conductivity. Regarding thin samples, Responses rate of the nematic LCEs matches that of the natural muscles [129,130].

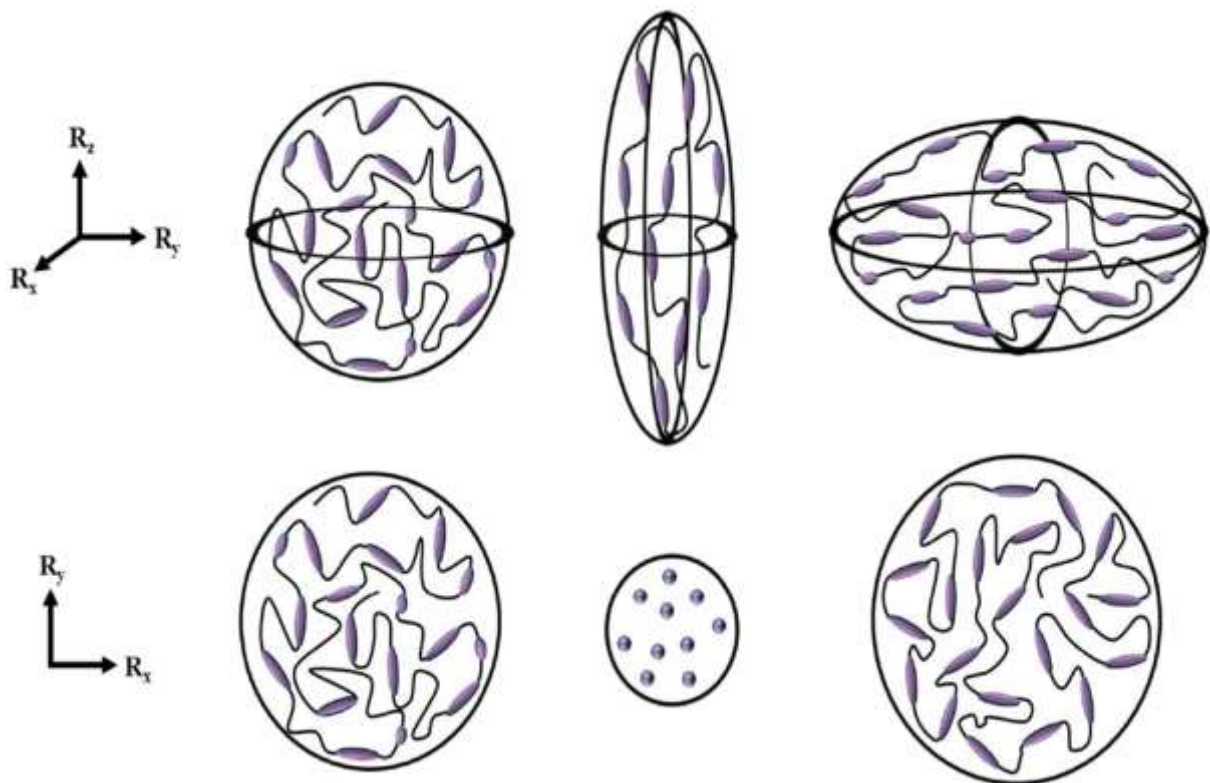


**Figure 2.17.** Global polymer chain conformations for main-chain LCEs [130].

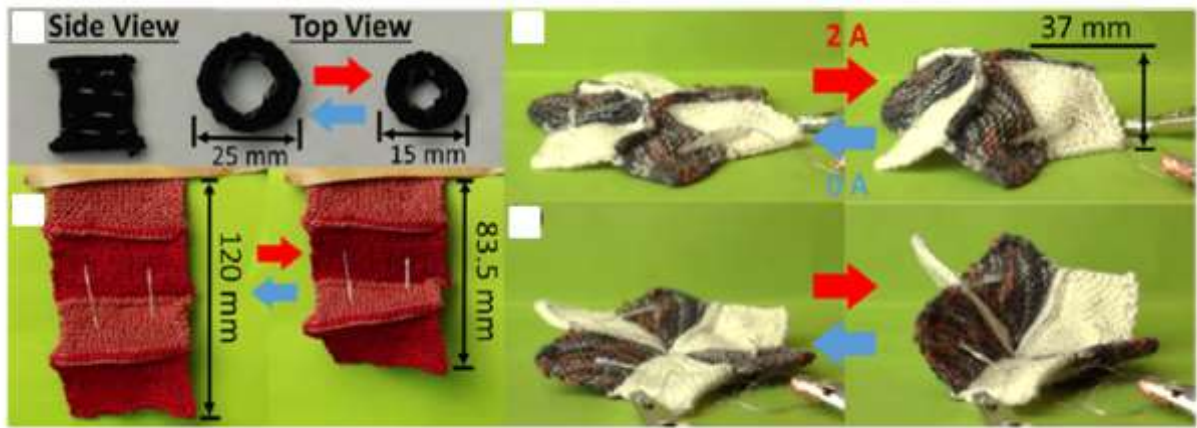


**Figure 2.18.** Knit textile achieving effective diameter shrinkage upon heating [131].

## 2.6. Laminated/coated and responsive textiles

In a material comprised of at least two layers and the one of them is the textile, closely connected by an additional adhesive of at least one component layer. Special types of fabric are produced by the attachment of more than one fabric layer. Naturally, laminated fabrics can be produced by the application of a fabric coating, where a fabric is coated with a continuous polymeric layer. A cost-effective and innovative personal thermal management technique by using self-adaptive, responsive SMP materials with tuneable thermal resistance, together with integrated thermoelectric (TE), the modules for active on-demand cooling and heating. Comfort with minimal power consumption and at least 4°F offset in HVAC set point in either direction causes over 15% in energy savings in the HVAC systems of buildings and a 2% saving in domestic energy usage and GHG emissions if widely implemented [133].

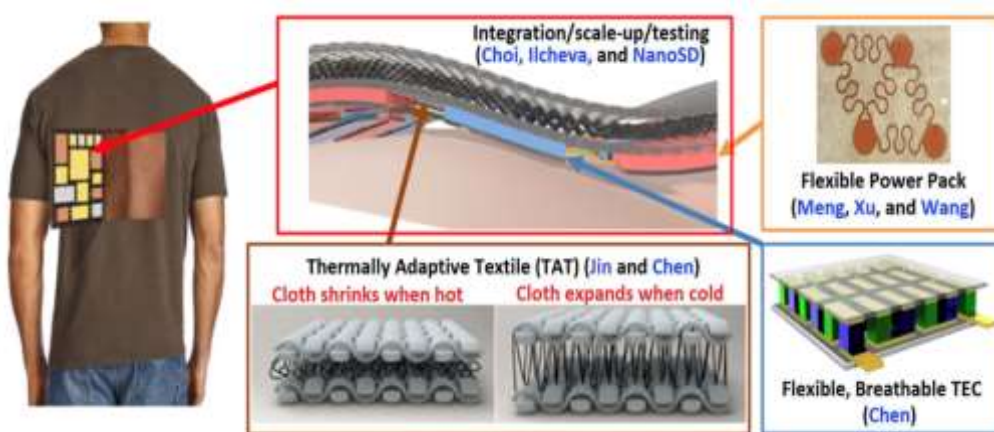


**Figure 2.19.** Personnel thermal management strategy by utilizing self- adaptive, temperature or humidity-responsive shape-memory material [132].

Climate change and energy consumption and are two of the biggest issues facing humans this century. The high energy consumption leads to excessive emissions of greenhouse gases, which majorly disturbs balance of the climate and leads to extreme weather as a result of global warming [134,135]. Therefore, many efforts are used for developing renewable energies such as ocean, wind, solar, carbon-neutral, and hydrogen fuels [136-138]. Conversely, reductions in current consumption of energy and improvements in efficiency rate energy are just as crucial. Yi Cui stated that nanoPE is a very good IR-transparent can be used for textile for cooling the human body. Nano porous polyethylene has interconnected porous structures which are normally 50-1000 nm (diameter). The size of the pores lengths are comparable with visible light wavelengths (400-700 nm), which scatters visible light, and that makes PE impervious to the human eye. Additionally, the pore size is much normally smaller comparing with IR wavelengths, this nanoPE membrane remains with a high transparency to the IR. Every feature, including fibres and pores, are scaled uniformly, however the

entire thickness remains fixed. Weighted-average the IR transmittance depends on human body IR begins at pore sizes of 1.2 (mm) and reaches up to minimum at 2.4 (mm). For nanoPE (thicker), the amount of nanoPE along with the light way shows an increase; therefore the transmittance variation is greater. Dimensions of fibres also control scattering properties; therefore, fixed the dimensions of the pore and conducted an investigation into fibre size effects. The transmittance dips also occurred, yet the magnitude is small because of low air-pore filling ratios. The nanoPE is available commercially and used widely in the lithium-ion batteries (as a separator) for preventing the electrical shorting among cathodes and anodes [138].

Endothermy has a crucial role in the maintenance of proper human functioning. This balance is achieved by thermoregulation measures, like metabolic rate, perspiration, blood circulation, shivering, etc [139]. Failing to maintain a core temperature (Human body) can cause a severe medical emergency. Today, even though medical needs are not as frequent, thermal comfort still affects health, economy and the productivity [140]. Thermal comfort (Indoor) is reached by the air conditioning the rooms or buildings; however it uses a lot of the energy. The USA, 12% of all energy used is for controlling the temperature indoors [141-143]. Without the air conditioning, the clothes are the only means by which to control the human body temperatures. Yet common clothes are restricted in their insulation (thermal), often failing to match up the changes in the weather. The large and sudden temperature (diurnal) variations can cause cardiac disease and respiratory infections [140-142]. Such issues require newer and better route to

manage the human body temperatures. Particularly, textile-based cooling management has a good chance as it normally focuses the temperature control nearer human body rather than the whole building [140-144].

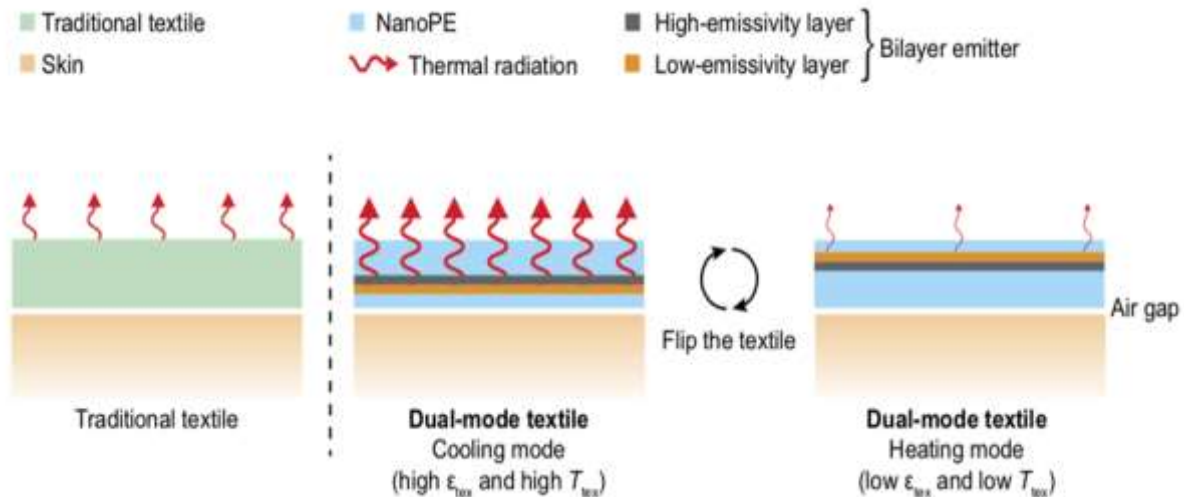


**Figure 2.20.** Schematic of dual-mode textile [140].

When body temperatures are lower, fabrics are less transmittable and maintain heat (body). When sweating, it permits water vapour to escape as moisture permeability is higher with increases in body temperatures. This releases heat from clothing. Because the fabric is rain resistant, the apparel is manufactured with coated/laminated SMP fabric and can be worn irrespective of weather. The application of shape memory polyurethane in textile including the followings, Protective Clothing (Thermal), Sportswear, Underwear, Leisurewear, Gloves, Outerwear, Socks, smart fabric and fibres (shape memory).

Temperature dependency of water vapour permeability is vital when considering the use of smart materials. The shape memory effect can be used on areas such as



smart fabrics that can control moisture permeability. The fabrics laminated or coated with SMPU can have higher water vapour transmission at a higher temperature and the low water vapor transmission at the lower temperature. This flexible barrier functions means the clothes can adjust their insulating property according to temperature fluctuations, ensuring good thermal management property and an increase in comfort. Thus, when shape memory polyurethane is activated in clothing, it provides greater versatility in protecting against extreme cold or heat. For clothing applications, the temperatures (reversible) for the effect of shape memory to be triggered should be closer to the body temperature.

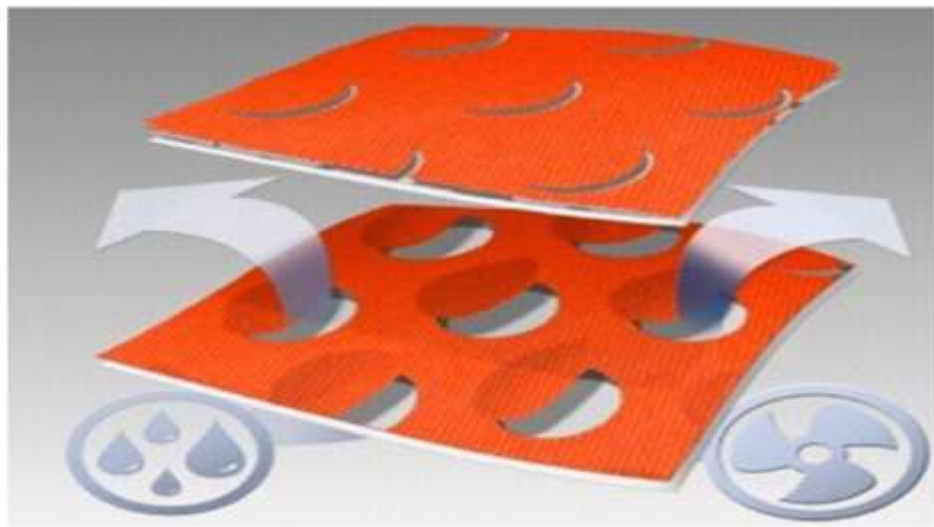


**Figure 2.21.** Back of a Nike ‘Sphere React Shirt’ with a smart vent structure

Ordinary SMPs can hold a temporary shape change and recover to their original shapes when properly stimulated. Over the past ten years, researchers have exerted great efforts towards achieving more controllable, complicated, stepwise and two-way SMEs. The smart moving is because of the environmental signals

and fundamental to the smart materials whereby they will not need an added the complex feedback (electrical) system. Much information exists about shape memory polymers, although these polymers are suggested for many different uses, their textile applications are limited because the reversible temperatures of the shape memory effect to be controlled is higher compare with the body temperature. Polyurethane-based shape memory polymers with broad variety of glass transition temperatures have drawn extensive interest in the textile field. The study of SMPU remains limited. Their shape memory mechanism, the relationship between effect and structure, particularly their applications towards garments and textiles still has high potential.

A number of limitations of in responsive polymer exist, for instance low strength (mechanical), permeability and the stress of recovery (low), these have been present since the 1st responsive polymer was invented, and a solution remains elusive. Through discussion of the problems faced by various responsive polymers, we intend that this review will inspire a solution.

## **2.7. Summery**

The high use of the energy directly/indirectly leads to the excessive emissions of the greenhouse gas, which cause extreme weather and global warming. Day by day, the global; temperature is increasing due to climate change, it's not an efficient way to solve global warming problem by using indoor or outdoor cooling because the use of energy is not sustainable way. To reduce the energy consumptions in space cooling and heating, thermo-regulating textile would play

a vital role. Current polyurethane composite film cannot fulfil the requirements of high permeability (water vapour and air), and other properties such as tensile strength and thermo-mechanical properties. Thus, to fulfil such requirements of permeability (water vapour and air) and mechanical property we have proposed polyurethane composite film, which can be used to make thermo-regulating textile.

Particulate leaching is the mostly used technique to make porous film due to easy processing; Salt particles are widely used for particulate leaching technique. There are many factors to be considered during this method including, the size of the particulate, amount, distribution and so no. The main disadvantage of this process is the leaching out time, normally for salt particle it needs 2-3 days to leach out the particle [125], which cannot be accepted for industrial purpose. To avoid this time consuming process, I proposed a quick water soluble silica particle for making the porous polymeric film, which is quick water soluble compare to salt particle leaching technique. The resulted membrane is highly water vapor permeable and water droplet resistant, this kind of films can be applied to make functional textile. Liquid crystal elastomers is a temperature sensitive materials, this can used to make temperature responsive textile. There is not much work has been done to make textile. In this study we used low temperature liquid crystal elastomers to make body temperature responsive textiles.

## Reference

1. Yang, Z., et al., The study of crosslinked shape memory polyurethanes. *Mater. Chem. and phy.*, 2006. 98: p. 368–372.
2. Qian, W., and jinlian H., Waterborne polyurethane based thermoelectric composites and their application potential in wearable thermoelectric textiles. *Com. Part B*, 2016. 107: p. 59-66.
3. Jinlian, H., et al., Quick water-responsive shape memory hybrids with cellulose nanofibers. *J. of polym. Sci. part a: polym. Chem.*, 2017. 55: p. 767-775.
4. Martien, A., et al., Emerging applications of stimuli-responsive polymer materials. *Nat.mater.*, 2010. 9: p. 543.
5. Simona, M., et al., Stimuli-responsive nano carriers for drug delivery. *Nat. mater.* 2013. 12: p. 654.
6. Harper, M. and Jinlian H., A brief review of stimulus-active polymers responsive to thermal, light, magnetic, electric, and water/solvent stimuli. *J. of intel. Mater. Sys. and struct.*, 2010. 21: p. 673.
7. Qinghao, M. and jinlian H., A review of shape memory polymer composites and blends. *Com.: part a*, 2009. 40: p. 1661–1672.
8. Jinlian, H., et al., Self-adaptive water vapor permeability and its hydrogen bonding switches of bio-inspired polymer thin films. *Mater. Chem. Front.*, 2017. 1: p. 2027.
9. Jinlian, H., et al., Recent advances in shape–memory polymers: structure, mechanism, functionality, modelling and applications. *Prog. in polym. Sci.*, 2012. 37: p.1720– 1763.
10. Senaratne, W., et al., Self-assembled monolayers and polymer brushes in biotechnology: Current applications and future perspectives. *Bio macro. mole.*, 2005. 6: p. 2427–2448.
11. Jhaveri, S. J., et al. Release of nerve growth factor from HEMA hydrogel- coated substrates and its effect on the differentiation of neural cells. *Bio macro mole.*, 2009. 10: p. 174–183.
12. Ho, M., origins and evolution of “controlled” drug delivery systems. *J. of Cont. Rel.*, 2008. 132: p. 153–163.
13. Bayer, C. L. and Peppas, N. A., Advances in recognitive, conductive and responsive delivery systems. *J. of Cont. Rel.*, 2008. 132: p. 216–221.
14. Mendes, P. M., Stimuli-responsive surfaces for bio-applications. *Chem. Soc. Rev.*, 2008. 37: p. 2512–2529.
15. Luzinov, I., et al., Responsive brush layers: from tailored gradients to reversibly assembled nanoparticles. *So. Matter*, 2008. 4: p. 714–725.
16. Menglian, w., et al., Stimuli-responsive polymers and their applications. *Polym. Chem.*, 2017, 8: p.127.
17. Harper, M. et al., Various shape memory effects of stimuli-responsive shape memory polymers. *Smart mater. and struct.*, 2013. 22: p. 23.
18. Wirpsza, Z., in: *Polyurethanes: Chemistry, Technology and Applications*. Ellis Horwood, New York, NY, 1993, p.11.

19. Wirpsza, Z., in: *Polyurethanes: Chemistry, Technology and Applications*. Ellis Horwood, New York, NY, 1993, p. 95.
20. Dieterich, D., et al., in: *Polyurethane Handbook*, G. Oertel (Ed.). Hanser, New York, NY, 1985, p. 6.
21. Lamba, N. M. K., et al., in: *Polyurethanes in Biomedical Applications*. CRC Press, Boca Raton, FL, 1998, p. 43.
22. Runumi, G., et al., Effect of soft segment chain length on tailoring the properties of isocyanate terminated polyurethane prepolymer, a base material for polyurethane bandage. *Inter. J. of rese. in engi. and techno.*, 2013. 02: p.10.
23. Xiao-dong, C., et al., Preparation and properties of cast polyurethane elastomers with molecularly uniform hard segments based on 2,4-toluene diisocyanate and 3,5-dimethylthioltoluenediamine. *J. of Biom. Sci. and Engi.*, 2009, 2: p. 245-253.
24. Mondal, S. and Jinlian H., Segmented shape memory polyurethane and its water vapor transport properties. *Desi. Mono. and Polym.*, 2006. 9(6): p. 527–550.
25. Mondal, S., The Hong Kong Polytechnic University, Hong Kong, Doctorate thesis, 2006.
26. Chu, B., et al., Microphase separation kinetics in segment polyurethanes: effects of soft segment length and structure. *Macro mole.*, 1992. 25: p. 5724-5729.
27. Hu, W. and Koberstein J.T., The effect of thermal annealing on the thermal properties and molecular weight of a segmented polyurethane copolymer. *J. Polym. Sci. Part B: Polym. Phy.*, 1994. 32: p. 437.
28. Takahashi, T., et al., Structure and properties of shape-memory polyurethane block copolymers. *J. of App. Polym. Sci.*, 1996. 60: p. 1061.
29. Leibler, L., Theory of Microphase Separation in Block Copolymers. *Macro mole.*, 1980. 13: p. 1602.
30. Dai, L., Phase separation of polyisoprene-polyacetylene copolymers. *Syn. Met.*, 1997. 84: p. 957.
31. Altena, F. W. and Smolders C. A., Calculation of liquid-liquid phase separation in a ternary system of a polymer in a mixture of a solvent and a nonsolvent. *Macro mole.*, 1982. 15: p. 1491.
32. Alig, I., et al., Curing kinetics of phase separating thermosets studied by DSC, TMDSC and dielectric relaxation spectroscopy. *Thermochimica Acta*, 1999. 330: p. 167-174.
33. Velankar, S. and Cooper, S. L., Microphase Separation and Rheological Properties of Polyurethane Melts. 2. Effect of Block Incompatibility on the Microstructure. *Macromolecule*, 2000. 33: p. 382-394.
34. <http://www.rsc.org/Education/Teachers/Resources/Inspirational/resources/4.3.1.pdf>.
35. Avila, A.F., et al., A dual analysis for recycled particulate composites: linking micro- and macro-mechanics. *Mater. Charac.*, 2003. 50: p. 281–291.
36. Nicoleta, I. and Hickel, H., Evaluation of the mechanical properties of dental adhesives and glass-ionomer cements. *Dent. Mater.*, 2009. 25: p. 810–819.

37. Bunsell, A.R. and Harris, B., Hybrid carbon and glass fibre composites. *Composites*, 1974. 5: p. 157-164.
38. Shaw, A., et al., A critical reliability evaluation of fibre reinforced composite materials based on probabilistic micro and macro-mechanical analysis. *Compo. Part B: Eng.*, 2010. 41: p. 446–453.
39. Josmin, P. J., et al., Advances in Polymer Composites: Macro- and Micro-Composites State of the Art, New Challenges, and Opportunities. *Polym. Comp.*, 2012. Chapter 1.
40. Harper, M. and Jinlian H., A brief review of stimulus-active polymers responsive to thermal, light, magnetic, electric, and water/solvent stimuli. *J. of intel. Mater. Syst. and struc.*, 2010. 21: p. 859-885.
41. Lee, K.P., et al., A review of reverse osmosis mem- brane materials for desalination— development to date and future potential. *J. of Mem. Sci.*, 2011. 370: p. 1–22.
42. Shannon, M.A., et al., Science and technology for water purification in the coming decades. *Nature*, 2008. 10: p- 452.
43. Humplik, T, et al., Nanostructured materials for water desalination. *Nanotechnology*, 2011. 22: p.292001/1–292001.
44. Burn, S, et al., Desalination techniques—a review of the opportunities for desalination in agriculture. *Desalination*, 2015. 364: p. 2–16.
45. Paul, D. R., and Ski Yampol, Y. P., *Polymeric Gas Separation Membranes (1<sup>st</sup> Edition)*. 1994, p. 1–640.
46. Khulbe, K. C., et al., Synthetic polymeric membranes. *Synth. Polym. Membr. Charact. At. Force Microsc.*, 2008.
47. Khosravi, A., et al., Polyurethane-silica nanocomposite membranes for separation of propane/methane and ethane/methane. *Ind. Eng. Chem. Res.*, 2014. 53: p. 2011–2021.
48. Kim, S., Lee, Y. M., High performance polymer membranes for CO<sub>2</sub> separation, *Curr. Opin. Chem. Eng.*, 2013, 2: p. 238–244.
49. Hassanajili, S., et al., Mixed matrix membranes based on polyether urethane and polyester urethane containing silica nanoparticles for separation of CO<sub>2</sub>/CH<sub>4</sub> gases. *Sep. Purif. Technology*, 2013. 116: p. 1–12.
50. Ho, B. P., et al., Gas separation properties of polysiloxane/poly- ether mixed soft segment urethane urea membranes. *J. of Mem. Sci.*, 2002. 204: p.257–269.
51. Karimi, M. B., et al., Vegetable oil-based polyurethane membrane for gas separation. *J. Mem. Sci.*, 2016. 527: p. 198-206.
52. Qian, W., and jinlian H.. Waterborne polyurethane based thermoelectric composites and their application potential in wearable thermoelectric textiles. *Com. part B*, 2016. 107: p. 59-66.
53. Ciobanu, G., et al., Mixed-matrix membranes based on polyurethane containing nanohydroxyapatite and its potential applications. *J. of Appl. Polym. Sci.*, 2015. p. 41813.

54. Cong, H., et al., Polymer-inorganic nanocomposite membranes for gas separation. *Sep. Purif. Technology*, 2007. 55: p. 281–291.
55. Herrera-Alonso, J. M., et al., Transport properties in polyurethane/clay nanocomposites as barrier materials: effect of processing conditions. *J. of Mem. Sci.*, 2009. 337: p. 208–214.
56. Sadeghi, M., et al., Enhancement of the gas separation properties of polybenzimidazole (PBI) membrane by incorporation of silica nano particles. *J. of Mem. Sci.*, 2009. 331: p. 21–30.
57. Wang, R., et al., The fabrication and tribological behaviour of epoxy composites modified by the three-dimensional polyurethane sponge reinforced with dopamine functionalized carbon nanotubes. *Appl. Surf. Sci.*, 2015.10: p. 222.
58. Du, S., et al., Tensile and flexural properties of graphene oxide coated-short glass fiber reinforced polyethersulfone composites. *Com. Part B*, 2016. 99: p. 407–415.
59. Zhang, Y., et al., A novel surface modification of carbon fiber for high-performance thermoplastic polyurethane composites. *Appl. Surf. Sci.*, 2016. 382: p. 144–154.
60. Fu, S., et al., Synergistic Effect on the Fracture Toughness of Hybrid Short Glass Fiber and Short Carbon Fiber Reinforced Polypropylene Composites. 2006. 323: p. 326–335.
61. Kootsookos, A., et al., Seawater durability of glass- and carbon-polymer composites. *Com. Sci. Technology*, 2004 64: p.1503–1511.
62. Zhang, Z., et al., Effect of carbon fibers surface treatment on tribological performance of polyurethane (PU) composite coating. *Wear*, 2008. 264: p. 599–605.
63. Luzinov, I., et al., Responsive brush layers: from tailored gradients to reversibly assembled nanoparticles. *So Matter*, 2008. 4: p. 714–725.
64. Cech, V., et al., The glass fiber – polymer matrix interface/interphase characterized by nanoscale imaging techniques, *Com. Sci. Technology*, 2013. 83: p. 22–26.
65. C.B.Y. Ftir-imaging, A.D.S.C. Techniques, To Study the Effect of Hygrothermal Ageing at the Interface of Glass/epoxy Micro-composites by FTIR-imaging and DSC Techniques, 2007.
66. Tsenoglou, C. J., Evaluation of interfacial relaxation due to water absorption in fiber-polymer composites. *Com. Sci. Technology*, 2006. 66: p.2855–2864.
67. Shalwan, A., et al., In State of Art: mechanical and tribological behaviour of polymeric composites based on natural fibres. *J. Materials*, 2012.
68. Park, J., et al., The change in mechanical and interfacial properties of GF and CF reinforced epoxy composites after aging in NaCl solution. *Compos. Sci. Technology*, 2015.
69. Almeida, J. H., Carbon fiber-reinforced epoxy filament-wound composite laminates exposed to hygrothermal conditioning. *J. of Mater. Sci.*, 2016. 51: p.4697-4708.
70. Tual, N., et al., Characterization of sea water ageing effects on mechanical properties of carbon/epoxy composites for tidal turbine blades. *Com. Part A*, 2015. 78: p.380–389.
71. Ionescu, M., Chemistry and technology of polyols for polyurethane (2<sup>nd</sup> edition), 2005. 1: p. 586.

72. Szycher, M., Szycher's Handbook of Polyurethanes (2<sup>nd</sup> edition). 2017. p. 269.
73. Chattopadhyay, D. K., et al., Influence of varying hard segments on the properties of chemically crosslinked moisture-cured polyurethane-urea. *J. Polym. Sci. Part B Polym. Physics*, 2006. 44: p. 102–118.
74. Velankar, S., et al., Microphase separation and rheological properties of polyurethane. *Macro mole.*, 2000. 33: p. 9181–9192.
75. Umair, B., et al., Preparation of an organic–inorganic polyurethane–Al<sub>2</sub>O<sub>3</sub> anion exchange fibrous composite and its application in the development of a membrane electrode for the determination of chromium(VI) in water. *RSC Adv.*, 2014. 4: p. 63831–63839.
76. Aleman, J. V., et al., Definitions of terms relating to the structure and processing of sols, gels, networks, and inorganic-organic hybrid materials (IUPAC Recommendations 2007)., 2009. 79 (10): p. 1801–1829.
77. "Guinness Records Names JPL's Aerogel World's Lightest Solid". NASA. Jet Propulsion Laboratory. 7 May 2002. Archived from the original on 25 May 2009.
78. Aegerter, M.A., et al., *Aerogels Handbook*. Springer publishing, 2011. ISBN 978-1-4419-7477-8.
79. Barron, R. F., and Gregory, F. N., *Cryogenic Heat Transfer* (2nd ed.). CRC Press. p. 682.
80. Kistler, S. S., Coherent expanded aerogels and jellies. *Nature*, 1931. 127: p. 741.
81. Kistler, S. S., Coherent Expanded-Aerogels. *J. of Phy. Chem.*, 1932. 36 (1): p. 52–64.
82. Pekala, R. W., Organic aerogels from the polycondensation of resorcinol with formaldehyde. *J. of Mater. Sci.*, 1989. 24 (9): p. 3221–3227.
83. Zahra, M. S., et al., The effect of the nano-structured aerogel powder on the structural parameters, water repellency, and water vapor/air permeability of a fibrous polyester material. *Mater. Chem. and Phy.*, 2016. 177: p. 99-111.
84. "What is Aerogel? Theory, properties and applications". 12 December 2013. [www.azom.com](http://www.azom.com).
85. Jones, R. G., et al., *Compendium of polymer terminology and nomenclature: IUPAC recommendations 2008*. RSC Publishing, Cambridge, UK, 2009. p. 1-443.
86. Groom, D.E. Abridged from atomic nuclear properties archived 27 February 2008 at the wayback machine. Particle Data Group: 2007.
87. "Ultra-light Aerogel Produced at a Zhejiang University Lab-Press Releases-Zhejiang University". [Zju.edu.cn](http://Zju.edu.cn). 19 March 2013.
88. Pierre A. C., et al., "Chemistry of aerogels and their applications". *Chem. Rev.*, 2002. 102: p. 4243–4265.
89. Gurav, J.L., et al., "Silica aerogel: synthesis and applications". *J. of Nanomater.*, 2010. p.1–11.



90. Lide, D. R., "Thermal conductivity" CRC Handbook of Chemistry and Physics (86th ed.), 2005. Section 12, p. 227.
91. Mecklenburg, M., "Aerographite: ultra lightweight, flexible nanowall, carbon microtube material with outstanding mechanical performance". *Advan. Mater.*, 2012. 24 (26): p. 3486–90.
92. Whitwam, R., Graphene aerogel is world's lightest material. The Wayback Machine. March 2013.
93. <https://www.zmescience.com/science/physics/graphene-lightest-material-26032013/>
94. Yan, B., et. Al., Effect of hollow silica spheres on water vapor permeability of polyacrylate film. *RSC Adv.*, 2015. 5: p. 11485–11493.
95. Liangxiao, T. and Bien T., Hypercrosslinked porous polymer materials: design, synthesis, and applications. *Chem. Soc. Rev.*, 2017. 46: p. 3322—3356.
96. Mu, X., et al., Porous polymeric materials by 3D printing of photocurable resin. *Mater. Hori.*, 2017. 4: p. 442--449.
97. Janik, H., and Marzec M., A review: Fabrication of porous polyurethane scaffolds. *Mater. Sci. and Eng. C*, 2015. 48: p. 586–591.
98. Hiroaki, S., et al., Hierarchical Porous Polymer Scaffolds from Block Copolymers. *Science*, 2013. 341: p. 10.
99. Dong, C. S., et al., Polyurethane (PU) scaffolds prepared by solvent casting/particulate leaching (SCPL) combined with centrifugation, 2010, 30: p. 78–85.
100. William, L. M., et al., Salt Fusion: An Approach to Improve Pore Interconnectivity within Tissue Engineering Scaffolds. *Tissue eng.*, 2002. 8(1): p. 43-52.
101. Draghi, L., et al., Microspheres leaching for scaffold porosity Control. *J. of Mater. Sci. Mater. in Med.*, 2005. 16: p. 1093– 1097.
102. Stephanie, G., et al., Polyurethane biomaterials for fabricating 3D porous scaffolds and supporting vascular cells. *J. of Biomed. Mater. Res. Part A*, 2006.82A: p. 802-809.
103. Zhang, J., et al., A comparative study of porous scaffolds with cubic and spherical macropores. *Polymer*, 2005. 46: p. 2979–2985.
104. Sin, C., et al., Polyurethane (PU) scaffolds prepared by solvent casting/particulate leaching (SCPL) combined with centrifugation, *Mater. Sci. Eng. C Mater. Biol. Appl.*, 2010. 30: p. 78–85.
105. Gioacchino, C., et al., A Versatile Technique to Produce Porous Polymeric Scaffolds: The Thermally Induced Phase Separation (TIPS) Method. *iMedPub J.*, 2017. 1: p. 2572-4657.
106. Heijkants, R. G. J. C., et al., Preparation of a polyurethane scaffold for tissue engineering made by a combination of salt leaching and freeze-drying of dioxane, *J. Mater. Sci.*, 2006. 41: p. 2423–2428.

107. Termonia, Y., Fundamentals of polymer coagulation, *J. of Polym. Sci. B Polym. Phys.*, 1995. 33: p. 279–288.
108. Rowlands, A. S., et al., Cooper-White, Polyurethane/poly (lactic-co- glycolic) acid composite scaffolds fabricated by thermally induced phase separation. *Biomaterials*, 2007. 28 (12): p. 2109–2121.
109. Jun, T. J., et al., Understanding the non-solvent induced phase separation (NIPS) effect during the fabrication of microporous PVDF membranes via thermally induced phase separation (TIPS). *J. of Mem. Sci.*, 2016. 514: p. 250–263.
110. Youn-Mook, L., et al., Preparation of porous poly(e-caprolactone) scaffolds by gas foaming process and in vitro/in vivo degradation behavior using g-ray irradiation. *J. of Ind. and Eng. Chem.*, 2008. 14: p. 436–441.
111. Marco, C. and Andrea B., Gas foaming technologies for 3D scaffold engineering. *Funct. 3D Tissue Eng. Scaffolds*, 2018.
112. Kim, H. J., et al., Gas foaming fabrication of porous bi-phasic calcium phosphate for bone regeneration. *Tissue Eng. Regen. Med.*, 2012. 9 (2): p. 63–68.
113. Gorna, K., and Gogolewski S., Preparation, degradation and calcification of biodegradable polyurethane foams for bone graft substitutes. *J. Biomed. Mater. Res.*, 2003. 67A: p. 813–827.
114. Kim, J., and Hollinger J. O., Recombinant human bone morphogenetic protein-2 released from polyurethane-based scaffolds promotes early osteogenic differentiation of human mesenchymal stem cells. *Biomed. Mater.*, 2012. 7: p. 045008.
115. Parks, K. L. and Beckman E. J., Generation of microcellular polyurethane foams via polymerization in carbon dioxide 2. Foam formation and characterization. *Polym. Eng. Sci.*, 1996. 36(19): p. 2417–2431.
116. Maio, E. D., et al., Structure optimization of polycaprolactone foams by using mixtures of CO<sub>2</sub> and N<sub>2</sub> as blowing agents. *Polym. Eng. Sci.*, 2005. 45 (3): p. 432–441.
117. Quirk, R. A., et al., Supercritical fluid technologies and tissue engineering scaffolds. *Solid State Mater.Sci.*, 2004. 8 (3–4): p. 313–321.
118. Ulrike, W., et al., Nano formulation and encapsulation approaches for poorly water-soluble drug nanoparticles. *Nanoscale*, 2016. 8: p. 1746–1769.
119. Grinberg, O., et al., Highly porous bioresorbable scaffolds with controlled release of bioactive agents for tissue-regeneration applications. *ActaBiomater*, 2010. 6 (4): p. 1278–1287.
120. Whang, et al., A novel method to fabricate bio-absorbable scaffolds. *Polymer*, 1995. 36 (4): p.837–842.
121. Spaans, C. J., et al., A new biomedical polyurethane with a high modulus based on 1, 4-butanediisocyanate and e-caprolactone. *J. of Mater. Sci. Mater. in Med.*, 1998. 9: p. 675–678.

122. Finoli, A., et al., Multiscale porous ceramic scaffolds for in vitro culturing of primary human cells. *Adv. Appl. Cera.*, 2012. 111: p. 262–268.
123. Jiang, X., et al., Fabrication and characterization of waterborne biodegradable polyurethanes 3-dimensional porous scaffolds for vascular tissue engineering. *J. of Bioma. Sci. Polym. Ed.*, 2010. 21: p. 1637–1652.
124. [https://arpaee.energy.gov/sites/default/files/10\\_UCSD%20Slides%20for%20PROGRAM%20REV-1-17-FINAL](https://arpaee.energy.gov/sites/default/files/10_UCSD%20Slides%20for%20PROGRAM%20REV-1-17-FINAL).
125. Oreskes, N., the Scientific Consensus on Climate Change. *Science*, 2004. 306: p. 1686.
126. Walther, G. R., et al., ecological response to recent climate change. *Nature*, 2002. 416: p. 389–395.
127. Chu, S., Majumdar A., Opportunities and challenges for a sustainable energy future. *Nature*, 2012. 488: p. 294–303.
128. Hu, J.L., et al., Recent advances in shape-memory polymers: Structure, bmechanism, functionality, modeling and applications. *Progress in Polyme.Sci.*, 2012. 37(12): p. 1720-1763.
129. Liu, C., H. Qin, and P.T. Mather, Review of progress in shape-memory polymers. *J. of Mater. Chem.*, 2007. 17(16): p. 1543-1558.
130. Sabina, W. Ula, Nicholas A. Traugutt, Ross H. Volpe, Ravi R. Patel, Kai Yu and Christopher M. Yakacki, Liquid crystal elastomers: an introduction and review of emerging technologies. *Liq. Crys. Rev.*, 2018, 6 (1): p. 78–107.
131. Devin, J. R., et al., Long Liquid Crystal Elastomer Fibers with Large Reversible Actuation Strains for Smart Textiles and Artificial Muscles *ACS Appl. Mater. Interfaces*, 2019. 11: p.19514–19521.
132. World Energy Outlook Special Report on Energy and Climate Change (International Energy Agency, 2015).
133. Po-Chun, H., et al., Radiative human body cooling by nanoporous polyethylene textile. *Sci.*, 2016. 353: p. 6303.
134. Kemp, T. S., The origin of mammalian endothermy: A paradigm for the evolution of complex biological structure. *Zool. J. of the Lin. Soc.*, 2006. 147: p. 473–488.
135. Carleton, T. A. and S.M. Hsiang S., Social and economic impacts of climate. *Science*, 2016. 353: p. 9837.
136. Chu, S., and Majumdar A., Opportunities and challenges for a sustainable energy future. *Nature*, 2012.488: p.294–303.
137. Hoyt, T., et al., Energy savings from extended air temperature set points and reductions in room air mixing, paper presented at the International Conference on Environmental Ergonomics, Boston, MA, 2 to 7 August 2009.
138. U.S. Energy Information Administration, Annual Energy Outlook 2016 with Projections to 2040 (U.S. Energy Information Administration, Office of Energy Analysis, 2016).

139. Po-Chun, H., et al., A dual-mode textile for human body radiative heating and cooling. *Sci. adv.*, 2017. 3: p. 1700895.
140. Lili, C., et al., Warming up human body by nanoporous metallized polyethylene textile. *Nature com.*, 2017.496: p. 1-8.
141. Jinlian, H., et al., Recent advances in shape-memory polymers: structure, mechanism, functionality, modeling and applications. *Progress in polym. Sci.*, 2012. 37: p.1720– 1763.
142. ([http://store.nike.com/?country=US&lang\\_locale=en\\_US&l=shop\\_pdp\\_ctr-inline/cid-100701/pid-240998#l=shop\\_pdp\\_ctr-inline/cid-100701/pid-240998](http://store.nike.com/?country=US&lang_locale=en_US&l=shop_pdp_ctr-inline/cid-100701/pid-240998#l=shop_pdp_ctr-inline/cid-100701/pid-240998)).
143. Jinlian, H., et al., A review of stimuli-responsive polymers for smart textile applications. *Smart mater. Struct.*, 2012. 21(5): p. 23.

# Chapter3. Experimental

This chapter introduces the experimental process in details, including the materials and equipment's used synthesis of different types of polyurethane, polyurethane, synthesis of liquid crystal elastomer, preparation of composite materials and membrane, preparation of porous polyurethane membrane, fiber preparation, and different polymer characterizations, properties and fabric performance tests.

## 3.1. Materials and equipment

The raw materials used in this project are tabulated in **table 3.1** and the main equipment used in this study are summarized in **table 3.2**

**Table 3.1.** Raw materials used in this study.

Raw materials	Abbreviation /Notes	Supplier
polyethylene glycol	PEG, Mn-1000, 2000 (g mol <sup>-1</sup> )	Alfa Aesar (USA).
Polytetramethylene Glycol	PTMG, Mn-1000, 2000 (g mol <sup>-1</sup> )	Alfa Aesar (USA).
Polycaprolactone	PCL, Mn-1000, 2000 (g mol <sup>-1</sup> )	Alfa Aesar (USA).
4,4-Methylene (di- isocyanate)	MDI, Mn- 250 (g mol <sup>-1</sup> )	Alfa Aesar (USA).
1,4-Butanediol	BDO, Mn- 90(g mol <sup>-1</sup> )	Alfa Aesar (USA).
N, N-dimethylacetamide	DMAc	Alfa Aesar (USA).
Silica aerogel	Size-10 $\mu$ m	Hengqiu Graphene Technology (Suzhou) Co., Ltd, China.
1, 4-Bis-[4-(6-	RM82, Mn-672 (g mol <sup>-1</sup> )	Wilshire Technologies, Inc

acryloyloxyhexyloxy)- benzoyloxy]-2- methylbenzene		
1,4-bis-[4-(3- acryloyloxypropyloxy) benzoyloxy]-2- methylbenzene	RM257, Mn-588 (g mol <sup>-1</sup> )	Wilshire Technologies, Inc
1, 3, 5-triallyl-1, 3, 5- triazine-2, 4, 6(1H, 3H,5H)trione	TATATO , Mn-249 (g mol <sup>-1</sup> )	Sigma-Aldrich
Ethylene glycol bis- mercaptoacetate	GDMP, Mn-238 (g mol <sup>-1</sup> )	Sigma-Aldrich
Triethylamine	TEA, Mn-101 (g mol <sup>-1</sup> )	Sigma-Aldrich
2,6-Di- <i>tert</i> -butyl-4- methylphenol	BHT, Mn-220 (g mol <sup>-1</sup> )	Sigma-Aldrich
2-Benzyl-2-dimethylamino- 1-(4-morpholinophenyl)- butanone-1	I-369, Mn-366 (g mol <sup>-1</sup> )	Sigma-Aldrich

**Table 3.2.** The main equipment used in this study.

Equipment	Supplier
Water vapor transmission machine	Haida International, China
Hydrostatic pressure	Haida International, China
Fourier Transform Infrared Spectroscopy-2000/FT-IR	Perkin-Elmer Inc. USA

Differential scanning calorimetry /DSC		Perkin-Elmer Inc. USA
Simultaneous Thermal analyzer (Mettler Toledo TGA/DSC 1)/TGA		Perkin-Elmer Inc. USA
Instron 5566		Instron Corporation, USA
Transmission Electron Microscopy /TEM, JEM-2100		Jeol Instrument, Japan
Scanning Electron Microscope		Jeol Instrument, Japan
Contact angle equipment		Contact Angle System SCA 20, DataPhysics Instrument GmbH, Germany
X-ray Diffractometer/XRD		Rigaku SmartLab, Japan

## 3.2. Preparation of functional polymers

### 3.2.1. Synthesis of polyurethane

Synthesis of polyurethane (PU) was carried out in a two-step process. Firstly, the macroglycol (PEG) was taken in three necked round bottom flask equipped with thermometer, mechanical stirrer and vacuum pump. PEG was degassed at 80°C for 1 hour under vacuum. Then, MDI was added in degassed PEG and continued the reaction at 80°C for 2.5 hour. At the second stage, the chain extender (BDO) was added to this pre-polymer and vigorously stirred to obtain the segmented PU.

### 3.2.2. Preparation of composite materials and membrane

Different percentages (0.5 and 1%) of silica particle were incorporated to fabricate the PU composite. The silica particle was added in PU solution (DMAc was used as solvent) and mixed by mechanically stirred for 30 min. After that, sonication was performed in order to get properly mixed the silica particle in PU matrix. Final PU composite membrane was obtained from the membrane casting. The thickness of the fabricated membrane was 25-28  $\mu\text{m}$ . Synthesis and fabrication details of composite membrane are in **figure 3.1** and **table 3.3**.

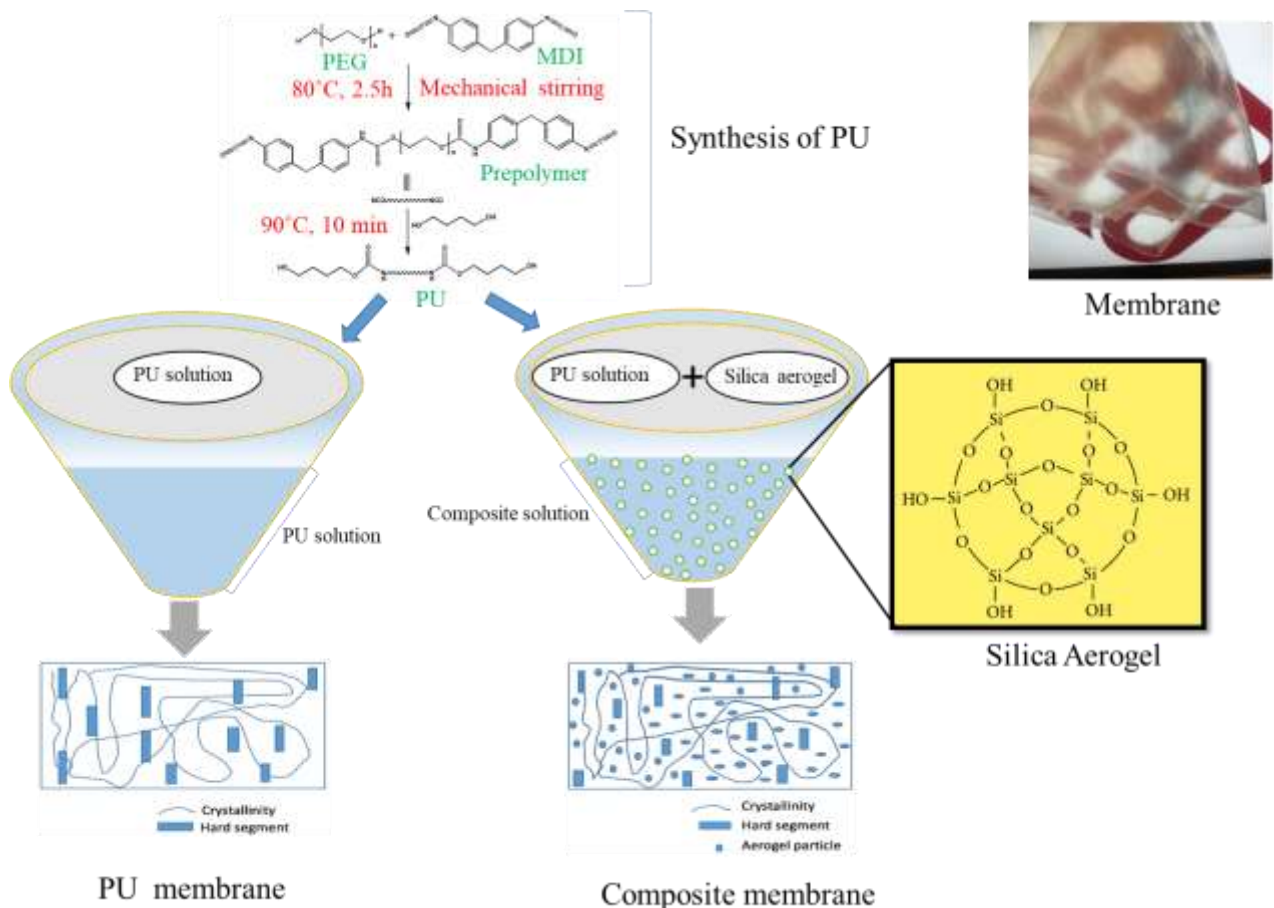


**Figure 3.1.** The fabrication process of PU and composite membranes.

**Table 3.3.** Synthesis details of samples

Sample	PEG(Polyol),	MDI (Di-	BDO (Chain-	Soft: Hard	Silica Aerogel
--------	--------------	----------	-------------	------------	----------------



	moL	Isocyanate), moL	extender), moL	Segment ratio of PU	(%)
PU	0.07	0.1068	0.0368	70:30	
Composite 0.5%	0.07	0.1068	0.0368	70:30	0.5
Composite 1%	0.07	0.1068	0.0368	70:30	1
Composite 2%	0.07	0.1068	0.0368	70:30	2

Scoured, bleached and dyed 100% cotton fabrics were used in twill weaving structure and then the fabric samples were cut into size 500 × 500 mm before laminating. The used fabric was -115 gms/sq.mt and 2/2 twill fabric. The twill line can be seen from both sides of the fabrics. Then these fabrics were laminated these fabrics with composite membranes by using hot press. Digital knight20 16” \*20” digital clamshell was used for the lamination. Temperature was kept at 150°C for the lamination and then cool down at room temperature. **Figure 3.2** is showing the picture of silica aerogel, composite membrane and laminated fabric.

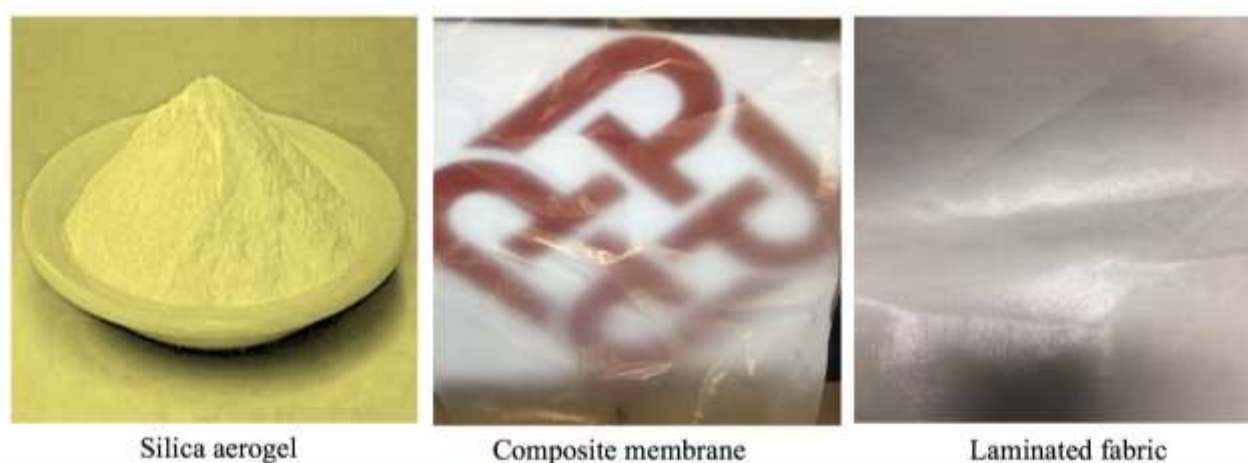


**Figure 3.2.** Silica aerogel particle, composite membrane, laminated fabric.

### **3.2.3. Preparation of porous polyurethane membrane**

Polyurethane (PU) was prepared via a pre-polymerization technique. At first, PEG was taken in a three-necked round bottom flask and degassed at 80°C for 1.5 h to remove any trapped moisture. After that, MDI was slowly added to the flask and the reaction was continued for 3h at 80°C under a nitrogen environment. After the formation of the pre-polymer, the temperature was cooled at room temperature and BDO was slowly added to the pre-polymer through high speed (1000 rotations per minute) stirring in a mechanical stirrer for homogeneous mixing. Finally, the mixture was heated for 1 h at 60°C for the chain extension process. The synthesized PU was then dissolved in DMAc (polymer content~30%). The synthesis process and their chemical structure has been shown in **Figure 3.3a**.

To fabricate the membrane, silica particles were added to a PU solution. The PU composite membrane was prepared by casting the mixture in a PTFE mold then kept at 80°C for 24 hours for the evaporation of solvent. The prepared PU composite membrane was then immersed in a water tank and sonicated for 5 min (PPU1 for 1 wt% & PPU2 for 2 wt%). A highly porous PU (PPU) membrane was obtained after drying it at 80°C for 24 hours. The fabrication process of the PU composite membrane is as shown in **Figure 3.3b**.

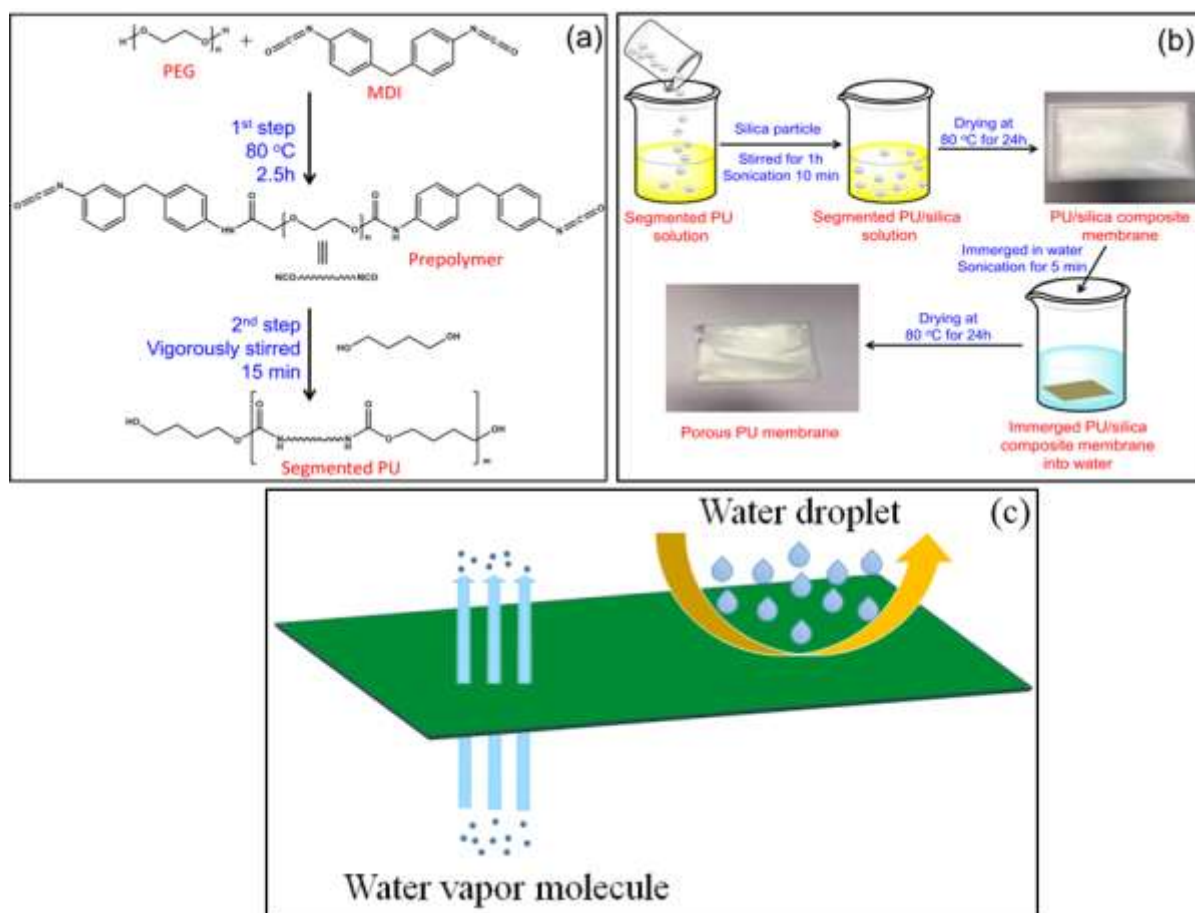


**Figure 3.3.** (a) synthesis of segmented PU, (b) fabrication of PPU membrane, and (c) schematic of water vapor transmission and water droplet resistance property of the porous membrane.

### 3.2.4. Synthesis and coating details

In this study, three different types of polyurethanes were synthesized for cotton fabric coatings, they are Polyethylene Glycol (PEG), Polytetramethylene Glycol (PTMG), and Polycaprolactone (PCL) based polyurethane. I have used three different types of polyol (PEG, PTMG, and PCL), with a molecular weight of 2000 g/mol. As a di-isocyanate we have used Methylene Diphenyl Isocyanate (MDI) with a molecular weight of 250 g/mol, and 1,4-Butanediol (BDO) with a molecular weight of 90 g/mol as a chain extender. Concentration and synthesis are detailed in

Table 3.4 and Figure 3.4, respectively.

**Table 3.4.** Concentration details of polyurethane synthesis

Sample	PEG (Polyol), mol	PTMG (Polyol), mol	PCL (Polyol), mol	MDI (di- isocyanate), mol	BDO (chain extender), mol	Soft: Hard segment ratio
Sample 1	0.082			0.282	0.200	65:35
Sample 2		0.082		0.282	0.200	65:35
Sample 3			0.082	0.282	0.200	65:35

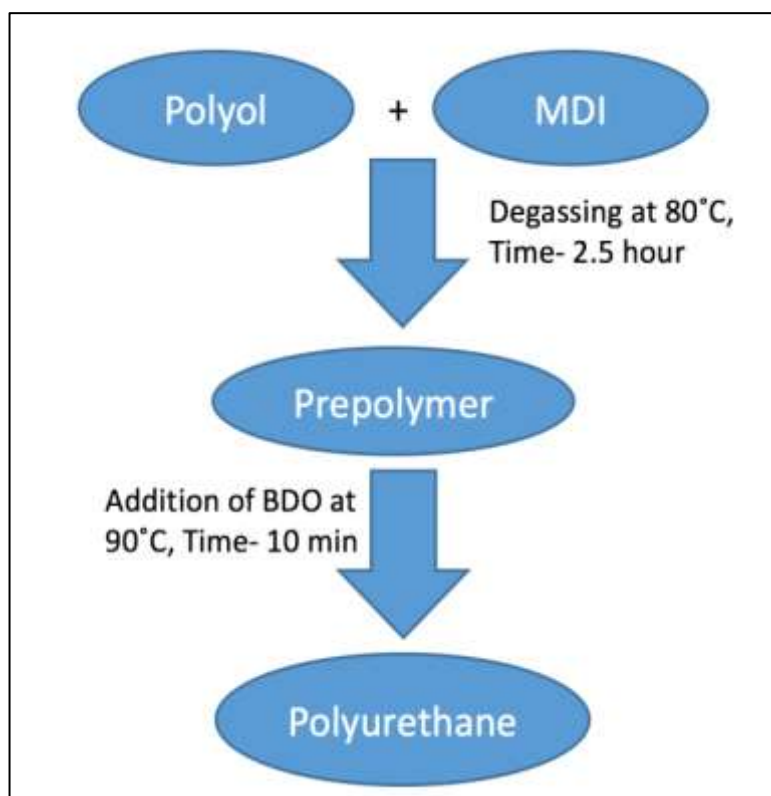


**Figure 3.4.** Synthesis procedure of polyurethane

Scoured, bleached, and dyed 100% cotton fabrics were used in a twill weaving structure, then the fabric samples were cut into 200 mm × 200 mm

sizes before coating. The twill fabric we have used is 115 gms/sq.mt, 2/2 twill fabric, so that the twill line can be seen from both sides of the fabric. Cotton fabrics were then coated by a knife over roller machine (Werner Mathis AG, Oberhasli, Switzerland). The coating roller speed was 0.2–0.5 m/min and the linear pressure was set to a 400 daN/cm (dekanewton/centimeter) maximum and applied in a single layer. The thicknesses of the uncoated and coated fabrics were 0.2 mm and 0.30–0.33 mm (Table 2), respectively, and measured by ETOPOO GL-65-75 thickness gauge (accuracy  $\pm 0.003$  mm). In order to easily identify the coated and uncoated fabrics, the uncoated and coated fabrics were coded and tabulated in Table 3.5.

**Table 3.5.** Coding and thickness of uncoated and different coated fabric

Sample code	Description	Thickness (mm)
UF	Uncoated fabric ( Control)	$0.20 \pm 0.01$
CFPEG	Fabric coated with PEG	$0.30 \pm 0.01$
CFPTMG	Fabric coated with PTMG	$0.32 \pm 0.01$
CFPCL	Fabric coated with PCL	$0.33 \pm 0.01$

The solution of the polyurethane has been added on to the fabric surface. We kept the same add-on percentage for all the fabric. The add-on % is the weight of the polyurethane solution that has been added on to the fabric

surface and controls the thickness and evenness of the sample. The add-on % on the coated cotton fabric was about 20% and calculated using the following formula

$$\text{Add-on (\%)} = [(Y - X)/X] \times 100 \quad (1)$$

where  $X$  is the weight of the uncoated fabric and  $Y$  is the coated fabric. Figure 3.5 shows the theoretical approach of fabric coating and water vapor transmission.

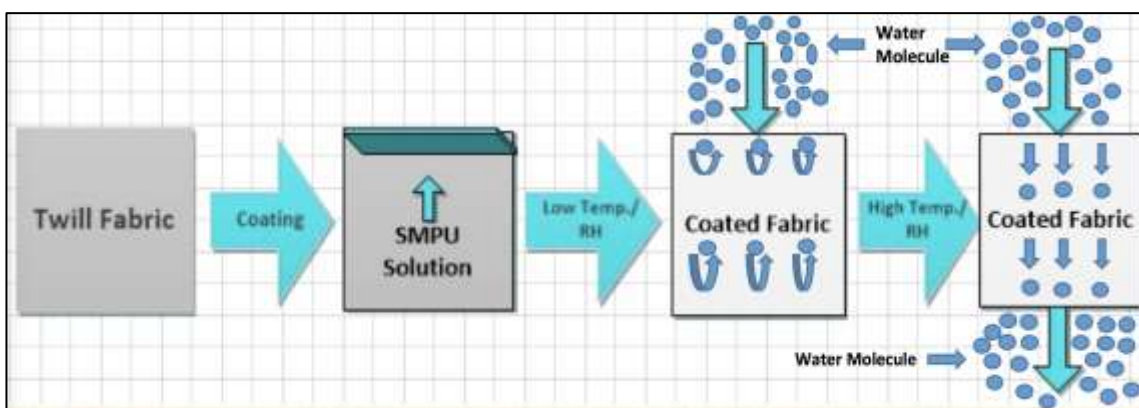


**Figure 3.5.** Theoretical approach of fabric coating and water vapor transmission.

### 3.2.5. Synthesis of liquid crystal elastomers (LCEs)

Thiol-terminated LC inks were synthesized via a thiol-acrylate Michael addition. Non-equimolar mixtures of LC monomers (RM82 and RM257) and dithiols were heated to 80°C and then mixed with 1 wt% of TEA, 2 wt% of BHT, 1.5 wt% of I-369 and TATATO. The ratio of thiol, acrylate, and vinyl functional groups was kept constant in all samples. The molar ratio used was 0.8 acrylate: 1.0 thiol: 0.2 vinyls, unless otherwise noted. After mixing, the solution was transferred into the

printing syringe or mold to complete oligomerization for 3h at 65 °C, forming thiol-terminated LC ink.

Liquid Crystal (LC) Ink Preparation. The LC ink is prepared by mixing RM82 and n-butylamine in a 1.1:1 molar ratio with 1.5 wt % of the photoinitiator, I-369, in a glass vial. The monomeric precursors are mixed with heat until a homogeneous solution is created. The LC ink solution is transferred into the printing syringe to oligomerize for 15h at 70 °C undergoing Michael addition. Different components of liquid crystal elastomers are shown in **Figure 3.6**.

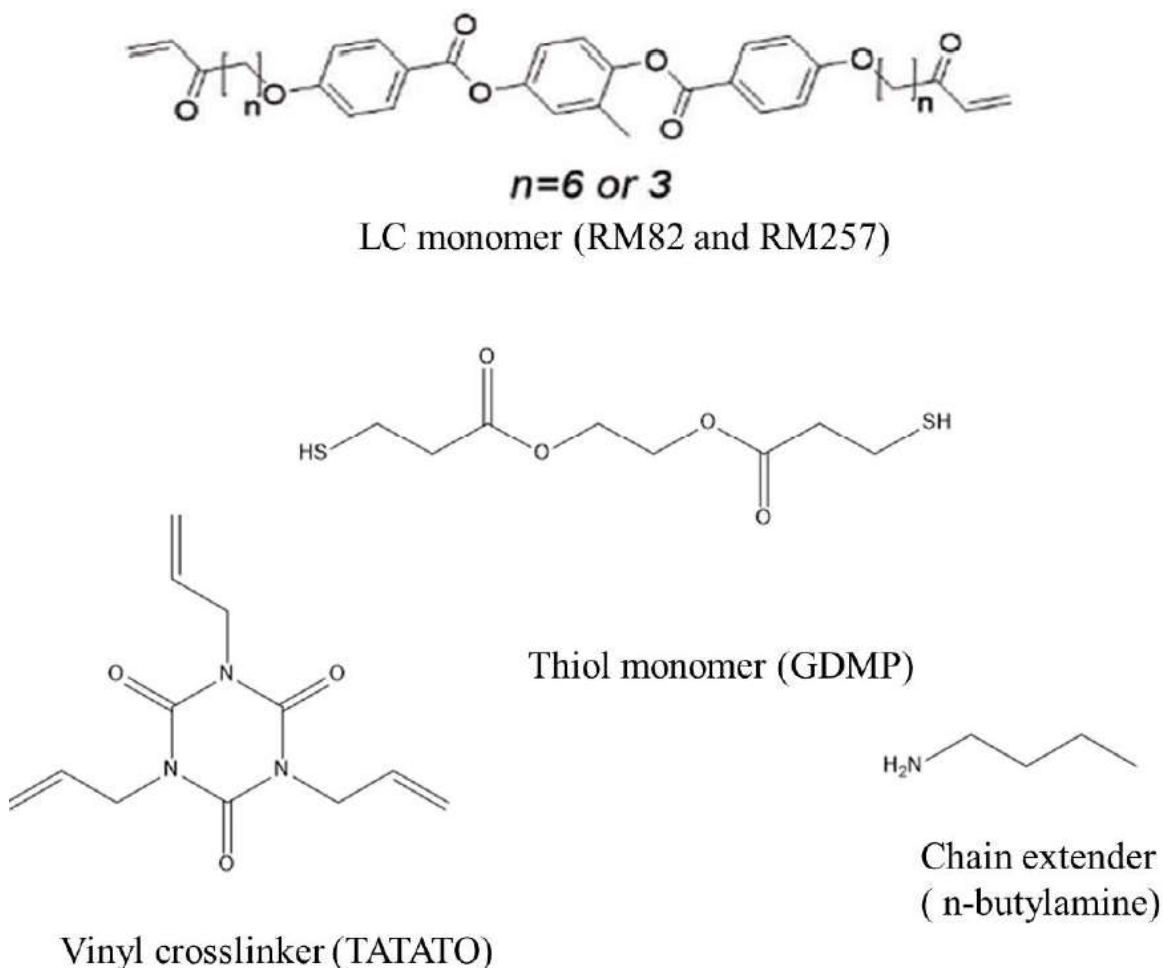


**Figure 3.6.** Chemical structures of different components of liquid crystal elastomers.

### 3.2.6. Fiber preparation

3D Printing: The LC ink within the printing syringe was then loaded into a KR-2 Extruder print head (Hyrel3D, Norcross, GA), which was an attachment of the system 30M 3D printer (Hyrel 3D, Norcross, GA). GDMP inks were printed at room temperature. These oligomers were crosslinked after printing by continuous irradiation from 365 nm LEDs located on the print head with an intensity of  $0.8 \text{ mW cm}^{-2}$ . Samples were then postcured under 365 nm UV light for 15 min. Preparation of fiber and radial structure by 3D printing are shown in **Figure 3.7**.

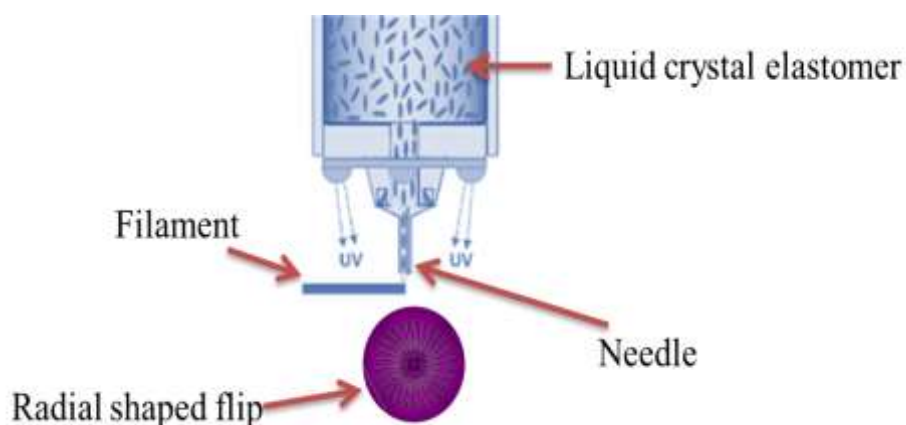


**Figure 3.7.** Preparation of fiber and radial shaped flip by 3D printing.



### 3.3. Characterization

#### 3.3.1. Water vapor transmission

Water vapour transmission tests were conducted in a climate chamber according to ASTM E96 BW standard by using Haida International Equipment (Model-HD-E702-100-4), It is a temperature, relative humidity and air velocity controlled climate chamber. Tests were conducted in different temperature and relative humidity. The air velocity in the chamber was 0.2-0.03 m/s. Test cup was half filled with water and the laminated sample was fixed on the top of the cup by grease. The test cup was placed into the test chamber for 4 h and then weight change was taken to calculate the WVT rate by following equation 3.2.

$$\text{WVT}=\text{G}/\text{tA} \quad (3.2)$$

where G is the weight change in grams; t the duration of test in hour and A is the test area in  $\text{m}^2$ . **Figure 3.8** is showing the apparatus measuring the WVT.

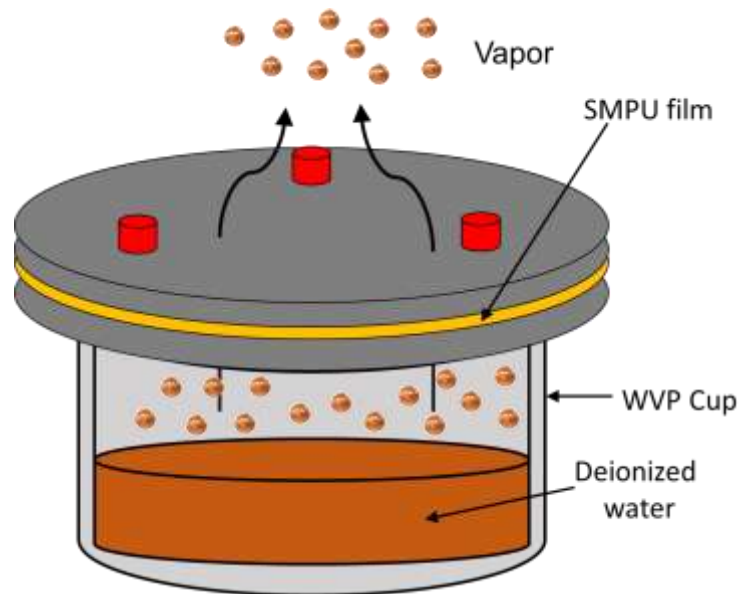


**Figure 3.8.** The apparatus for measuring WVT.

### **3.3.2. Water resistant/Contact angle**

The contact angle of the membranes was measured according to ASTM D7334 to investigate the water resistance property of the membrane. The contact angle was measured using the tatec contact angle meter. The specimen was placed in the instrument and a drop of de-ionized water was placed on the surface using a syringe at room temperature. The contact angle was determined graphically.

### **3.3.3. Mechanical property**

Mechanical properties (strength and elongation at break) of the samples were tested according to ASTM D882 standard by using by using an Instron 4411 (Boston, MA, USA). The samples were cut into 100 x 10 mm (L x W) squares. Tests were performed at room temperature (25°C), relative humidity 70%.

### **3.3.4. SEM**

The surface morphology of the porous membrane was observed using a Scanning Electron Microscope (SEM) with (TESCAN VEGA3). The samples were cut from two different regions of the sample and then fixed in a carbon tape for gold coating. After the gold coating was conducted, it was placed into the SEM instrument for analyzing and for taking the microscopic image. The roughness after leaching out the silica was evaluated from SEM image using imageJ analyzing software.

### **3.3.5. FTIR**

The Fourier transform infrared (FTIR) spectra of the SMPUs were measured over the wavenumber range 4000–500 $\text{cm}^{-1}$  with a Perkin-Elmer model Spectrum 100 FTIR spectrometer. Spectra were recorded with a resolution of 4 $\text{cm}^{-1}$  and a scan number of 4.

### **3.3.6. XRD**

Wide angle X-ray diffraction (WAXD) patterns were collected using a Rigaku SmartLab X-ray diffractometer through Cu  $K\alpha$  radiation. The samples were scanned at a diffraction angle of  $2\theta=10^\circ$  to  $80^\circ$  at a scan speed of  $10^\circ/\text{min}$ .

### **3.3.7. TGA**

Thermogravimetric analysis (TGA) was carried out under a nitrogen atmosphere (50 ml/min) in the TG analyser (METLER TOLEDO, TGA). A heating rate of  $10^\circ\text{C}/\text{min}$  was used in the analysis.

### **3.3.8. DSC**

Differential scanning calorimetry (DSC) was done using PerkinElmer DSC 8000. A 5mg sample was cut and put into a sealed aluminium pans. It was then loaded into the DSC chamber to analyse the melting behaviour of the sample. The samples were heated from room temperature to  $150^\circ\text{C}$  at a rate of  $10^\circ\text{C}/\text{min}$  followed by a cooling cycle at  $5^\circ\text{C}/\text{min}$  until reaching  $-30^\circ\text{C}$ . Finally, samples were heated again at a rate of  $10^\circ\text{C}/\text{min}$  until  $150^\circ\text{C}$ . Data from the second heating cycle was considered for analysis of thermal properties of the materials.

### **3.3.9. Absorbency**

The water absorbency of the membrane were measured in order to check the absorbability of different membranes. Testing time 4 hour and condition were recorderd. Absorbaility was calculated according to equation 3

$$\text{Absorbency} = 100 - \left( \frac{\text{Initial weight}}{\text{Final weight}} \times 100 \right) \quad (3)$$

### **3.3.10. Wicking distance**

The wicking test was performed according to AAATCC TM 197. The testing samples were cut into 2cm wide stripe and dipped into distilled water. Then the water started to climb up the testing sample due to capillary force.

### **3.3.11. Abrasion resistance**

For checking the hardness and adhesion properties of the laminated fabric we have done the Martindale abrasion resistance test of the laminated sample according to ASTM D4966 standard, we rub 1000 times (50 per min) with 9 kPa load on the upper surface and under lower surface there was a plain twill fabric, after testing we investigate the sample and found very good abrasion resistance properties which means it has very good adhesion property.

### **3.3.12. Porosity**

The bubble point method was used for characterizing pore size, by using a capillary flow porometer (CFP-1100AI, Porous Materials Inc., USA). The porosity of the fibrous membranes was calculated using the below equation:

$$\text{Porosity (P)} = \frac{D_b - D_a}{D_b} * 100\% \quad (4)$$

Where  $D_b$  represents the density of the pristine PU materials and  $D_a$  represents the density of the porous polyurethane. Thickness of the membrane was measured using an ETOPOO GL-65-75 thickness gauge (accuracy  $\pm 0.003$ ).

### **3.3.13. Hydrostatic pressure**

The hydrostatic pressure of the membranes was examined according to the JIS L1092 B standard method using the Henbert Hydrostatic Pressure Machine (China).

### **3.3.14. Air permeability**

To observe the breathability of the membrane, the air permeability testing of the laminated fabric was performed according to ASTM D737-96 by using SDL international textile testing equipment.

### **3.3.15. Shape memory property**

Shape memory properties of the polyurethane were measured using an Instron 5566 (Canton, MA, USA). The shape memory property was measured under the condition of heating the sample at  $60\text{ }^{\circ}\text{C}$  for 10 min then elongating it up to 100% and holding it for 10 min, then cooling it at room temperature. The number of cycles was four and the size of the sample was  $8\text{ cm} \times 1\text{ cm}$ . The shape fixity and shape recovery ratio were calculated from the below equations ( $\varepsilon_u$ : fixed strain;  $\varepsilon_m$ : maximum strain;  $\varepsilon_p$ : plastic or residual strain).

$$\text{Shape fixity (\%)} = \frac{\varepsilon_u}{\varepsilon_m} \times 100 \quad (5)$$

$$\text{Shape recovery (\%)} = \frac{(\varepsilon_m - \varepsilon_p)}{\varepsilon_m} \times 100 \quad (6)$$

### **3.3.16. IR transmittance**

The IR transmittance of membranes were tested by using Fourier Transform Infrared Spectroscopy (FTIR), Perkin Elmer model Spectrum 100. Spectra for the membrane was recorded in the range of 2 -18 $\mu\text{m}$  and 7 -14  $\mu\text{m}$ .

# **Chapter4. Water vapor transmittable and resistant textile**

## **4.1. Introduction**

Comfort is a satisfying state of physical and emotional harmony between the human being and the environment atmosphere [1–3]. Water resistance and water vapor transmission (WVT) through textiles has a great effect on the thermo-physiological comfort of the human body. Thermal comfort is maintained by perspiring in vapor form and transmitting it from inside the garment to the outside environment [4]. When the heat transmission from the clothing inside (skin) to the environment decreases, the sweat glands begin to produce liquid perspiration as well. The perspiration in vapor form is known as insensible perspiration and the perspiration in liquid form is known as sensible perspiration [5,6]. When the vapor perspiration is transported to the outside atmosphere it carries body heat, thus reducing or maintaining the body temperature. Body temperature can influence the skin temperature [7]. Therefore, the garment being worn must allow the vapor perspiration to pass through; otherwise, it will cause discomfort [8]. The level of skin wetness is the main reason affecting the perception of discomfort. During sweating, if a garment's water vapor transfer rate is slow or limited, the relative humidity levels of the garment inside the microclimate will increase the evaporation of perspiration. This will increase body temperature and cause heat stress [9].

Water vapor transmission through textile fabrics plays a major role in

maintaining the wearer's body comfort, both in hot and cold weather and during normal and high activity levels [10]. Hence, a clear consideration of the role of water vapor transmission through clothing in relation to body comfort is important for designing high-performance fabrics for specific end applications. To provide wearing comfort to the wearer, textile materials should have a high-capacity of water vapor transmission so that perspiration can evaporate and be transmitted from the body surface to the environment. Shape memory polyurethane (SMPUs) could possibly be the next candidate of smart textile material in the coming decade [11,12].

The contact angle is defined as the angle formed by the intersection of the liquid-solid interface and the liquid-vapor interface. The SMPUs coated fabrics are expected to improve water resistance to a certain extent. Therefore, SMPUs coated cotton fabrics should have low wettability so that the coated fabrics may bead up the water droplets and drip on the surface of the garment. This also indicates a certain level of hydrophobicity of the coated fabric. The lower the contact angle, the greater the wettability of the fabric. When the contact angle equal to  $0^\circ$ , the complete wetting occurs. In contrast, fabric with large contact angles is represented with lower wettability but higher hydrophobicity. When the contact angle equal to  $0^\circ$  or  $\cos\theta = 1$ , complete wetting occurs. When the contact angle is greater than  $90^\circ$  it generally means that the surface of the sample is water resistant. For super hydrophobic surfaces, the contact angles are generally greater than  $150^\circ$ . This means almost no contact between the liquid droplet and the solid surface. The contact angle is closely related to wettability and surface energy



[13,14].

The coating is one of the important techniques for adding value to textiles. Coating extends the range of the functional performance properties of textiles and the use of these techniques is increasing rapidly as the application for functional textiles become extensive. The coating technique imparts smart properties to fabrics. Having widespread applications across a range of technical textile sectors increases functionality and durability as well as value.

SMPU is a new functional material that is continuously improving the aesthetic as well as the comfort of the products created from it. It has attracted greater attention in recent years [15–17]. A responsive material is a material that changes in shape as a result of a change in temperature/RH; SMPU is a class of polyurethane (PU) that is different from conventional polyurethane in that it is known to originate from the phase-separated structure between hard and soft segments, and the reversible phase transformation of the soft segment. The use of SMPU in clothing textiles is a new concept. In SMPU, the soft segment is responsible for behavior changes according to temperature and humidity and allows the water vapor to pass through [18,19]. When shape memory polyurethane is laminated/coated with a fabric [20–22], a smart fabric is formed. Its permeability changes as the wearer's environment and body temperature change to form an ideal combination of thermal insulation and vapor permeability for army clothing [23–26]. When the body temperature is low, the fabric remains less permeable and keeps the body heat. When the body is in a sweat condition, it allows the water vapor to escape into the air because

its moisture permeability becomes very high with increasing body temperature [27–30]. It can also keep our body warm by resisting water during rain.

In this chapter, I have produced a coated fabric with water resistance and permeability properties. Such a coated fabric can be used during rainy weather to protect the body from the rain or some other extreme condition, when both water resistance and permeability are required. In this study, three different types of polyurethane were synthesized and coated on to cotton fabric surfaces. I then investigated the water resistance and water vapor transmission property of the coated fabrics.

## **4.2. Results and discussion**

### **4.2.1. Water Resistance/Contact Angle**

The wettability and water resistance property of the coated and uncoated fabrics were measured by the contact angle measurement of a water droplet at its sample surface (**Figure 4.1**). In **Figure 4.1(A–C)**, the water contact angle changes from  $113^{\circ} \pm 1$  to  $92^{\circ} \pm 1$ , implying the change of the contact angle from good water resistance to water resistance. In **Figure 4.1(D–F)**, the water contact angle changes from  $38^{\circ} \pm 1$  to  $0^{\circ}$ , implying the change of the contact angle from slightly wetted to completely wet. As we can see in **Figure 4.1 (E,F)** the surface is not so smooth because there are some protruding fibers that absorb water. From **Figure 4.1E**, we can see that the contact angle of the uncoated fabric after 20 s is  $0^{\circ}$ , which means it is wetted completely, and the contact angle of CFPEG, CFPTMG, and CFPCL is

$94.5^\circ \pm 1$  (**Figure 4.1B**), and after 2 min the contact angle of the coated sample is  $92^\circ \pm 1$  (**Figure 4.1C**), which means still water-resistant. However, after a drop of de-ionized water was placed on the sample surface, we immediately observed the contact angle and found that the uncoated fabric was slightly wetted and the coated fabrics were water-resistant. From the result of the contact angle of our experimented sample, we can say that our coated samples are water-resistant where the uncoated sample is not. **Figure 4.2** shows the contact angle of CFPTMG, CFPCL, CFPEG and uncoated with time variation. The polyurethane we synthesized easily passes the water molecule (water vapor transmission result are in **Figures 4.3 and 4.4**) but it can resist the water droplet (normally the size of the water molecule is about  $2.75 \text{ \AA}$  where the size of the water droplet is about 2 mm). The contact angle is mainly dependent on the cohesive forces of the molecule (surface tension) of the surface of the polymer. The coated polyurethane has enough surface energy to keep liquid together, meaning droplet spread-out will not occur.

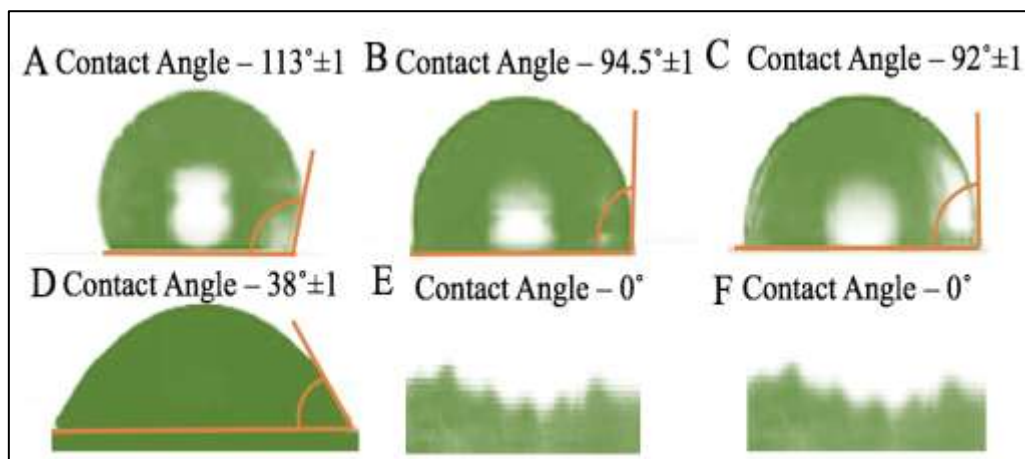


**Figure 4.1.** Contact Angle of coated and uncoated fabric. A) Coated after 0 s, B) Coated after 20 s, C) Coated after 2 min, D) Uncoated after 0 s and E) Uncoated after 20 s, and F) Uncoated after 2 min.

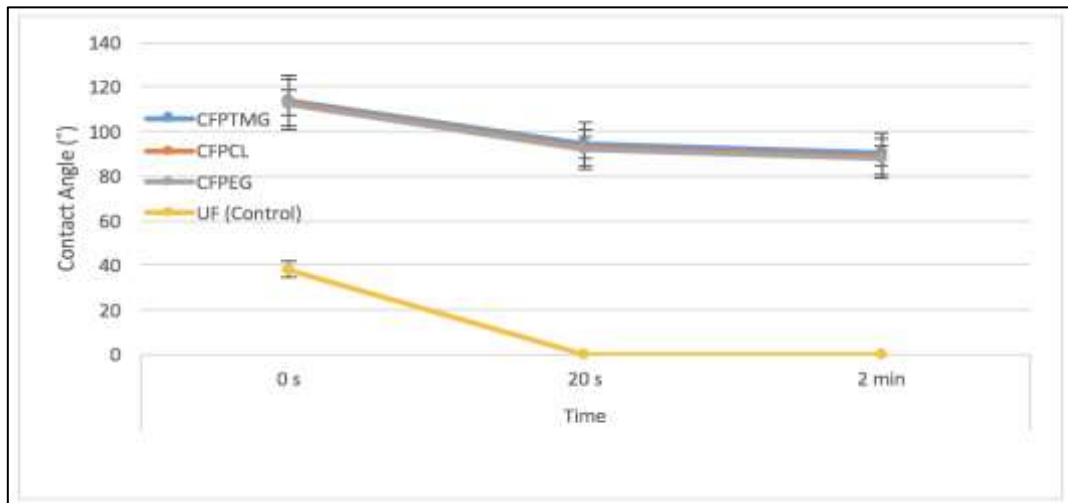


**Figure 4.2.** The contact angle of CFPTMG, CFPCL, CFPEG and uncoated with time variation.

#### 4.2.2. Water Vapor Transmission of Coated Fabric

The water vapor transmitting ability of UF (Control), CFPEG, CFPTMG and CFPCL are plotted in Figures 6 and 7. The water vapor transmitting ability of the coated fabric was measured, in order to compare the water vapor transmitting ability of coated fabric with different polymeric materials. The results of the water vapor transmitting ability of UF (control fabric) and the coated fabric CFPEG, CFPTMG, and CFPCL are shown in **Figures 4.3 and 4.4.**

As shown in **Figure 4.3**, we can see that the WVT for the uncoated fabric increased linearly with the increase of relative humidity (constant temperature (20 °C)) and the WVT of the CFPEG coated fabric shows a better WVT than

the all coated fabric during the whole period. **Figure 4.3** shows that the WVT of the CFPTMG and CFPCL coated fabrics was always lower than the CFPEG and the uncoated fabric.

The WVT of all coated fabric was similar at the beginning; however, the WVT of all coated fabric increased significantly when enhancing the RH %. The slope of all coated fabrics was so similar that they raised steadily at RH 25% to 65%, but CFPEG increased significantly at RH 65% to 95%. CFPEG has showed significantly better water vapor transmission compared with CFPTMG and CFPCL after RH 65%. As we can see from **Figure 4.3**, CFPEG increased significantly after RH 65% and nearly touches the uncoated fabric. The WVT increases with such a high relative humidity because of the matrix between the relative humidity, constant temperature (20 °C) in the chamber, room temperature water (23 °C), and the air velocity in the chamber 0.3 m/s. The results of the water vapor transmitting ability of the uncoated (control fabric) and the coated fabric, CFPEG, CFPTMG, and CFPCL against temperature are shown in **Figure 4.4**.

As shown in **Figure 4.4**, we can see that the WVT for the uncoated and coated fabrics increased gradually with the increase of temperature from 15 to 40 °C (constant relative humidity (70%)). It shows that the WVT of the CFPEG coated fabric was similar to the uncoated fabric throughout the whole period. **Figure 4.4** shows that the CFPEG is very near to the uncoated fabric after 30 °C. After 25 °C, CFPEG increases significantly compared with CFPTMG and CFPCL. Sinem et al. [13] tried to improve

the breathability of the coated fabric via micro-cracking and tested the water vapor permeability of the coated fabric according to EN ISO 11092, but their result reveals that the water vapor permeability did not improve enough; from their results the coated sample can pass around 12% of water, where the uncoated sample can pass around 35% of water from the test cup, which means the uncoated fabric is much more water vapor permeable than the coated fabric. The difference between the uncoated and coated fabric is too high. In contrast, the water vapor permeability property of our coated fabric is very near to the uncoated fabric. Our coated fabric is able to transmit water vapor more efficiently because of its soft and hard segment ratio, and the molecular weight of the polyols.

The effect of temperature or RH on the water vapor transmitting ability of CFPEG, CFPTMG, and CFPCL is highly related by their hard and soft segment ratio and their –OH group. The CFPTMG and CFPCL molecular structure have less change or movement with the increase of temperature or RH compared with CFPEG, and water vapor transmission largely depends on the water affinity of the functional group of those polymers. As we can see, CFPEG attracts and passes more water vapor molecule when compares with CFPTMG and CFPCL. According to the above results, WVT increased with the increase of temperature and RH %. However, for shape memory polyurethane there is a transaction when temperature or RH is high and the soft segments of the SMPU change their state according to

temperature or RH in order to facilitate the passing of water vapor. From **Figures 4.3 and 4.4** we can see that the CFPEG showed better WVT compared with the CFPCL and CFPTMG because of the number of the –OH group in the structure. WVT depends on a hard and soft segment ratio of the polymer and the number of –OH groups in the structure. As we know from the structure, PEG has more affinity to water molecules compared with PCL and PTMG because of its branched structure and number of –OH groups.

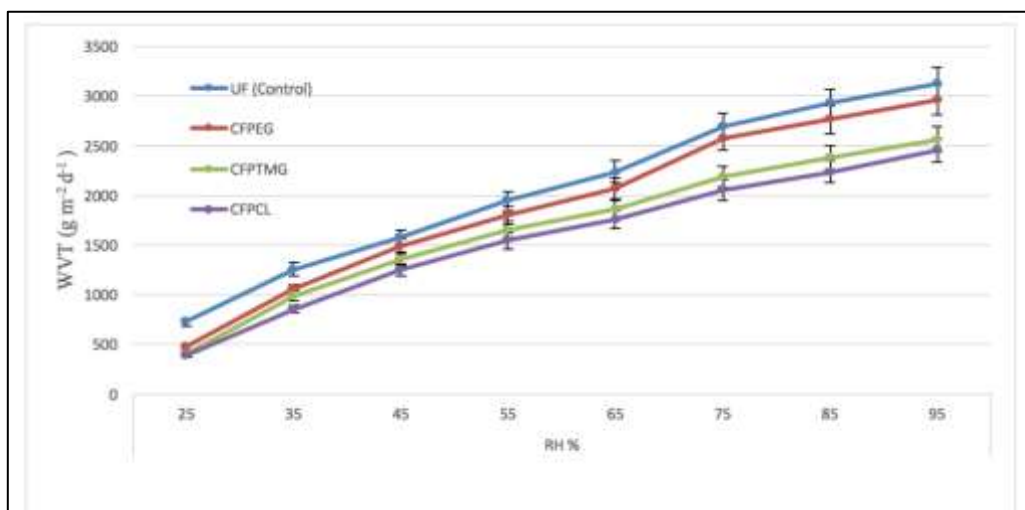


**Figure 4.3.** WVT of UF (control), CFPEG, CFPTMG, and CFPCL

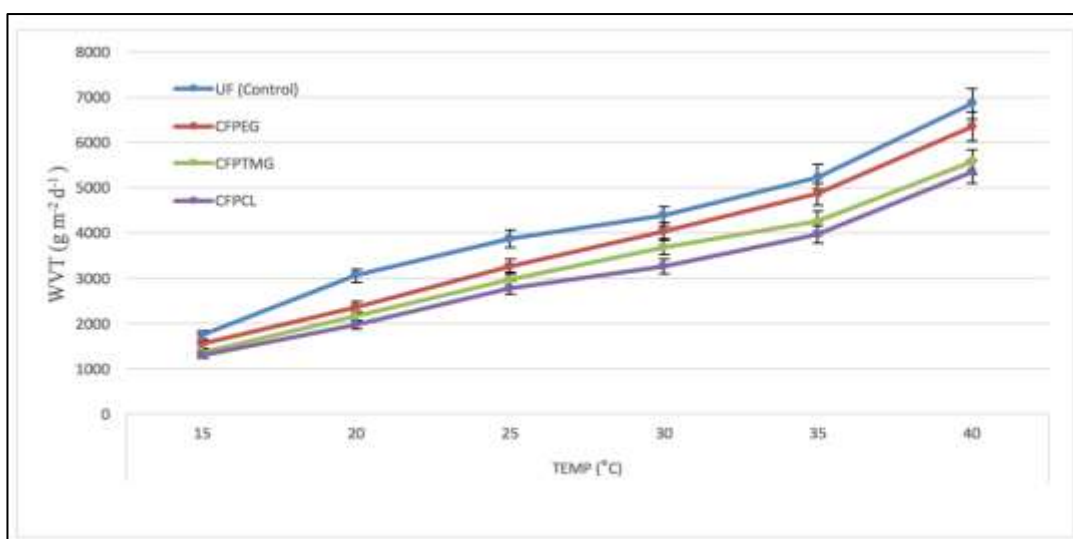


**Figure 4.4.** WVT of UF (control), CFPEG, CFPTMG, and CFPCL

### **6.2.3. Mechanism of Water Transmittance and Resistance Property of the Coated Fabric**

Non-porous polymeric membranes are a dense polymer; PEG, PCL, and PTMG are all hydrophilic polymers that can absorb and diffuse water molecules and can produce a wicking action that attracts water molecules. A membrane allows the water molecule to transmit. When the water vapor arrives at the surface of the membrane, the membrane absorbs the water molecule because of its hydrophilic nature. The chemical structure and film thickness are the main determinants of transmission ability of the water vapor in a membrane and also the surroundings (Temperature and Relative humidity). In **Figures 4.5 and 4.6**, we explain the factors that influence the water vapor transmission and resistance. **Figure 4.5** reveals that the hydrophilic polymeric membrane can be triggered by temperature and relative humidity that is why we call our polymer a responsive polymer. Furthermore, permeability occurs through the membrane at the molecular level of sorption-absorption/diffusion-evaporation; therefore, the structure of the polymer plays the main role in controlling the water vapor transmitting ability of the polymer. The polymer interaction and the primary structures of the polymer itself are very important for understanding polymer functions such as sorption, and the permeability of small water molecules. Furthermore, from the above WVT result we can say that fabric coated with PEG has better permeability compared with PCL and PTMG, as we know from the structure that the



functional group of PEG is more water absorbent than PCL and PTMG. PEG contains more hydroxylic groups and branched structures that cause the improvement of water molecule passes.

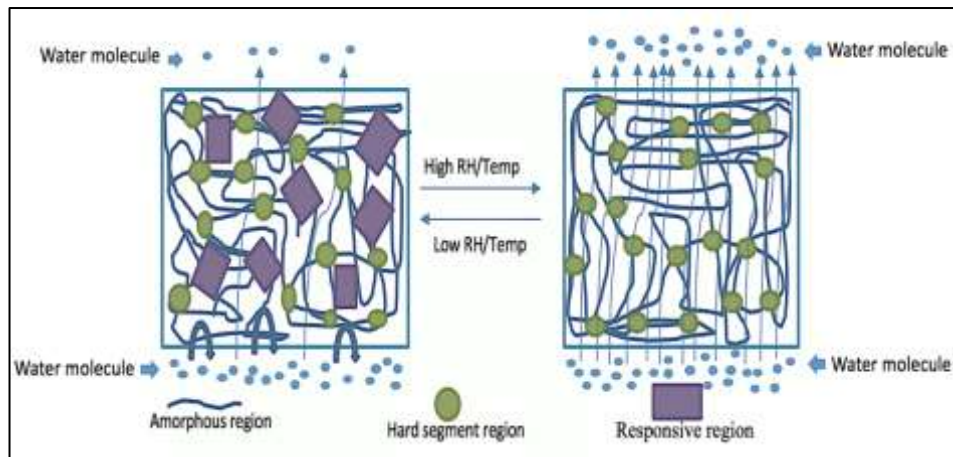


**Figure 4.5.** Molecular structure design of responsive polyurethane.

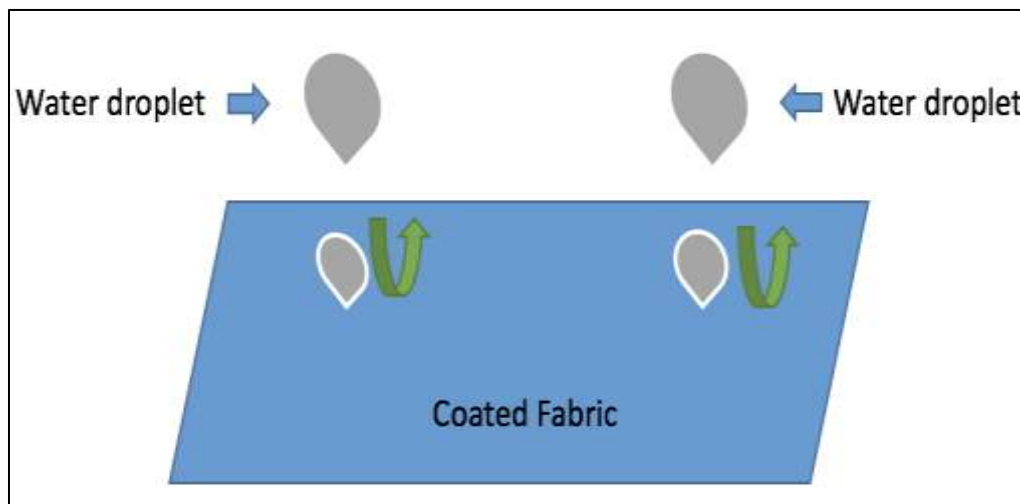


**Figure 4.6.** Water resistance of coated fabric

The water-resistant property of coated fabric was measured and it was found that all the coated fabric is water-resistant while the uncoated one was fully water absorbent. The terms water vapor transmittable and water resistance are seemingly contradictory, but water vapor transmission happens through the interaction of the water molecule and the hydrophilic

polyurethane, while water-resistance happens by resisting the water droplet. It is easy for the polyurethane to resist the water droplet because it comes with a number of water molecules together. **Figures 4.5 and 4.6** shows the mechanism of the water vapor transmitting ability and water resistance ability, and the size of the water molecule and the water droplet. As we know, the size of the water droplet is about 2 mm, which is 20 million times higher than the water molecule (the size of the water molecule is about 2.75 Å). Furthermore, normally, the twill structure of the cotton fabric does not have any issue with water vapor transmission; however, it can absorb water very easily (Figure 6.3). The moisture regain percentage of cotton is about 7.1–8.5%. To avoid the water absorbent property of the cotton fabric we coat them in polyurethane in order to get a water-resistant (rainproof) cotton fabric, and achieve at the same time better water vapor transmission.

#### **4.2.4. Thermo-Mechanical Properties**

Shape memory polyurethane is usually a thermally induced process, though it can be triggered by temperature and humidity. Thermally induced SMPUs have the capability of sensing and responding to external stimuli, such as temperature and humidity, in a predetermined way. The polyurethane we have synthesized is segmented polyurethane. It has two different phases (soft and hard). When the temperature or the humidity rises, the soft part of the polyurethane starts to switch its state, which leads to the improvement of WVT with increasing temperature. **Figure 4.7** reveals the melting temperature of the polyurethane. The transition temperature depends on the

hard/soft phase ratio and the molecular weight of the polyols. In addition, the crystallinity increases with the increase in soft segment content and molecular weight. As we can see from the **Figure 4.7**, the transition temperature of polyurethane is (35–37) °C, which means it can switch in this temperature range. The soft segment influences the water vapor transmission of the polyurethane by the free volume and hydrophilicity of the polyurethane, and it is revealing that the PEG has the lowest transition temperature among these three types of polyurethane.

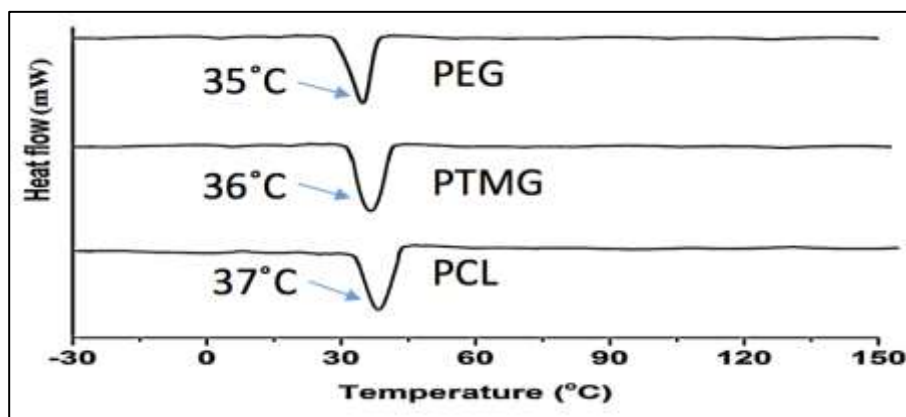


**Figure 4.7.** DSC of different polyurethane

The shape memory property of different polyurethanes are tabulated in **Table 4.1**. All the synthesized polyurethane has shown the shape memory property. It can be said that the existence of the irreversible elongation and recovery trend happened as a result of the hard segment network, which gives rise to the ratio of shape recovery and the ratio of fixity shape, which describes the shape memory property of the material. The deformation is normally conducted at a temperature higher than the transition temperature

and this deformation can be fixed in the cooling process. when we release the stress of the polyurethane from 0.85 MPA to 0.00, the PEG can keep 100% strain till 0.45 MPA, while PCL and PTMG can keep 100% strain till 0.55 MPA. Then the strain goes down along with stress. As we can see, the strain of PEG, PCL, and PTMG is fixed at  $79.4 \pm 1.5\%$ ,  $79.5 \pm 1.5\%$ , and  $80.1 \pm 1.5\%$ , respectively, with zero stress. After cooling it at room temperature we found the shape recovery of PEG, PCL and PTMG are  $85.3 \pm 1.5\%$ ,  $86.2 \pm 1.5\%$  and  $86.7 \pm 1.5\%$ , respectively. The plasticity of the polyurethane depends on the shape recovery. We found the plasticity of the polyurethane after deducting the shape recovery from the maximum strain (100%). From these three different types of polyurethane, we can see that the shape fixity and recovery of PTMG is comparatively higher than PCL and PEG, while the fixity and recovery of PTMG is higher because of the crystalline structure of the soft segment.

**Table 4.1.** The shape memory properties of different polyurethanes

Polyurethane	Shape Fixity (%)	Shape Recovery (%)	Plasticity (%)
PEG	$79.4 \pm 1.5$	$85.3 \pm 1.5$	$14.7 \pm 1.5$
PTMG	$80.1 \pm 1.5$	$86.7 \pm 1.5$	$13.3 \pm 1.5$
PCL	$79.5 \pm 1.5$	$86.2 \pm 1.5$	$13.8 \pm 1.5$

Thermogravimetric analysis (TGA) is the method of study of the thermal behavior of the polymer. **Figure 4.8** provides the information about the decomposition of a different kind of polyurethane, and from it we can observe that the decomposition occurs in three steps. According to the first step, the polyurethane showed an initial weight loss (decomposition around 20%) in the range of 50 to 380 °C, which is related to the mass loss of the volatile compound, like some additives which has been used during the synthesis process of polyurethane.

The second step is the decomposition of the urethane (around 60% decomposition of the polyurethane) in the range of 380 to 450 °C, and in the third step, the ester groups decompose (around 20% of the polyurethane) in the range of 450 to 650 °C. The thermal stability of these polyurethanes strongly depends on the urethane groups per unit volume.

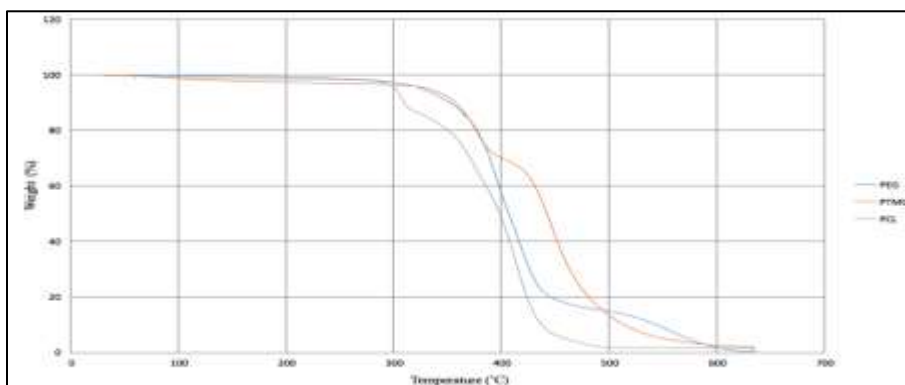


**Figure 4.8.** Thermogravimetric curves of three different polyurethane

#### **4.2.5. Mechanical Properties**

The tensile properties of the SMPU coated fabric were measured to investigate the mechanical strength of the coated fabric. The tensile strength of the coated fabrics increased compared with the uncoated control (uncoated) fabrics that have many pores, which would permit sufficient penetration of SMPU to achieve some chemical and mechanical adhesion of the film. The coated fabric is a composite of polymer and fabrics, and the final tensile strength of the polymer coated fabrics is a function of the base fabrics and SMPU materials. Tensile properties and the elongation of the coated fabrics

are almost the same. As we can see from **Table 4.2**, the elongation and strength of the CFPEG and CFPTMG are similar. The strength of the coated fabric is much better than the uncoated fabric. As we can see from Table 4, the breaking strength of the coated samples is very close and the uncoated one is too low compared with the coated sample, which is the reason the standard deviation for the breaking strength is so large while the standard deviation among the coated samples is 0.58 MPA.

**Table 4.2.** Tensile strength and elongation of uncoated and coated fabric.

Sample	Breaking load (MPA)	Breaking elongation (%)
UF (Control)	27 ± 1	21 ± 1
CFPEG	36 ± 1	22 ± 1
CFPTMG	36 ± 1	21 ± 1
CFPCL	37 ± 1	20 ± 1

#### 4.2.6. Scanning Electron Microscopy (SEM)

The surface morphology and properties of the uncoated and coated fabrics were examined by SEM. The cross-section of the above-mentioned specimens was further investigated to determine the changes in the fiber morphology as well as the fabric properties. **Figure 4.9A** shows the surface morphology of the uncoated fabric. The uncoated fabric surface contained many protruding fibers. The surface was not flat. The cross-section view of the uncoated fabric was not compacted. The cotton fibers were loose in the weaving structure and the fibers were easily eliminated. **Figure 4.9(B–D)** shows the surface morphology of the CFPEG, CFPTMG, and CFPCL. All coating concentrations became flattened compared to the control fabric. The fibers were controlled by the polymer coating. The cross-section view was compacted and thinner when compared with the uncoated one. The cotton fibers were controlled by the coating.



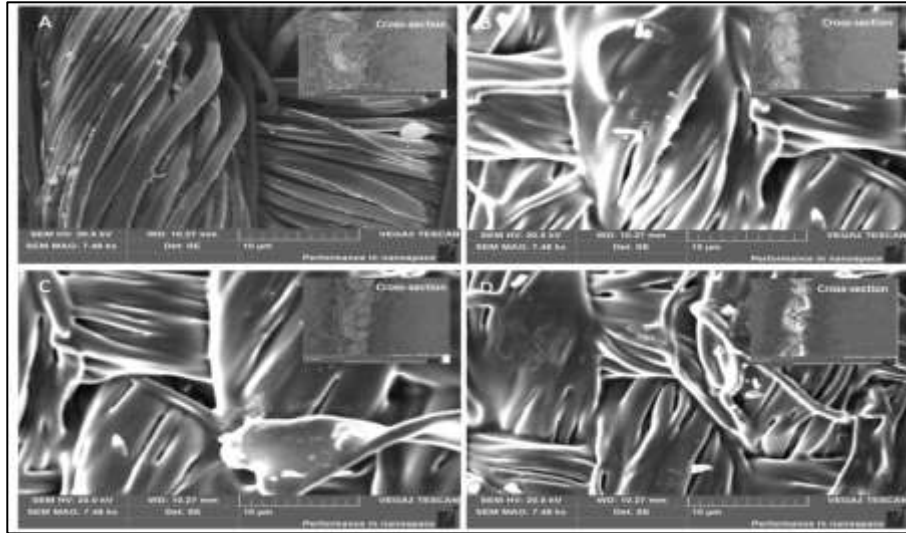


**Figure 4.9.** Surface morphology and cross section of (A) control fabric (uncoated), (B) CFPEG, (C) CFPTMG, (D) CFPCL coated fabric.

### 4.3. Summery

The use of SMPU in clothing is a new concept, particularly with water sensitivity (water-resistant and permeable). When SMPU is coated to a fabric, a functional fabric is formed. Its permeability changes as the body temperature and humidity change to form an ideal combination of thermal insulation and vapor transmitting ability for the garment. As we can see from the contact angle, the uncoated cotton fabric is not water-resistant where all the coated fabrics are water-resistant. From the results of the water vapor transmission test, it was observed that the WVT curve of the CFPEG significantly changed when both relative humidity and temperature were altered, whereas the CFPTMG and CFPCL were less sensitive to both the temperature

and relative humidity compared with CFPEG. The WVT curve of the CFPEG changed more significantly against both the temperature and relative humidity linearly with the uncoated fabric. It was concluded that the segmented CFPEG is water resistant, thermal, and moisture sensitive. In moisture-sensitive SMPU, the fabric remains less permeable and keeps body heat when the body humidity is low and can resist water droplets when needed. When the body is in a sweat condition, it allows more water vapor molecules to escape into the air because its moisture permeability becomes very high, at the same time it can protect our body from the rain because of its water-resistant property.

Published work “Jahid, M. A., et al., Fabric Coated with Shape Memory Polyurethane and Its Properties. *Polymers*, 2018. 10: p. 681.”

## Reference

1. Mustafa, E., et al., Analysis of thermal comfort properties of fabrics for protective applications. *J. Text. Inst.*, 2017. 109: p. 1091–1098.
2. Li, Y., *The Science of Clothing Comfort*. *Text. Prog.*, 2001. 1: p. 31.
3. Hu, J.L. and Mondal, S. *Temperature Sensitive Shape Memory Polymer for Smart Textile Application*; Woodhead in Association with the Textile Institute: Cambridge, UK, 2006. p. 104–121.
4. Wong, K.H., *Study of Water Vapor Permeability of Fabric Coated with Shape Memory Polyurethane*. Bachelor's Thesis, The Hong Kong Polytechnic University, Hong Kong, China, 2016.
5. Bartels, V.T. and Umbach, K.H., Water Vapors Transport through Protective Textiles at Low Temperatures. *Text. Res. J.*, 2002. 72: p. 899–905.
6. Parsons, K.C., *Human Thermal Environments*; Taylor & Francis Group: London, UK, 1993.
7. Xu, X., et al., Relationship between core temperature, skin temperature, and heat flux during exercise in heat. *Eur. J. Appl. Phys.*, 2013. 113: p. 2381–2389.
8. Mondal, S., et al., Shape Memory Polyurethane for Smart Garment. *Res. J. Text. Appar.*, 2002. 6: p. 75–83.
9. Zhang, P., et al., Thermoregulatory Responses to Different Moisture-transfer Rates of Clothing Materials during Exercise. *J. Text. Inst.*, 2001. 92: p. 372–378.
10. Mondal, S. and Hu, J.L. Water vapor permeability of cotton fabrics coated with shape memory polyurethane. *Carbohydr. Polym.* 2007. 67: p. 282–287.
11. Cho, J.W., et al., Water Vapor Permeability and Mechanical Properties of Fabrics Coated with Shape-Memory Polyurethane. *J. Appl. Polym. Sci.*, 2004. 92: p. 2812–2816.
12. Behl, M. and Lendlein, A. Shape Memory Polymers. *Mater. Today*, 2007. 10: p. 20–28.
13. Sinem, G., et al., The improved breathability of polyurethane coated cotton fabric via micro-cracking. *J. Text. Inst.*, 2017. 108: p. 1815–1821.
14. Yuan, Y. and Lee, T.R., *Contact Angle and Wetting Properties*. In *Surface Science Techniques*; Springer: Berlin/Heidelberg, Germany, 2013. 51: p. 3–34.
15. Chen, S.J., et al., Properties and Mechanism of Two-way Shape Memory Polyurethane Composites. *Compos. Sci. Technol.*, 2010. 70: p. 1437–1443.
16. Hu, J.L., et al., Shape Memory Polymers and Their Applications to Smart. *Text. Prod. J. China Text. Univ.*, 2002. 19: p. 89–93.
17. Jeong, H.M., et al., Water Vapor Permeability of Shape Memory Polyurethane with Amorphous Reversible Phase. *J. Polym. Sci.*, 2000. 38: p. 3009–3017.
18. Yang, J., et al., A New Type of Photo-Thermo Staged-Responsive Shape-Memory Polyurethanes Network. *Polymers*, 2017. 9: p.287.
19. Chung, Y.C., et al., Graft Polymerization of Polyacrylonitrile or Poly(methyl methacrylate) onto Polyurethane for the Improvement of Mechanical Properties and Water Vapor Permeability. *Bull. Korean Chem. Soc.*, 2015. 36: p.1418–1425.
20. Hu, J.L. and Zhuo, H., Shape Memory Polymers in Coating and Laminates for Textiles. In *Smart Textile Coatings and Laminates*; Woodhead in Association with the

- Textile Institute: Cambridge, UK, 2010. p. 222–233.
21. Xiao, Y., et al., Effect of phase separation on the crystallization of soft segments of green waterborne polyurethanes. *Polym. Test.*, 2017. 60: p. 160–165.
  22. Zhu, Y. et al., Effect of steaming on shape memory polyurethane fibers with various hard segment contents. *Smart Mater. Struct.*, 2007. 16: p. 969.
  23. Zhou, H., et al., Study of Water Vapor Permeability of Shape Memory Polyurethane Nano fibrous Nonwovens. *Text. Res. J.*, 2011. 81: p. 883–891.
  24. Hayashi, S., Room-temperature-functional Shape-memory Polymers. *Plast. Eng.*, 1995. 51: p. 29–31.
  25. Hornbogen, E., Comparison of Shape Memory Metals and Polymers. *Adv. Eng. Mater.*, 2006. 8: p. 101–106.
  26. Cui, B., et al., High performance bio-based polyurethane elastomers: Effect of different soft and hard segments. *Chin. J. Polym. Sci.*, 2016. 34: 901–909.
  27. Hu, J.L., *Shape Memory Polymers and Textiles*; Woodhead in Association with the Textile Institute: Cambridge, UK, 2007.
  28. Jassal, M., et al., Waterproof Breathable Polymeric Coatings Based on Polyurethanes. *J. Ind. Text.*, 2004. 33: p. 269.
  29. Ruckman, J.E. Water Vapor Transfer in Waterproof Breathable Fabrics. *J. Cloth. Sci. Technol.*, 1997. 9: p. 141–153.
  30. Gu, L., et al., Bio-based polyurethanes with shape memory behaviour at body temperature: Effect of different chain extenders. *RSC Adv.*, 2016. 6: p. 17888–17895.

# **Chapter5. Composite membrane for thermo-regulative textile.**

## **5.1. Introduction**

Climate change is one of the fundamental challenges for human civilization, with the current challenge being to keep global warming below a rise of 2°C. To keep within this limit, deployment of negative emissions technologies (NETs) is required [1, 2]. According to the Hong Kong Observatory, climate change is making Hong Kong warmer; it was reported that the temperature and relative humidity during the summer could be around 35.4°C and 95% respectively. Such hot weather can have a negative impact on human body, like heat stroke, dehydration, elevated heart rate, etc. [3, 4]. Personal cooling technology could play a vital role in controlling body heat in hot environments.

The requirement for a personal microclimate controlling system has existed for a long time. Active cooling, passive cooling and combo cooling are the three major types of cooling process. Combo cooling is the combination of active and passive cooling. Active cooling includes ventilated air cooling such as liquid supplies or external air connections, active cooling reduces both thermoregulatory and cardiovascular strain [5-9]. Phase change materials act as passive cooling materials and can reduce thermal stress and improve thermal comfort [10]. Thermo-physiological comfort is the ideal state between the environmental atmosphere and

physical and emotional harmony of the body [11]. Thermoregulation is the biological process which keeps the body temperature within the correct range when the outdoor temperature can vary. If the human body cannot maintain a normal core temperature, and it increases significantly above normal temperature, then hyperthermia can occur when the core temperature rises above 45°C. During hyperthermia proteins and enzymes may be destroyed, which can lead to death. On the contrary, when the core temperature decreases below normal temperature, then hypothermia occurs at a core temperature lower than 35°C. Hypothermia can slow the metabolism process of the human body. During exercise the body's ability to thermoregulation is affected. Metabolism (metabolism maintains the reactions which occur in the human body) produces heat as a by-product. The human body is 25% efficient; therefore, we lose approximately 75% of energy as heat [12, 13]. According to Arthur Guyton, the hypothalamus in the brain controls the body temperature.

The hypothalamus responds to different temperature receptors in the body, it uses thermo-physiological adjustment to maintain a comfortable core temperature. For example, when the surroundings are hot the skin will pass the signal on to the hypothalamus to adjust the core temperature by increasing radiation through the sweat rate (evaporation), convection and conduction. The heat exchange between the human body and the environment plays an important role in the body's

thermoregulation [14-16]. The human body releases heat by evaporation, radiation, conduction and convection. Sweat evaporation is one effective way by which to cool the human body, evaporation of sweat from the skin to the environment provides effective body cooling for individuals exposed to hot/dry environments [17]. Heat from the skin converts sweat (water) to sweat vapor, around 25% of body heat is released by sweating. During high intensity heat the human body loses up to one liter of sweat per hour. Temperature and relative humidity play a key role in controlling the sweating level. Water and electrolytes (sodium, potassium and chloride) produce the sweat, the hypothalamus in the brain senses when the core temperature is high and responds by stimulating the sweat glands to maintain a normal core body temperature. The emission of radiation is the most effective way to release heat from the skin into the environment, around 45% of body heat is released by radiation. Jonathon et al developed an infrared-transparent-visible-opaque fabric which provides passive cooling through the transmission of thermal radiation from the body to the environment [18]. It does not provide evaporative and convective behavior, which is very related to thermoregulation of the human body. Hsu et al. demonstrated a nanoporous polyethylene (nanoPE) which is transparent to mid-infrared human body radiation but which is opaque to visible light because of the pore size distribution, they then developed a textile that promotes effective radiative cooling [19], however the mechanical properties of

nanoPE are inferior compares to PE or cotton. For thermal comfort of the human body air conditioning (convection) plays a vital role. Approximately 15% of body heat can be transferred to the environment by convection. Convective cooling of the human body in hot weather improves thermal comfort [20], convective cooling facilitates the hypothalamus to control core temperature. Nowadays, most people keep their house warm in the winter and cool in the summer via air conditioning, however this consumes a lot of energy [21, 22]. Passive personal body cooling may be a better solution to overcome such a problem. Currently, there are several personal body cooling clothing materials available on the market. However, such clothing is fabricated for high performance applications, such as protective clothing and sports clothing, which is not suitable for regular use [23-26].

To overcome such challenges, we developed an Evaporative-Radiative-Convective Fabric (ERCF) that provides passive cooling by means of evaporation of perspiration, air convection and emission of radiation directly into the environment. The microclimate control fabric plays a very vital role in controlling human body temperature by transferring body heat into the environment in different ways during the summer season when the surrounding temperature is too high (**Figure 5.1 (A-D)**). One of these methods is evaporation, the prepared composite membrane was super evaporative, most textile fibers are either water absorbent or resistant, but the ERCF we prepared is water vapor permeable.



Therefore, this kind of evaporative behavior may provide evaporative cooling to the wearer. A limited range of body heat can be transported from the skin into the environment by air convection, the ERCF has air permeability behavior which can provide air convection to the human body. When there is no wind convective cooling occurs by temperature or density difference, which can be called “free convection”. Usually, convective cooling during high speed winds is better for comparing temperature or density difference. Emission of radiation is the most effective way to release body heat, transporting the heat via electromagnetic waves. Radiative cooling provides an effective way to surpass conventional ways of microclimate controlling. Radiative thermal management can be achieved by controlling transmissivity, emissivity and reflectivity [27-30]. The ERCF provides the necessary body cooling for an individual to feel comfortable at different temperature levels. The proposed super evaporative composite membrane was prepared using a hydrophilic segmented polyurethane (PU) solution along with hollow silica aerogel. Different weight percentages of silica aerogel were added (0.5 & 1wt %, named as composite 0.5% & composite 1%, respectively). This kind of responsive PU has the capability to respond to specific changes in their surroundings (temperature and relative humidity). Hydrophilic segmented PU is composed of soft (polyol) and hard segments (di-isocyanate and chain extender).

Soft segment (polyol) is the responsive part of the PU and hard segment gives the PU its mechanical properties.

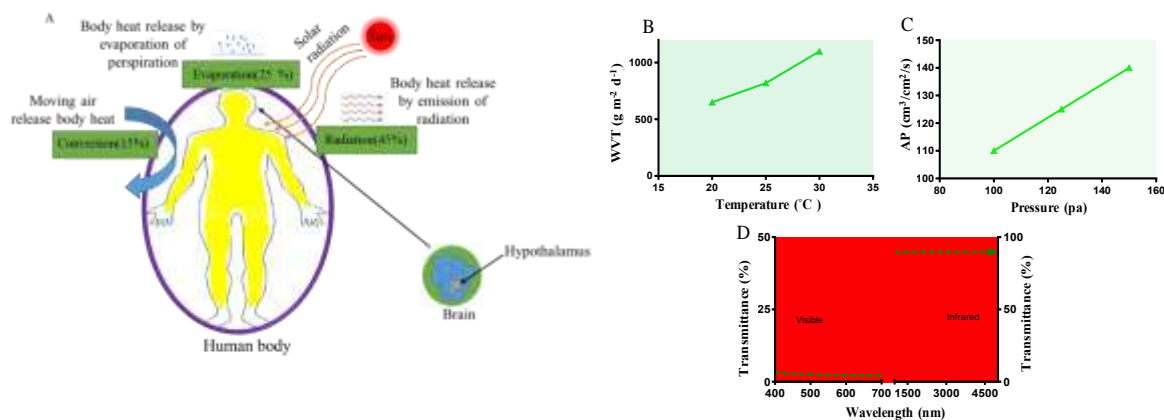


**Figure 5.1.** Thermal management of human body **A)** the way human body release heat (emission of radiation, evaporation of perspiration, releasing heat by air convection), **B)** water vapor transmission (WVT) of laminated fabric, **C)** Air permeability (AP) of laminated fabric, **D)** Transmittance of visible light and infrared radiation composite membrane.

## 5.2. Results and discussion

### 5.2.1. Water vapor transmission mechanism of composite membranes

Hydrophilic silica aerogels are nanoporous, and low density with an open pore structure. Highly porous three-dimensional silica aerogel networks (**Figure 4.2(A-B)**) contain some extraordinary properties, such as low thermal conductivity (~0.02

W/mK), high specific surface area (450-950 m<sup>2</sup>/g), etc. Porous silica aerogel contains lots of hydroxyl (-OH) on its backbone (**Figure 4.2 (C)**), such structures have led to silica aerogel being used in a wide variety of scientific and industrial applications [229,230], after making the composite membrane we laminated (**Figure 5.2(D)**) them with woven fabric (cotton). These hydroxyl (-OH) groups on silica aerogel facilitate the achievement of water vapor permeability of the composite membrane. A self-adaptive water vapor permeability membrane has many applications such as laminated textiles, gas separation, food packaging, wound dressing [33,34], etc. Porous skin covers the human body, which perspires all the time; it contains more than 60% of water under normal core temperature (36-37°C). It would be a crucial property of a textile to have the ability to transport such perspiration from the body surface to the environment for controlling the thermo-physiological comfort of the human body. Thermal comfort is controlled by body sweat in vapor form and its transmission from inside the fabric to the environment. The sweat glands begin the production of perspiration while heat transmission from the skin to the environment decreases. Normally, the body sweat in vapor form is termed insensible perspiration, and the body sweat in liquid form is termed sensible perspiration [11]. When perspiration is transported from skin to the environment it contains body heat, thus adjusting the body heat level. If the water vapor transmitting ability rate is low or limited then it increases body

temperature and causes heat stress in hot environments. Water vapor permeability through fabric plays a significant role in adjusting body comfort during both hot and cold environments, or during high activity levels. To provide wearing comfort, the fabric should have a high level of water vapor transmission so that body sweat can evaporate and be transmitted from the skin to the environment.

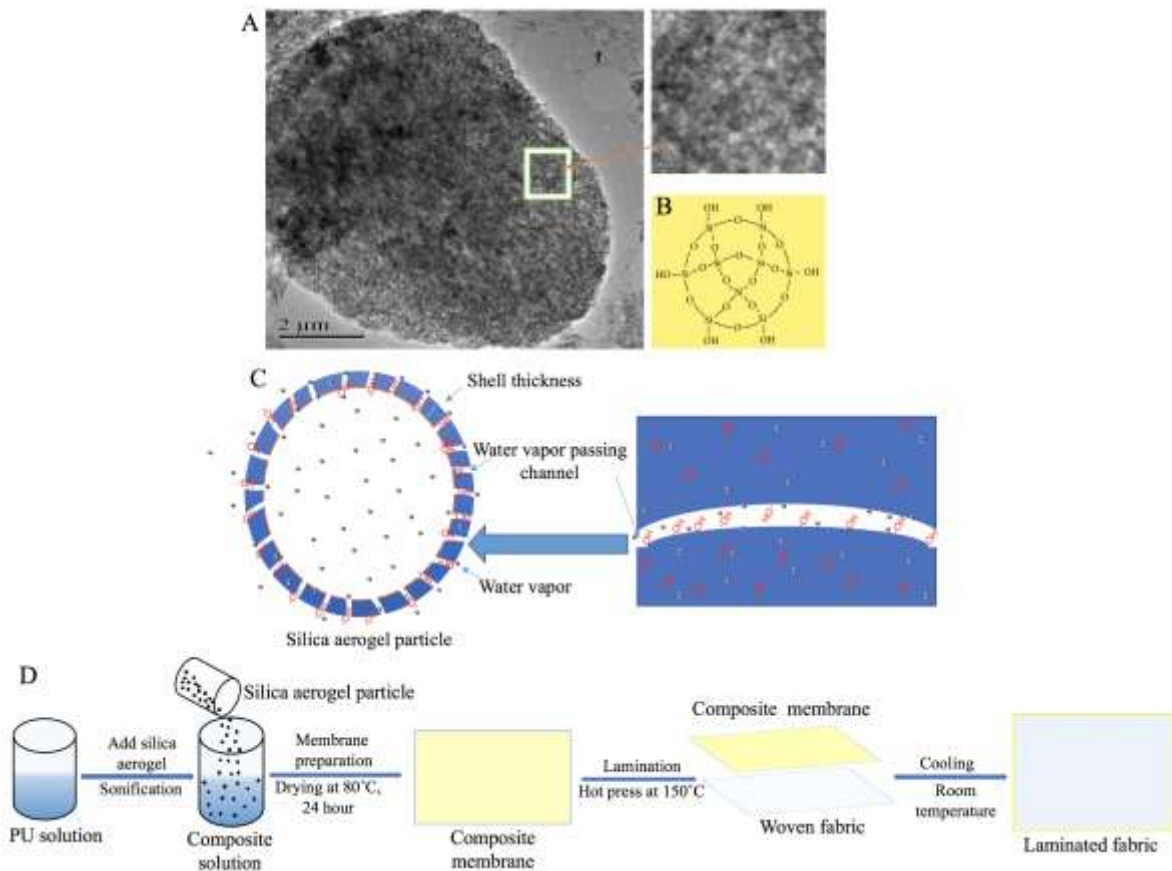


**Figure 5.2.** A) TEM image of silica aerogel particle (scale 2μm, 50nm), B) Structure of silica aerogel, C) Schematic of hollow silica aerogel and water vapor passing channel, D) The fabrication process laminated fabric.

### **5.2.2. Water vapor transmission**

Nowadays, energy efficient and environmentally friendly cooling systems are receiving huge attention. Air conditioning systems consume more energy, to reduce the energy consumption of air conditioning systems evaporative cooling can be a better alternative [35,36]. Evaporative cooling is the reduction of heat by evaporation of perspiration, this moves latent heat from the skin into the environment. Evaporative cooling is different from typical air conditioning; in evaporative cooling the water absorbs a huge amount of latent heat during evaporation. When the core temperature of the body increases, the hypothalamus attempts to control the core temperature by releasing heat through perspiration. To pass this perspiration from the surface of the body into the environment we have developed an evaporative cooling fabric (**Figure 5.3(A-E)**); the relationship between WVT, temperature, relative humidity is shown in (**Figure 5.3(F)**). Cotton is a highly water absorbent cellulosic material; the moisture absorption rate of cotton is around 7-8%. To make the evaporative cooling fabric, we laminated the cotton weaved fabric via a highly evaporative thermo-moisture responsive PU composite membrane. The composite membrane was prepared by adding hydrophilic hollow silica aerogel with PU. Segmented hydrophilic PU was synthesized, then super moisture absorbent hollow silica aerogel was added in order to make a highly evaporative film. Our composite membrane and laminated

fabric has a high water vapor permeability property to control the personal microclimate of the human body, as seen in **Figure 5.3(D)**, composite 1% has better WVT ( $1859 \text{ g m}^{-2} \text{ d}^{-1}$ ) than PU alone ( $1065 \text{ g m}^{-2} \text{ d}^{-1}$ ) or cotton fabric ( $1190 \text{ g m}^{-2} \text{ d}^{-1}$ ) at  $40^\circ\text{C}$  temperature. Furthermore, WVT of composite 1% has  $859 \text{ (g m}^{-2} \text{ d}^{-1})$  where PU has only  $440 \text{ (g m}^{-2} \text{ d}^{-1})$  at relative humidity 90% (**Figure 5.3(E)**). This type of microclimate controlled cooling fabric has been developed to minimize body heat related diseases such as heat stroke and other heat related injuries in extreme weather. A hot environment reduces the working efficiency of the body. Evaporation of perspiration is an extremely effective way by which to cool the body in a hot environment. Moreover, when the core temperature of the body increases it directly influences physical performance and metabolism. Uncontrolled metabolism can cause serious physical defects and cause the body to work inefficiently. Research has shown that if human thermoregulation can be controlled and body efficiency increased, then the risk of heat related disease is limited. Personal cooling fabrics can enhance working time by keeping the body cool. When metabolic heat is produced it passes the signal to the hypothalamus which distributes the heat to different parts of the body via blood circulation to release body heat by evaporation of perspiration, convection, radiation and conduction. Thus, the hypothalamus controls the core temperature of the body. Water vapor permeability through the membrane strongly depends on the

microstructure and hydrophilicity of the PU. The physical and chemical properties mostly depend on the soft and hard segment ratio, and the molecular weight of the monomer and processing parameter. Incorporating hollow silica aerogel makes the PU membrane more water vapor and air permeable, radiative, and robust. The hollow silica aerogel has a super affinity to moisture and can pass water molecules to the environment by using its hollow water vapor passing channel. **Figure 5.4** is showing the methods of water vapor transmission, and **Figure 5.5** is showing the relationship between water vapor transmission, relative humidity and temperature.

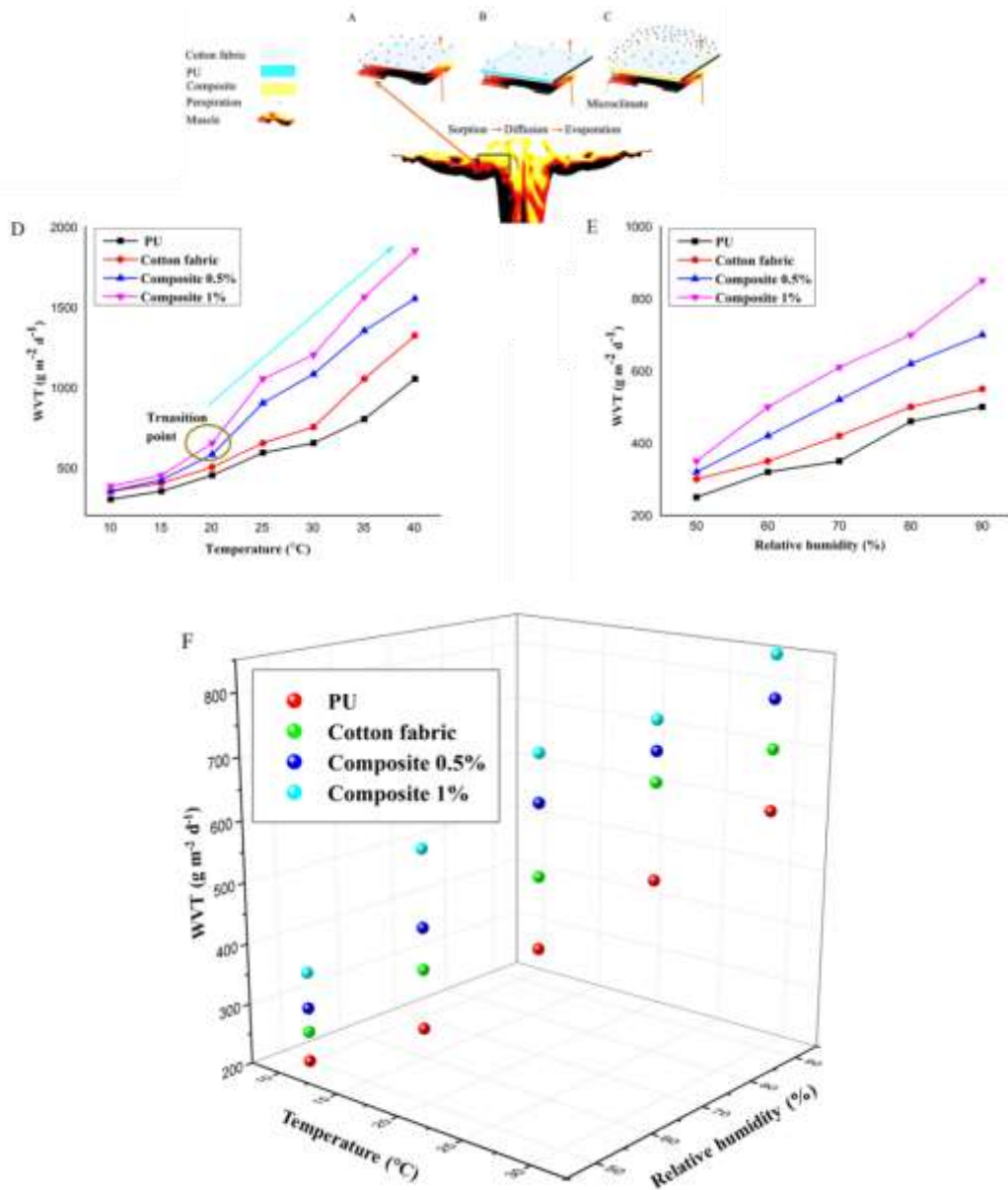


**Figure 5.3.** Mechanism of evaporation of perspiration **A,B,C)** Evaporation of perspiration with fabric (cotton), PU layer and with composite layer, **D)** Water vapor transmission results of laminated fabric of PU, composite 0.5%, composite 1%, and cotton fabric as a function temperature, **E)** Water vapor transmission results of laminated fabric of PU, composite 0.5%, composite 1%, and cotton



fabric as a function of relative humidity, F) The relationship between water vapor transmission, temperature, and relative humidity.

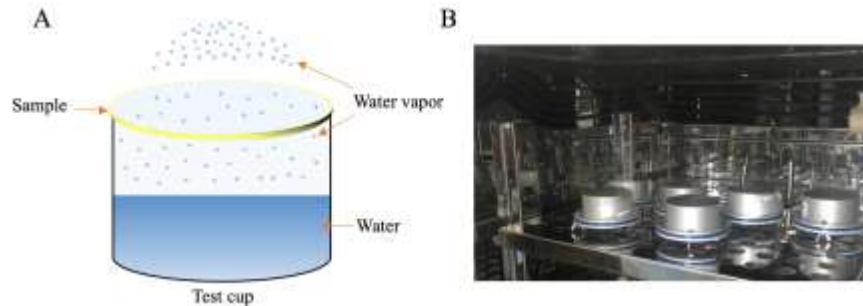


**Figure 5.4.** A) Testing mechanism of water vapor transmission, and B) Temperature and relative humidity controlled climate chamber where water vapor transmission testing took place.

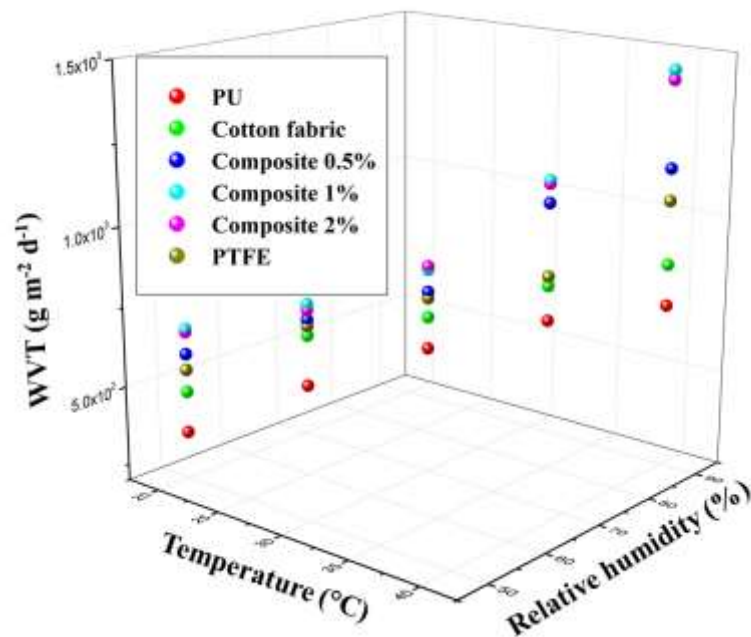


**Figure 5.5.** The relationship between water vapor transmission, temperature, and relative humidity.

**Figure 5.5**, There are several membranes has been using for making laminated textile, Polytetrafluoroethylene (PTFE) is one mostly used membrane for laminated textile, company like Gore-Tex has been using PTFE membrane for a long time for breathable textile. From WVT data, we can see that the water vapor transmission rate of composite 1 and 0.5% is significantly higher than the PTEF, at some point, it's around 30% higher. We also tried with composite 2% here and found that composite 2% has an almost similar result as composite 1%, it's because silica aerogels compactness probably, that is the reason we tried with composite 1% only, which showed significantly better result compare with all the membranes we used.

### **5.2.3. Air permeability, mechanical property, absorbency of membranes.**

Convection is one heat transfer mechanism of the body; convection contributes to the transportation of body heat from the body's surface into the environment. During the convection process air removes body heat from the skin to the environment and cools down the body during high activity. Heat stroke is a common reason of death during extreme weather or high activity such as marathon running; convective clothing could play a significant role in minimizing these deaths, our composite membrane and laminated fabric has the ability to cool down

our body by air convection (**Figure 5.6(A, B)**), and warm the body during high activity levels and in extreme weather. Nowadays, heat related diseases are increasing greatly because of global climate change, diseases range from neurological diseases, cellular damage, to many more heat related illnesses, and may cause death. Li et al has reported the devastating effects on human health from recent heat waves in China as a consequence of extreme heat stress [37]. It has also been suggested that children and the elderly are most affected during summer, because of high temperatures. Air convection play a major role in minimizing such heat related diseases, our laminated fabric has the ability to circulate air in hot conditions. Air permeability was measured on an instrument designed to pressure air through the laminated fabrics. The rate of air passing through the test specimen was significant, except for the PU laminated fabric. Cotton fabric has better air permeability ( $160 \text{ cm}^3/\text{cm}^2/\text{s}$  at 150 pa pressure) because of its porous woven structure, whereas composite membranes ( $140 \text{ cm}^3/\text{cm}^2/\text{s}$  at 150 pa pressure (composite 1%), and  $100 \text{ cm}^3/\text{cm}^2/\text{s}$  at 150 pa pressure (composite 0.5%)) also have better air permeability. Normally, air permeable material allows water vapor to pass through and therefore water vapor transmission is closely related to the air passing ability of the material. Water vapor permeability also depends on the material's chemical structure. The pore from the woven fabric structure and porous silica aerogel facilitates the air permeability of the laminated fabric. For thermo-

physiological comfort, air permeability is a very important property of a fabric. The first step of water vapor transmission is absorption, followed by diffusion and evaporation. Additionally, water vapor transmission mostly depends on the water absorbance ability of the material (**Figure 5.6(D)**). The water absorbency of composite samples is significantly higher than the cotton fabric and PU. As seen in **Figure 5.6(C)**, composite materials re-enforce the laminated fabric, composite samples are significantly strong and elastic compare with cotton fabric. Toughness and tensile modulus also showed the similar result that composite samples are significantly stronger compare with PU (**Figure 5.8**). The wicking height rate reveals the moisture absorbency ability of the material. Normally, composite materials has better wicking height in both a warp and weft directions because its water absorbent ability and hydrophilic group in the backbone ((**Figure 5.7 (E, F)**)). Cotton fabric also has a good wicking height compared with PU membrane. To check the adhesiveness and abrasion resistance of the laminated fabric we performed an abrasion resistance test (**Figure 5.7(G)**) and found that there was almost no weight loss; there is also no yarn breakage after rubbing the laminated fabric 1000 times (50 per min) with 9 kPa load, which means the laminated fabric has very good abrasion resistant property.

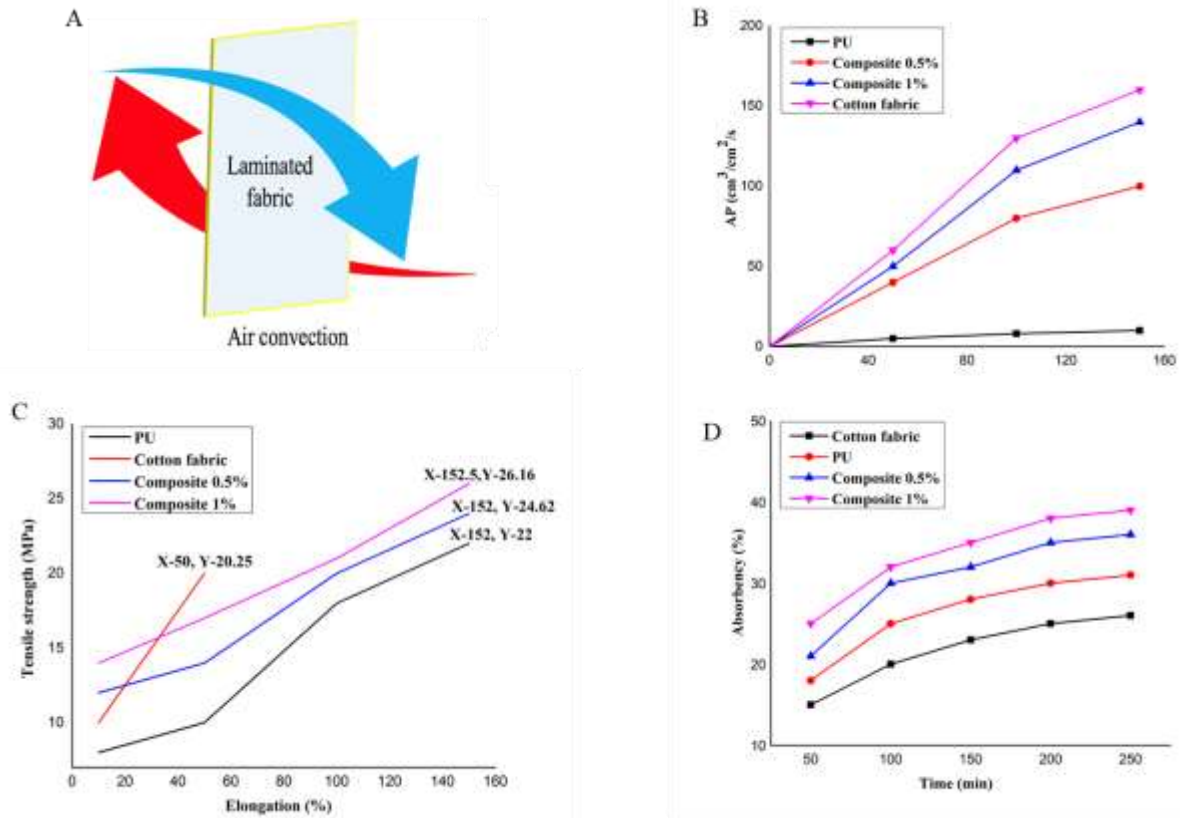


**Figure 5.6.** A) Air convection of laminated fabric, B) Air permeability result of laminated fabric (PU, Composite 0.5% and 1%) and control (fabric), C) Mechanical properties of laminated fabric D) Water absorbency of laminated fabric.

## 5.2.4. Wicking height and mechanical property of membranes.

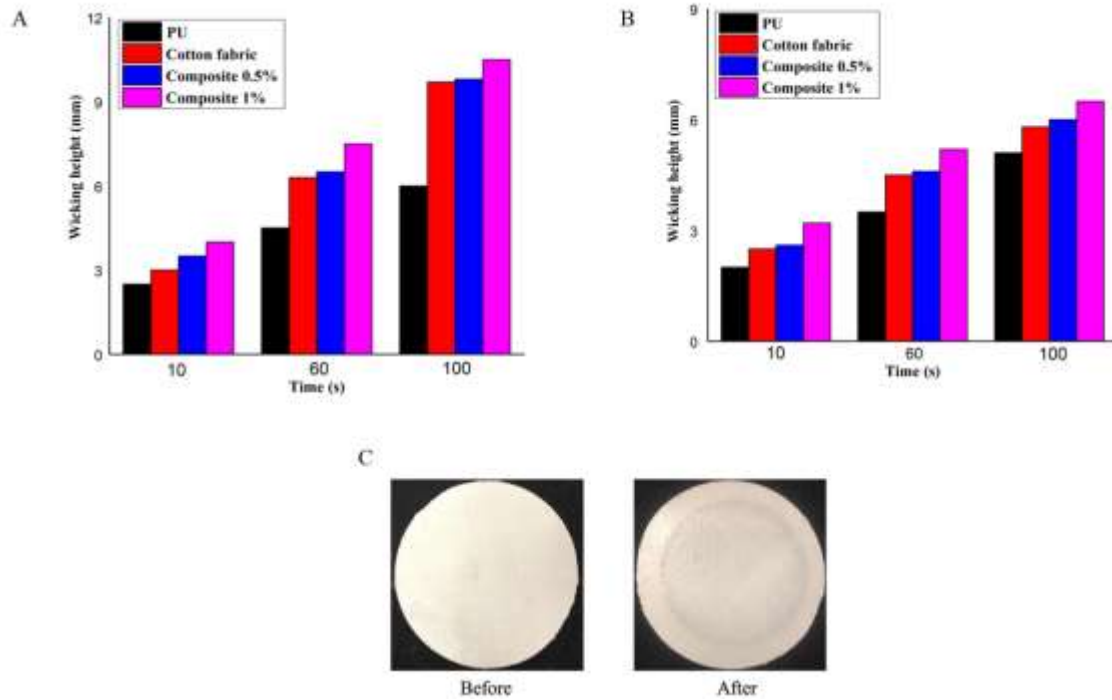


**Figure 5.7.** A) Wicking properties of laminated fabric (warp direction), B) Wicking properties of laminated fabric (weft direction), C) Abrasion resistance property of laminated fabric.

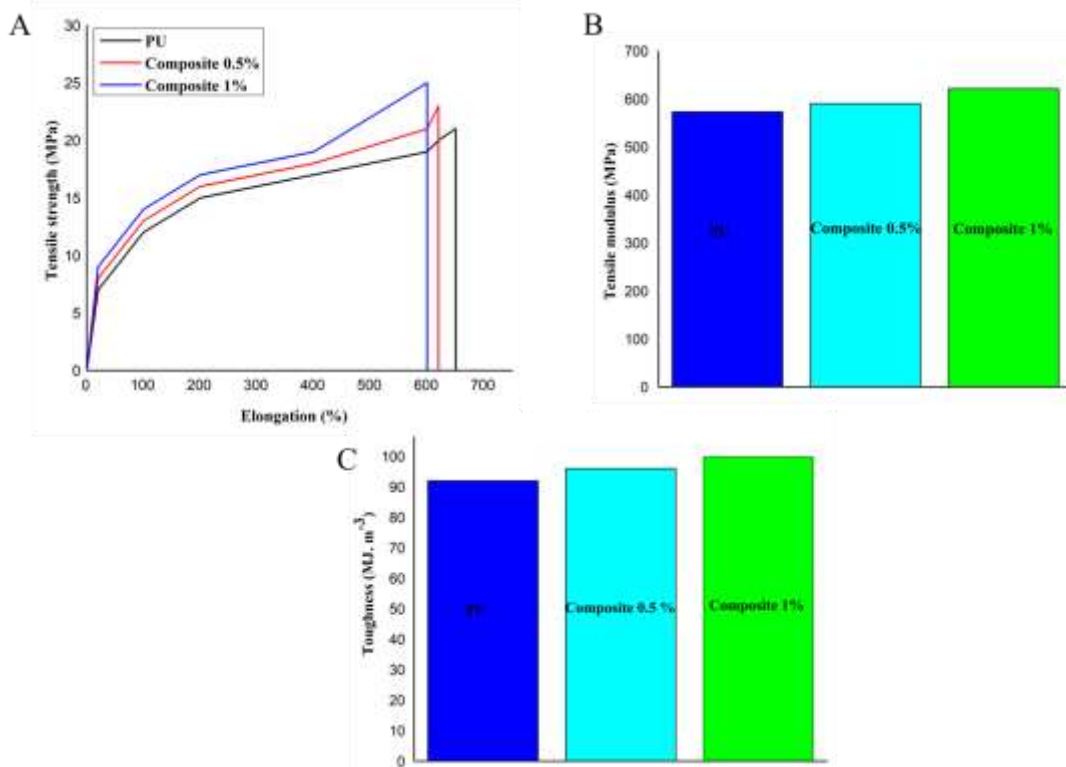


**Figure 5.8.** A) Stress strain profile, B) Tensile modulus and C) Toughness of PU, composite 0.5% and composite 1% membranes.

The tensile strength, elongation, tensile modulus, toughness of membranes showed in **Figure 5.8 (A-C)**. In **Figure 5.8 (A)**, all the materials we used are mechanically strong and highly elastic. The resistance to elastic deformation of the material is also higher, as we can see from **Figure 5.8 (B)**, all the materials we used required a higher stress to deform, which reveals the higher tensile modulus of the materials, tensile modulus of composite 1% is 621 MPa, composite 0.5% is 590 MPa and PU is 573 MPa, which means the tensile modulus of composite 1% is better to compare with composite 0.5% and PU. The toughness also a very important

property of a material, which reveals the material's strength and ductility. To see how much energy our materials can absorb before rupturing, the toughness of materials (**Figure 5.8 (C)**) showed that, composite 1% ( $99.8 \text{ MJ.m}^{-3}$ ) has better toughness compare with composite 0.5% ( $95.9 \text{ MJ.m}^{-3}$ ) and PU ( $91.8 \text{ MJ.m}^{-3}$ ).

### **5.2.5. Radiative property of membranes**

Radiative heat emission is an effective way by which to release heat from the skin to the environment. Approximately 45% of body heat is released into the environment by the emission of radiation. The human body is mid-infrared radiative in the wavelength range between 7 to  $14\mu\text{m}$  [19, 38]. The traditional textile is not IR transparent and our human skin is a super IR emitter, therefore the IR transmittance textile provides thermal comfort to the body. Since textile materials are very heat absorbent, fabric temperature rises rapidly when exposed to thermal sources [37]. Silica aerogel and composites made by using silica aerogel can be considered as semi-transparent materials capable of absorbing, emitting, and radiating heat [39-41]. Our fabricated composite membrane successfully transmitted more than 90% of inferred radiation with a wavelength longer than  $7 \mu\text{m}$  (**Figure 5.9 (B, C)**). The schematic of ERCF (**Figure 5.9 (A)**) shows that the outer surface of the laminated fabric (cotton) reflects solar radiation and the inner surface of laminated fabric (composite membrane) transmits IR from the body. The



presence of silica aerogel has improved the IR transmittance of the laminated fabric (**Figure 5.9(B,C)**). Consequently, PU composites showed better transmittance compared to pristine PU, where cotton fabric showed almost zero transmittance. To maintain the human thermoregulation system and a constant body temperature, our developed ERCF could play a vital role.

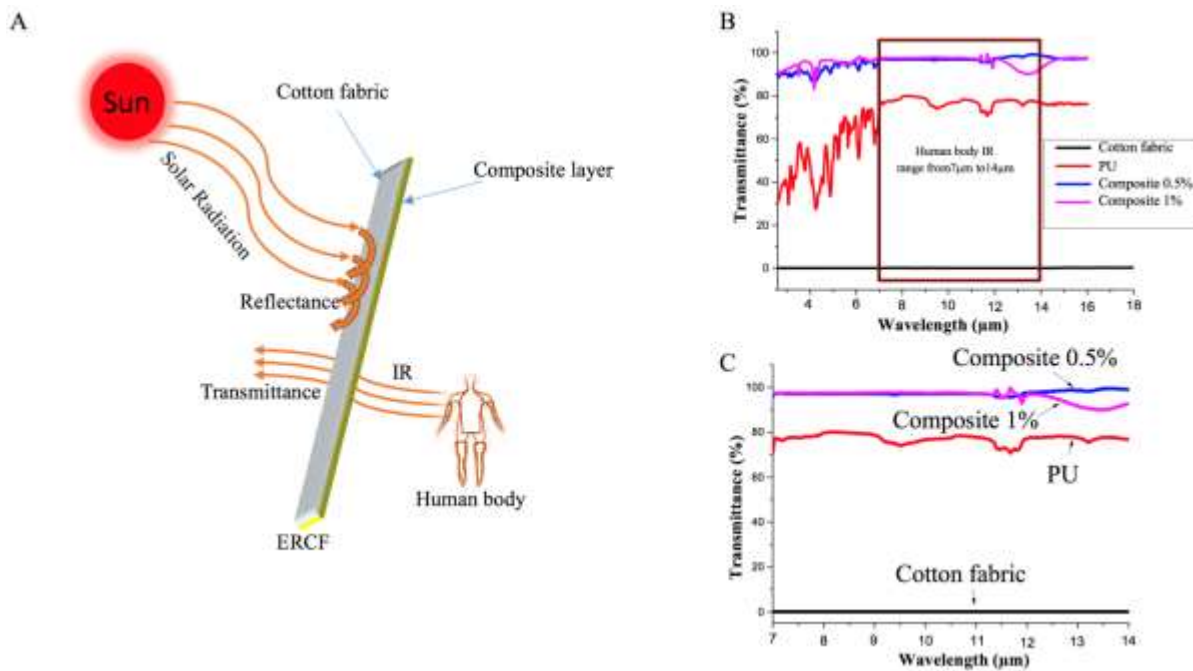


**Figure 5.9.** A) The behavior of ERCF with solar radiation and IR radiation, B) IR transmittance percentage of Cotton fabric, PU, Composite 1% and Composite 0.5% (range 3-18 $\mu\text{m}$ ), C) IR transmittance percentage of Cotton fabric, PU, Composite 1% and Composite 0.5% (range 7-14 $\mu\text{m}$ ).

### 5.2.6. SEM and DSC of samples

Figure 5.10 is showing the SEM of laminated, fabric and cross-section of laminated fabric, Figure 5.11 is showing the DSC of polyurethane and composites.

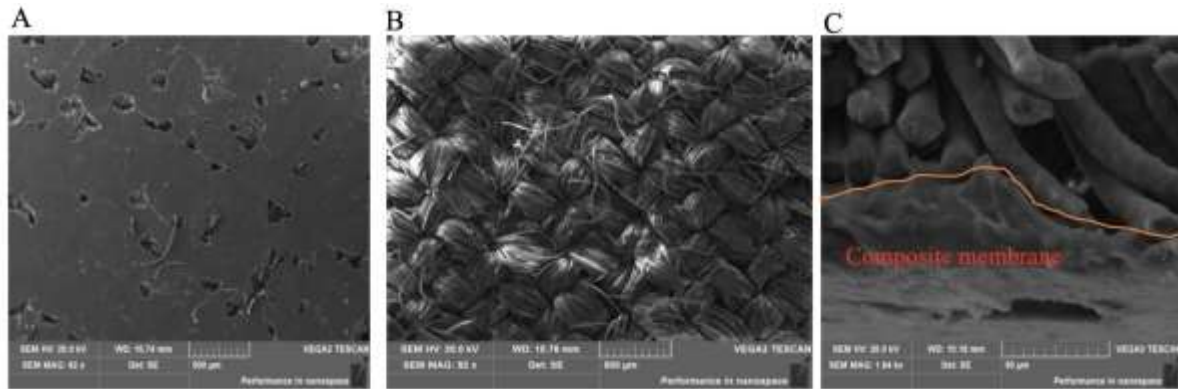


Figure 5.10. Scanning Electron Microscopy (SEM) images of A) Laminated fabric, B) Woven fabric, and C) Cross-sectional view of laminated fabric.

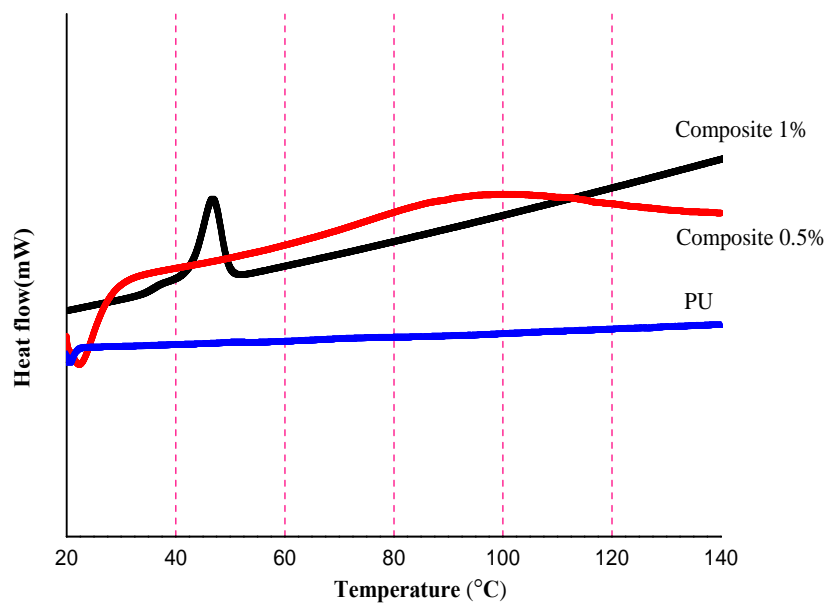


Figure 5.11. DSC of PU, composite 0.5% and composite 1% membranes.

### **5.3. Summery**

Developed ERCF can control 85% of body heat. Climate change is increasing the global temperature daily, the current challenge is to keep the global temperature below a variation of 2°C, to do so requires sustainable and significant global mitigation. Hot outdoor environments can have a negative impact on the body, such as heat stroke, dehydration, elevated heart rate, etc. During high activity, or in a hot environment, metabolism produces heat as a by-product. The body is 25% efficient; therefore, we lose around 75% of energy as heat. To overcome such challenges our ERCF can play an important role by providing passive cooling by evaporation of perspiration, air convection and emission of radiation from the body directly to the environment. ERCF has a vital role in controlling body temperature by transferring body heat through various mean into the environment during the summer season or when the surrounding temperature is too high. Approximately 25% of body heat is released by evaporation of perspiration; the evaporative behavior of the ERCF could provide evaporative cooling by releasing 25% of body heat during extreme weather. Air convection can transport around 15% of body heat from the skin to the environment; the ERCF has an air permeability behavior which can provide air convection to the human body. Emission of radiation is the most effective way by which to release body heat, around 45% of body heat can be

transported by emission of radiation through electromagnetic waves. Radiative cooling provides an effective way by which to surpass conventional methods of controlling the microclimate. The ERCF I have developed provides the necessary body cooling for an individual to feel comfortable at different temperature levels.

## Reference

1. Glen, P.P., et al., The challenge to keep global warming below 2°C. *Nature Clim. Change*, 2013. 3: p. 4-6.
2. Pete, S., et al., Biophysical and economic limits to negative CO<sub>2</sub> emissions. *Nature Clim. Change*, 2016. 6: p. 42-50.
3. Study on the effectiveness of personal cooling equipment for protecting workers from heat stroke while working in a hot environment. Occupational safety and health council, Hong Kong, 2013. p. 1-44.
4. Maxwell, F., et al., The relationship between outdoor thermal conditions and acute injury in an aluminum smelter. *Inter. J. Ind. Ergono.*, 2005. 35: p. 47–55.
5. Selkirk, G. A., et al., Active Versus Passive Cooling During Work in Warm Environments While Wearing Firefighting Protective Clothing. *J. Occup. Environ. Hyg.*, 2004. 1: p. 521–531.
6. Perez, M. S., et al., Novel shape-memory polyurethane fibers for textile applications. *Text. Res. J.*, 2019. 89: p. 1027-1037.
7. Meng, Q. and Hu, J. L. A temperature-regulating fiber made of PEG-based smart copolymer. *Solar Ene. Mat. And Solar cells*, 2008. 92: p. 1245-1252.
8. Yong, Z., et al., Shape memory effect of PU ionomers with ionic groups on hard-segments. *Chi. Jour. of Polym. Sci.*, 2006. 24: p. 173-186.
9. Zhang, L., et al., All-Textile triboelectric generator compatible with traditional textile process. *Adv. Mat. Tech.*, 2016. 1: p. 160047.
10. Randi, E. R., et al., Optimizing the Performance of Phase-Change Materials in Personal Protective Clothing Systems. *Inter. J. Occup. Safe. Ergono.*, 2008. 14: p. 43–53.
11. Jahid, M. A., et al., Fabric Coated with Shape Memory Polyurethane and Its Properties. *Polymers*, 2018. 10: p. 681.
12. Meng, Q., et al., Thermal sensitive shape recovery and mass transfer properties of polyurethane/modified MWNT composite membranes synthesized via in situ solution pre-polymerization. *J. Membr. Sci.*, 2008. 319: p. 102-110.
13. Yang, X., et al., Moisture-responsive natural fiber coil-structured artificial muscles. *ACS Appl. Mater. Interfaces*, 2018. 10: p. 32256-32264.

14. Wu, Q. and Hu, J. L., A novel design for a wearable thermoelectric generator based on 3D fabric structure. *Smart Mater. Struct.*, 2017. 26: p. 045037.
15. Aizezi, M., et al., High-Strength Triple Shape Memory Elastomers from Radiation Vulcanized Polyolefin Elastomer/Polypropylene Blends. *ACS Appl. Polym. Mater.*, 2019. 1: p. 1735-1748.
16. Dusan, F., et al., A computer model of human thermoregulation for a wide range of environmental conditions: the passive system. *The Amer. Physio. Soci.*, 1999: p. 1957-1972.
17. Uwe, R., and Ravindra, S. G., Fabric Cooling by Water Evaporation. *Jour. of Fib. Bioeng. and Infor.*, 2016. 9: p. 237-245.
18. Jonathan, K. T., et al., Infrared-Transparent Visible-Opaque Fabrics for Wearable Personal Thermal Management. *ACS Photo.*, 2015. 2: p. 769–778.
19. Po-Chun, H., et al., Radiative human body cooling by nanoporous polyethylene textile. *Science*, 2016. 353: p. 1019-1023.
20. Yoshihito, K., et al., Convective Heat Transfer Coefficients of the Human Body under Forced Convection from Ceiling. *Jour. of Ergono.*, 2014. 4: p. 1000126.
21. Micheal, W. B., and Katherine, A. C, Heat related illnesses. *Am. Fam. Physician*, 1998. 1: p. 749-756.
22. Steven, C. and Arun, M, Opportunities and challenges for a sustainable energy future. *Nature*, 2012. 488: p. 294-303.
23. Hu, J. L., et al., Self-adaptive water vapor permeability and its hydrogen bonding switches of bio-inspired polymer thin films. *Mater. Chem. Front.*, 2017. 1: p. 2027- 2030.
24. Thakur, S., et al., Mechanically strong shape memory polyurethane for water vapour permeable membranes. *Polym. Inter.*, 2018. 67: p. 1386-1392.
25. Meng, Q. H. and Hu, J. L., A temperature-regulating fiber made of PEG-based smart copolymer. *Sol. Ener. Mate. and Sol. Cel.*, 2008. 92: p. 1245-1252.
26. Mondal, S. and Hu, J. L., Structural characterization and mass transfer properties of nonporous segmented polyurethane membrane: influence of hydrophilic and carboxylic group. *J. Membr. Sci.*, 2006. 274: p. 219-226.
27. Norman, N. S., et al., Keeping cool: Enhanced optical reflection and radiative heat dissipation in Saharan silver ants. *Science*, 2015. 349: p. 298-301.
28. Aaswath, P. R., et al., Passive radiative cooling below ambient air temperature under direct sunlight. *Nature*, 2014. 515: p. 540- 544.
29. Winslow, C. E. A., et al., The influence of air movement upon heat losses from the clothed human body. *Amer. Physio. Soci.*, 1939. P. 505- 518.
30. Po-Chun, H., et al., A dual-mode textile for human body radiative heating and cooling. *Sci. Adv.*, 2017. 3: p. 1-8.
31. Hrubesh, L. W., The world's lightest solids, *Chem. And Ind.*, 1990. 24: p. 824-827.
32. Mulder, C. A. M and Van Lierop, J. G., in: J. Fricke (Ed.), *Aerogels*, Springer, Berlin, 1986. 68:.
33. Catherine, O., et al., Methods of Evaluating Protective Clothing Relative to Heat and Cold Stress: Thermal Manikin, Biomedical Modeling, and Human Testing. *J. Occup. Environ. Hyg.*, 2011. 8: p. 588–599.
34. Boateng, J. S., et al., Wound healing dressings and drug delivery systems: a review. *J. Pharm. Sci.*, 2008. 97: p. 2892–2923.
35. Hu, J. L., et al., Recent advances in shape–memory polymers: Structure, mechanism, functionality, modeling and applications. *Prog. in Poly. Scie.*, 2012. 37: p. 1720– 1763.

36. Devin, J. R., et al., Long liquid crystal elastomer fibres with large reversible actuation strains for smart textiles and artificial muscles, *ACS Appl. Mater. Interfaces*, 2019. 11: p. 19514-19521.
37. Bai, L., et al., The effects of summer temperature and heat waves on heat-related illness in a coastal city of China, 2011–2013, *Environ. Res.*, 2014. 132: p. 212–219.
38. Zdraveva, E., et al., The efficacy of electrospun polyurethane fibers with  $\text{TiO}_2$  in a real time weathering condition, *Text. Res. J.*, 2018. 88: p. 2445-2453.
39. Hui, Z., et al., Transmittance of Infrared Radiation Through Fabric in the Range 8–14  $\mu\text{m}$ . *Tex. Res. J.*, 2016. 80: p. 1516–1521.
40. Cheng, D., et al., Surface Characterisation of Polyelectrolyte/Silver Nanocomposite Films. *Polym. & Polym. Com.*, 2017. 25: p. 635-642.
41. Jin, S., et al., Preparation of breathable and superhydrophobic polyurethane electrospun webs with silica nanoparticles, *Text. Res. J.*, 2019. 86: p. 1816-1827.

# **Chapter6. Porous membrane for smart textile application.**

## **6.1. Introduction**

The structures and properties of 3D polymeric porous membranes are of great importance in various applications such as laminated fabric, cell seeding, bio-material, and tissue engineering. Porous polymeric membranes are produced in different ways. For example, through the leaching of soluble particles, gas foaming, solvent removal by freeze-drying, liquid-solid phase separation, liquid-liquid phase separation, etc. The properties and surface morphology of the emergent porous membrane is mainly dependent on the phase separation mechanism and the varying amounts of leachable particles [1,2]. A porous polyurethane membrane was used to investigate the various applications mentioned because of its exceptional mechanical properties and flexibility.

Particulate leaching is a frequently used and simple method for preparing porous polymeric membranes. It usually uses NaCl salt or organic compounds such as saccharose to produce the pores [3]. The particulate leaching technique involves the dissolution of a water-soluble solute (sugar, salt) from a polymer/solute composite system [4]. The shape and size of the pores are proportional to the dimensions and size of the leached particles. Usually, the pores take over the particle size, therefore the membrane pore size can be controlled through the

selection of an appropriately sized particle. Additionally, the effect of pore size on the membrane's mechanical properties also needs to be considered [5]. The central benefit of the particulate leaching technique is the simple approach of specialized equipment without requirements. The primary disadvantage of such a technique is that it requires a lot of time and that there is the potential difficulty of controlling the material's porosity [6]. To increase the inter-connectivity between pores, other methods for preparing the membranes have been suggested which combine particulate leaching with other fabrication methods. For example emulsion freeze-drying, phase separation, and gas foaming [7]. Thermally induced phase separation (TIPS) is another method that is frequently used to produce highly porous polymeric scaffolds. The TIPS quenches the polymer solution below the freezing point of the solvent and this induces liquid-liquid separation [5]. Two different phases are formed, such as a polymer-rich phase and a polymer-poor phase. The polymer-rich phase solidifies, whilst the polymer-poor phase crystallizes. Highly porous structures form (about 90%) when the crystals are removed [8,9]. The polymer solution concentration controls the porous membrane structure, which also depends on the quenching rate and quenching temperature [10]. The pore shapes can be controlled by altering the TIPS method. However, the TIPS method only produces a laminated range of pore sizes and it has difficulty producing a diameter greater than 200 $\mu\text{m}$ . It is also difficult to control the porous membrane's



micro-structure [11]. Gas foaming is also used to prepare porous membranes. Foaming can be achieved by reacting the components with one another or by releasing the gas, which is produced by the thermal degradation of the gas foaming agent.

For example, a preparation of PU foams when water is added to the reaction mixture. this then reacts with the isocyanate group and forms the carbamic acid derivative, subsequent to which decarboxylation produces carbon dioxide. This method is rarely used for preparing the porous membrane. It is difficult to control the diameter of the pores. Usually, the porous PU material is prepared by a gas foaming method and it is primarily used for bone generation [12-14]. The benefit is that organic solvents are not required when using the gas foaming method. There is some difficulty in terms of controlling pore size and interconnection, as usually the foaming process creates closed pores inside the polymer structure, which is a disadvantage [15-17]. Melt moulding and emulsion freeze-drying are also used to prepare a polymeric scaffold.

Highly permeable and selective microporous membranes are attractive for liquid and gas separation processes such as evaporation and distillation, which are used in the oil, energy, gas, and pharmaceutical industries [18-21]. These highly porous membranes are also used to obtain laminated water vapor permeable and droplet resistant textile [22-26].

In this chapter, highly water-soluble silica particles were used for preparing the PU composite membrane. The particles were leached out using the sonication method (5min). The studied particulate leaching technique provided a very high and homogeneous porous PU membrane. The prepared water vapor transmittable and water droplet resistant porous PU membrane was then used for apparel applications. Scanning electron microscopy was used to investigate the surface morphology. To prove the co-existence of the water droplet resisting and water vapor transmitting properties of the porous membrane, we used a water droplet resistant and water vapor transmission test.

## 6.2. Results and discussion

### 6.2.1. Water vapour transmission property of porous membranes

A temperature, relative humidity and air velocity controlled chamber was used to measure the water vapor transmission (WVT) in accordance with the ASTM E96BW method. WVT is dependent on a thickness and porous structure in the membranes. The WVT of PPU was used in a comparison with the respective pure PU membrane (nonporous). **Figure 6.1 (a)** shows that the WVT increases with increased temperature. This is due to diffusivity increases with increasing of the temperature. At high temperature, motion of the polymer segments is increased and also energy levels of the permeating molecules are increased, thus WVT increases with temperature [27]. PPU<sub>s</sub> displayed a higher WVT compared to pristine PU because of porosity in PPU<sub>s</sub>, WVT increased with porosity and PPU<sub>2</sub> displayed a higher WVT than PPU<sub>1</sub>, revealing the surface effect on WVT. PPU<sub>2</sub> possesses high amount of silica particles than PPU<sub>1</sub>. Therefore, PPU<sub>2</sub> produced more porous structure than PPU<sub>1</sub> after leach out of silica. **Figure 6.1 (b)** shows that WVT against the relative humidity displays similar effects, such as, against temperature, PPU<sub>1</sub> and PPU<sub>2</sub> having higher WVT than pristine PU. **Figure 6.1 (c)** shows the relationship between the WVT, temperature and relative humidity. The WVT increases alongside the porosity percentage of the membrane increases. Incorporating silica particles into the PU was performed. The particles were

then leached out which produced the porous membrane increases of the WVT. Water penetration and transportation through the porous membrane is dependent on the size and the amount of the pores formed in the membrane. The porosity of the membranes determines the properties of water vapor transmission. **Figure 6.2** (a,b) is showing the sample preparation and test method for water vapor transmission test. **Figure 6.3, 6.4 and 6.5** is showing the relationship between the water vapor transmission, temperature and relative humidity.

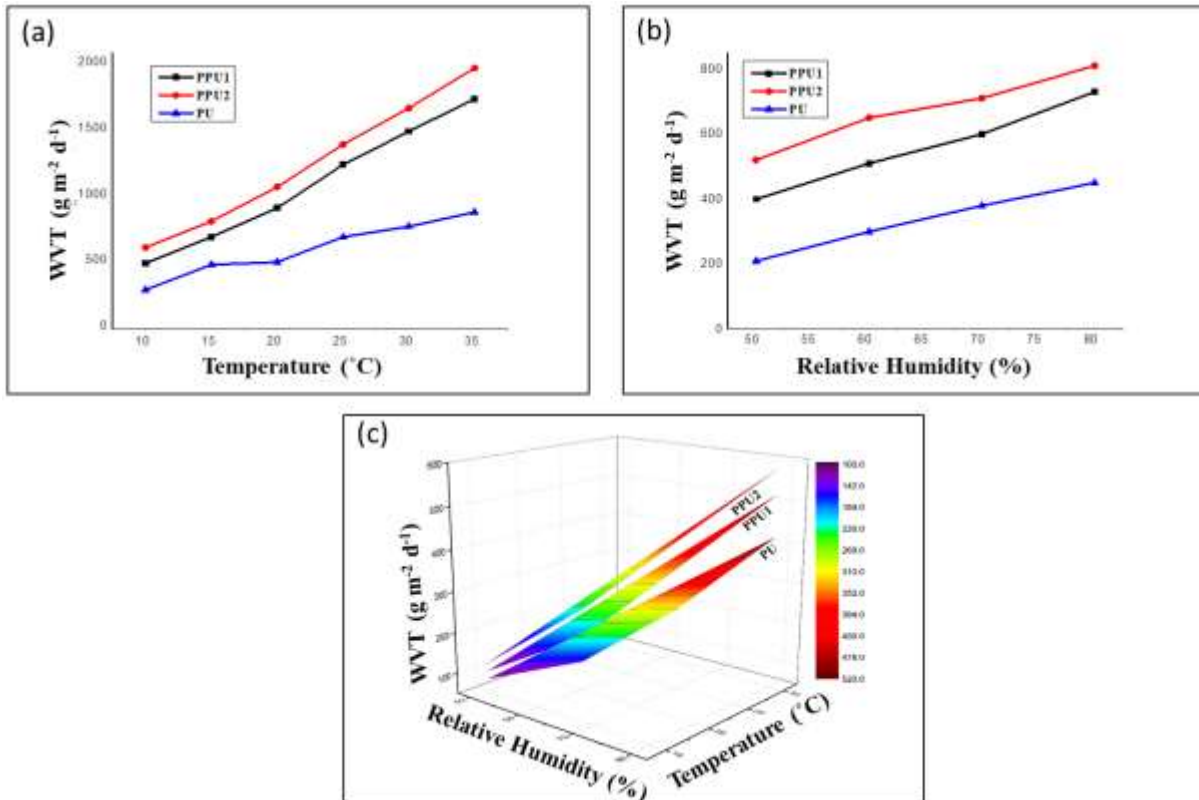


**Figure 6.1.** Water vapor transmission of different membranes, (a) against temperature, (b) against relative humidity, and (c) the relationship between the water vapor transmission, temperature and relative humidity.

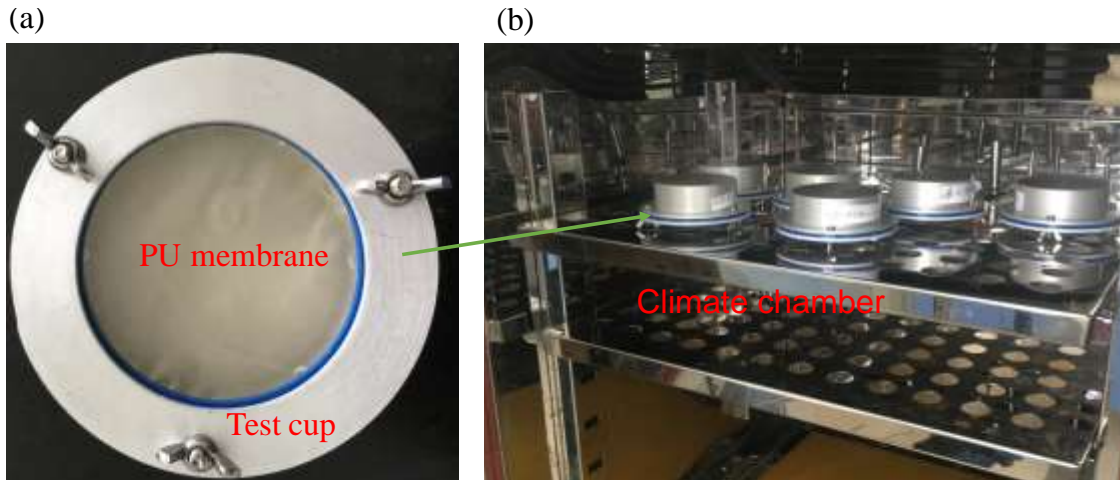


**Figure 6.2.** (a) Cup for water vapor transmission test, and (b) Temperature and relative humidity controlled climate chamber where water vapor transmission testing took place.

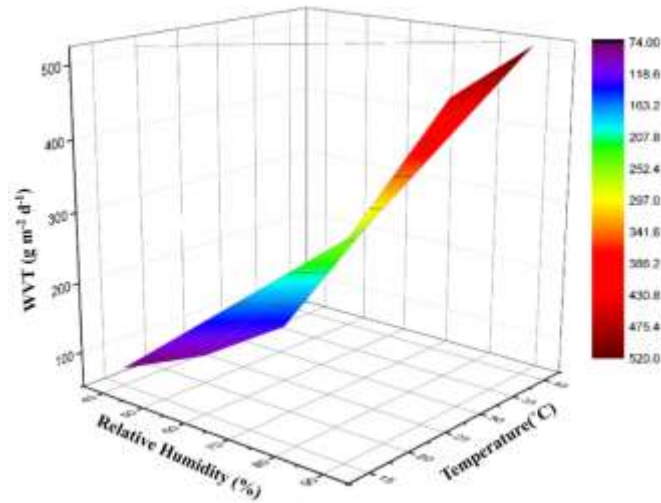


**Figure 6.3** The relationship between the water vapor transmission, temperature and relative humidity of PU membrane.

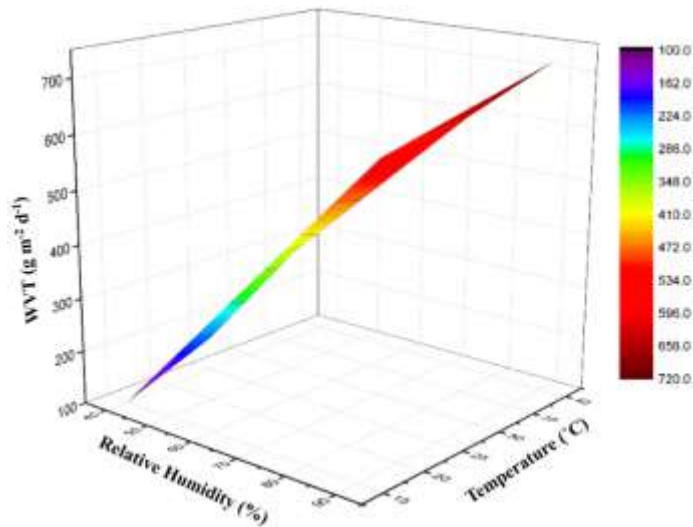


**Figure 6.4.** The relationship between the water vapor transmission, temperature and relative humidity of PPU1 membrane.

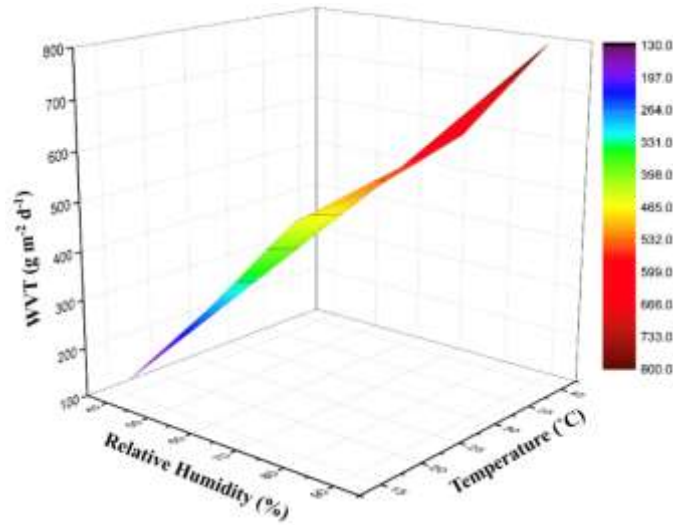


**Figure 6.5.** The relationship between the water vapor transmission, temperature and relative humidity of PPU2 membrane.

### 6.2.2. Water droplet resistant property of membranes

The membranes' water resistance properties were measured using the contact angle measurement of a water droplet at the surface of the membranes (**Figure 6.6a**).

The water contact angle changed from  $116^{\circ}\pm 1$  (1s) to  $96^{\circ}\pm 1$  (120s) for PU, from  $112^{\circ}\pm 1$  (1s) to  $93^{\circ}\pm 1$  (120s) for PPU1 and from  $111^{\circ}\pm 1$  (1s) to  $92^{\circ}\pm 1$  (120s) for PPU2. This indicates that both PU and PPU are hydrophobic as water contact angles are higher than  $90^{\circ}$ . The water contact angle of PU, PPU1 and PPU2 after 1s, 60s, 120s was measured. The fabricated porous PU is easy to pass the water

vapour due to porous structure through (the WVT result is in **Figure 6.1 (a, b, c)**) but the water droplets can be resisted due to hydrophobic nature. The contact angle usually depends on the cohesive forces of the surface tension of the membrane surface. The porous PU has sufficient surface energy to keep the liquid together, meaning that the droplet spread-out does not happen (**Figure 6.7b**). As shown in (**Figure 6.6b**), PPU2 exhibits decreased hydrostatic pressure (10200 mmH<sub>2</sub>O) compared with PPU1 (11000 mmH<sub>2</sub>O) and PU (12000 mmH<sub>2</sub>O). The hydrostatic pressure dropped from 12000 mmH<sub>2</sub>O to 10200 mmH<sub>2</sub>O, thus indicating that the water resisting properties decreased regularly when the incorporation of silica particles increased, because due to the increased porosity.

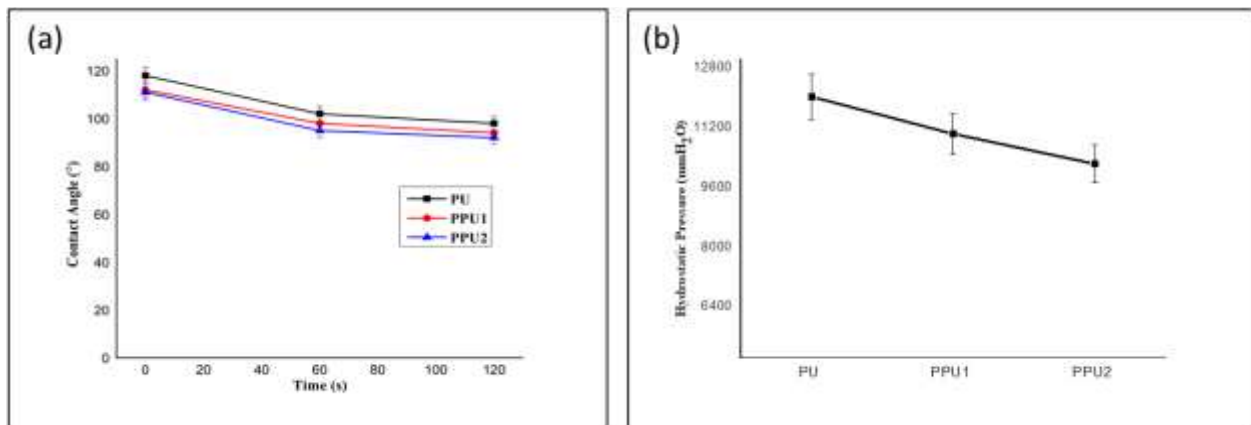


**Figure 6.6.** (a) water contact angle of membranes and (b) hydrostatic pressure of membranes.



### **6.2.3. Water vapor transmission and resistant mechanism, SEM and porosity of membranes**

Via the membranes, WVT happens in three stages; sorption, diffusion and evaporation.

During sorption, the water molecules come to the membrane's surface which then absorbs the water molecules. The sorption rate primarily depends on the membrane's surface properties along with the porosity. Usually the porous surface has a greater sorption rate. In diffusion, the water molecules penetrate across the membrane. The diffusion rate primarily depends on the hydrophilic group and membrane porosity. In evaporation, the water molecules evaporate from the membrane's surface and into the environment. The evaporation rate depends strongly on the surrounding environment (relative humidity or temperature) and pore volumes in the membrane. The fabricated porous membranes were 7000 times higher than a single water vapor molecule (the size of the water molecules is about  $2.75\text{\AA}$ ) and 1000 times smaller than a water droplet (the size of a water droplet is about 2mm). **Figure 6.7 (a, b)** shows the water vapor transmission and the resistant mechanism of the porous membrane.

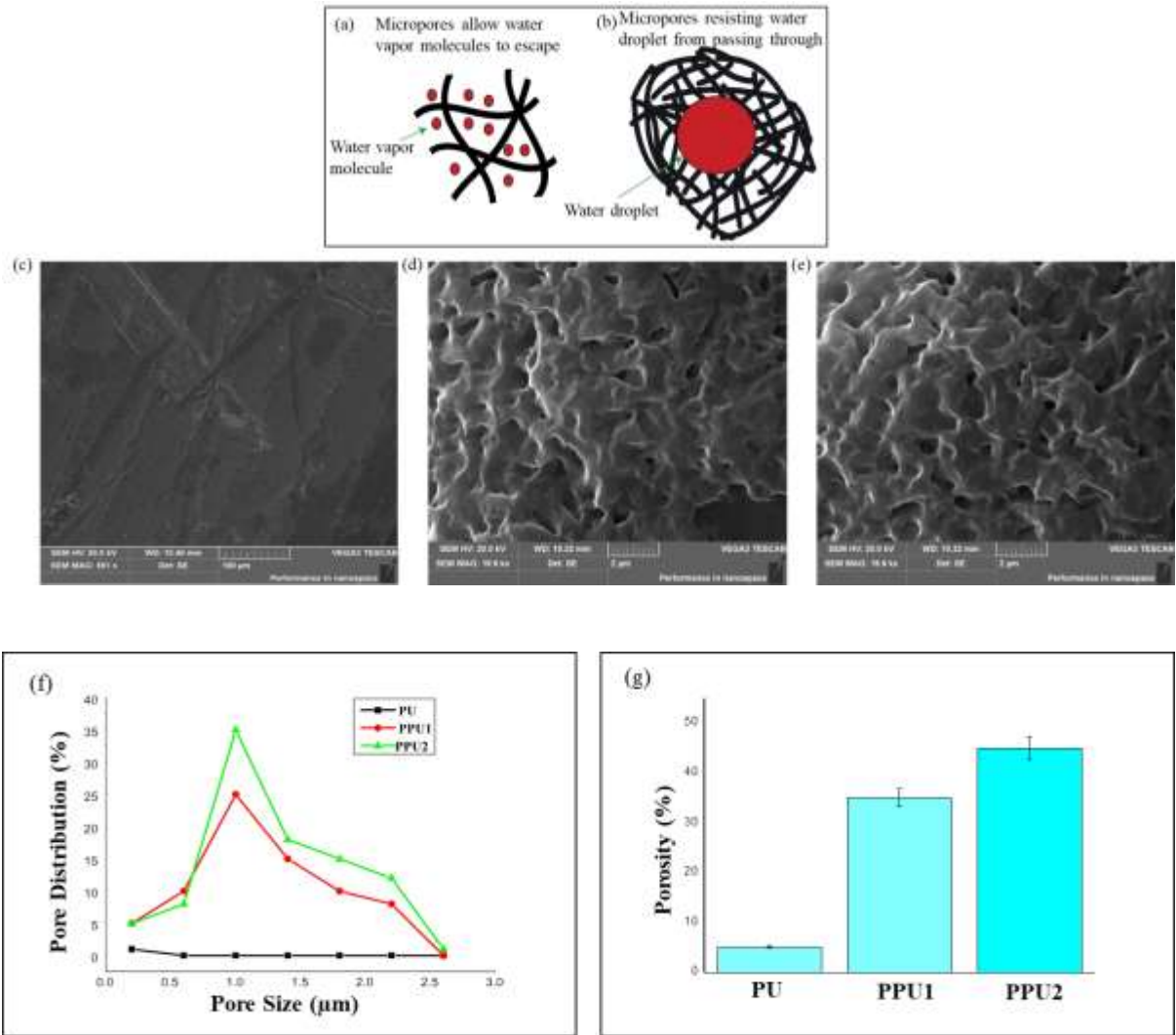


**Figure 6.7.** Schematic of the mechanism of (a) water vapor transmission, (b) water resistant, and SEM of the surface (c) PU, (d) PPU2, (e) PPU1 membrane, (f) pore size distribution and (g) porosity.

The PU and PPU membrane surface morphology and properties were examined using scanning electron microscopy. **Figure 6.7 (d, e)** shows the PPU membrane's porous structure and **Figure 6.7c** shows a nonporous smooth surface. The pore sizes are relatively small, with the maximum pore size being about 2 $\mu$ m. **Figure 6.7 (d, e)** show that the scaffolds can be prepared using the particulate leaching method which is particularly time-saving in comparison with the salt leaching method. The irregular porous structure is paired with pore inter-connectivity within the porous matrix. Additionally, it indicates that no distinct skin layer is formed on the membrane surface by the silica particles. **Figure 6.7f** shows that the porous polyurethane membranes were fabricated with different silica percentages (1 and 2%), exhibiting maximum pore sizes of 0.8, 1, 1.5, 2 and 2.3 $\mu$ m, respectively. The porosity percentage of the PPU2 membranes was more than that of the PPU1. The porosity and pore size distribution increased along with the percentage of silica particles added. As shown in **Figure 6.7g**, PPU2 exhibits around 45% porosity where PPU1 exhibits 35% porosity. The roughness of the samples were investigated from surface SEM images by ImageJ software and shown in **Figure 6.8**. The images revealed that pristine PU possessed smooth surface with very less roughness. However, PPU1 and PPU2 possessed high rough surface due to leach out of water soluble silica particles. The leach out of silica particles creates porous structure and hence surface become rougher compare to PU.

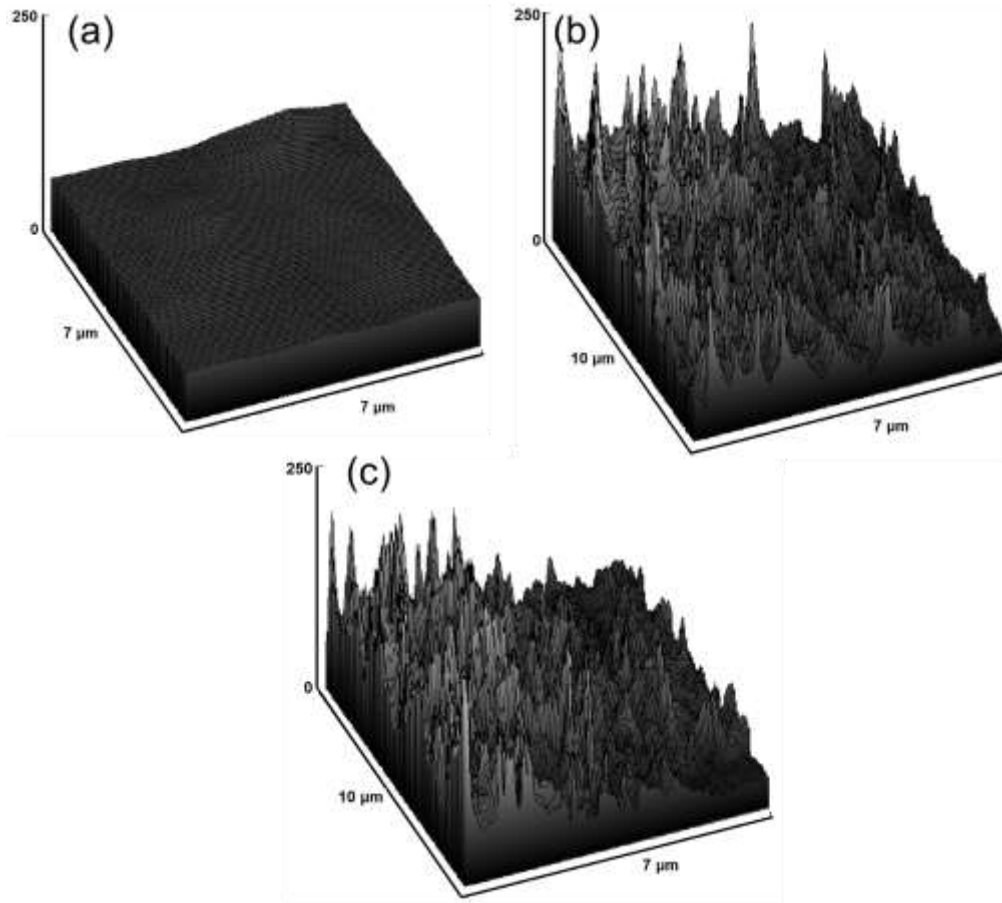


**Figure 6.8.** Surface roughness of (a) PU, (b) PPU1 and (c) PPU2 which were obtained by processing SEM image through ImageJ software.

#### **6.2.4. Mechanical property, TGA, DSC and XRD of membranes**

The mechanical properties mainly depend on particulars such as the presence of hydrogen bonds, the molecular weight, the polar groups within the polymeric chains, the existence of inter- and intra-molecular interactions, the rigidity of the polymer, the entanglement of the chains, the compositions, the nature of reactants, etc. [28, 29]. The PU tensile strength increased in comparison with the porous membranes. This is because porous membranes have many pores. This can weaken the membranes compared with PU, which is why porous 1% is mechanically stronger than porous 2%. The tensile properties and elongation of the porous membranes have similarities. **Figure 6.9a** shows that the elongation and strength of porous 1% and porous 2% are similar, whereas PU has significantly better tensile strength and elongation.

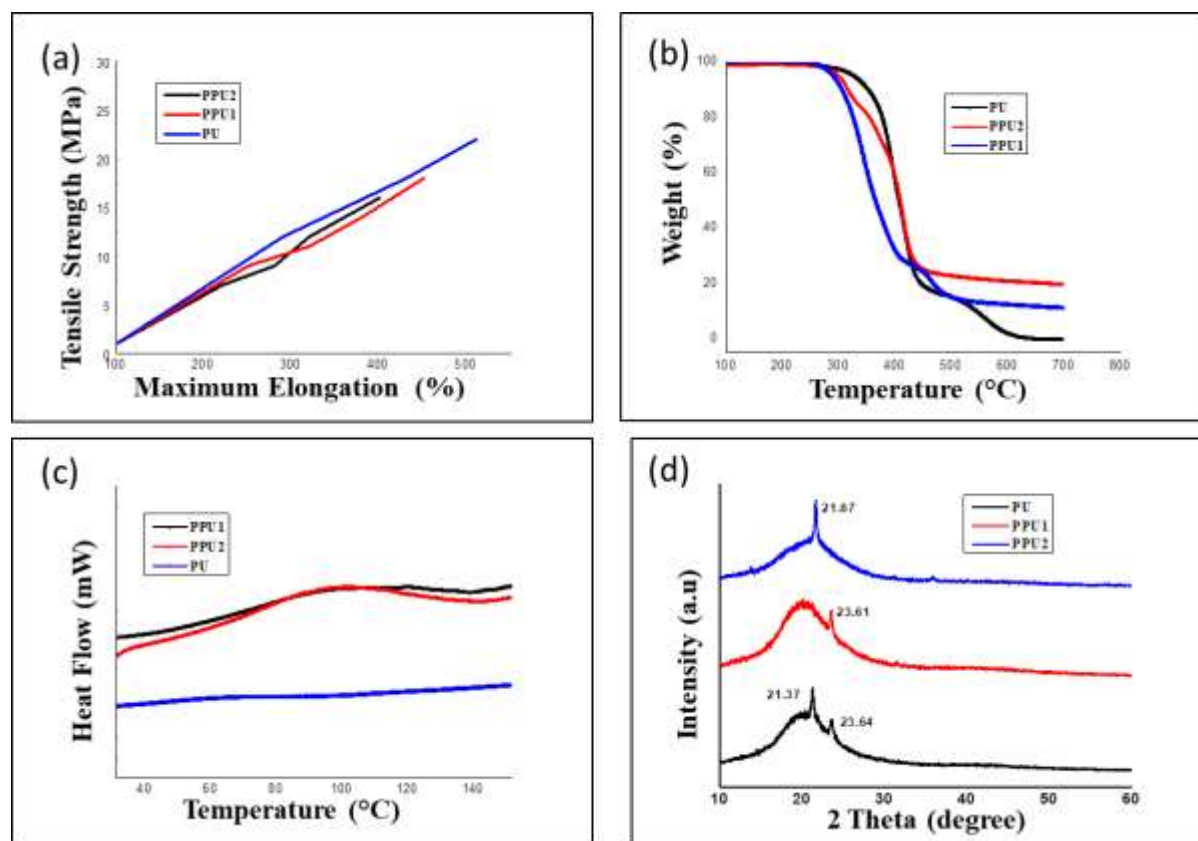


**Figure 6.9** (a) Mechanical property, (b) TGA curve, (c) DSC curve, (d) XRD patterns of PU, PPU1 and PPU2.

The pristine PU and PPU TGA curves have been shown in **Figure 6.9b**. The pristine PU and PPU1 is displayed two-step degradation. The first step involves all of the membranes showing a primary weight loss (with a decomposition of approximately 10%) from 100 to 300°C, which is related to the weight loss of the volatile compound. This is like some of the additives included during the nonporous and porous membrane synthesis process. The second step was urethane link decomposition (around 70% polyurethane decomposition) between 300 and

500°C. In the third step, the ester groups decomposed (around 20% of the polyurethane) between 500 and 700°C. These PU decompositions mainly depend on urethane groups per unit volume as shown in **Figure 6.9b**. PUs are normally a thermally induced material, although they may be triggered by relative humidity and temperature. These thermally triggered PUs can sense and respond to external stimuli. The PU and porous membranes synthesized in this research consist of segmented polyurethane with two phases - soft and hard. **Figure 6.9c** reveals polyurethane's melting temperature. However, there is no sharp peak of melting point in any of the sample. This indicates the amorphous character of the synthesized PU and PPU. The DSC curves of PPU also showed different characteristic compare to pristine PU. The porous structure influences melting behavior [30], so the nature of the curve is changed in PPU. Both the PPU samples showed a similar characteristic curve. The transition temperature is dependent on the molecular weight of the polyols and the hard /soft phase ratio. The soft segment influences the membranes' water vapor transmission by the free volume of the polyurethane.

The PU and porous PU membrane XRD patterns have been displayed in **Figure 6.9d**. All of the samples showed a broad peak of around  $2\theta=15-25^\circ$  because of the presence of a crystalline soft segment. The PU XRD patterns showed double sharp peaks noticeable at  $2\theta \sim 21^\circ$  and  $23.6^\circ$ . These peaks are allocated to the highly

crystalline structure of the soft domains (PEG based soft segment) and match well with the reported peak positions of the PEG based PU [31,32]. There were no separate peaks observed in the XRD patterns for the silica particles, suggesting that there was complete removal of water soluble silica particles from the membrane surface.

Such highly water vapor transmittable, water drop resistant and mechanically strong porous membranes can be utilized for laminated textiles. The lamination method adds properties to the textile fabric such as rainwear, permeable textiles, water resistant textiles, three-dimensional fabric etc [33]. Laminated fabrics have multiple uses in the technical and functional textiles fields. Usually, the reverse side of the woven fabric surface is laminated. This is so then it does not affect the textile fabric look from the front. The water vapor transmissible and water-resistant laminated fabrics are effective clothing in the heat and rain [34,35]. **Figure 6.10** shows the lamination technique of the membranes of the textile fabric (woven structure).



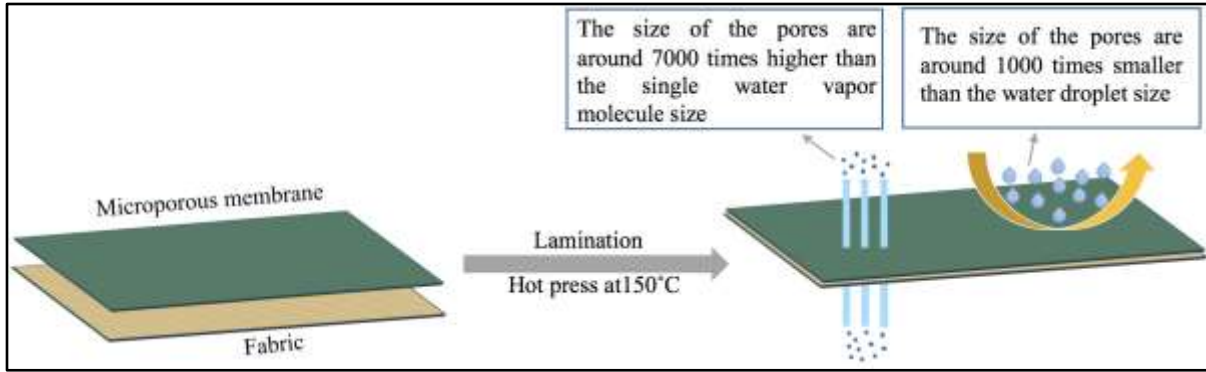


**Figure 6.10.** Lamination technique of fabric.

### 6.2.5. Abrasion resistant property of laminated fabric

To check the adhesiveness and abrasion resistance of the laminated fabric we performed an abrasion resistance test (**Figure 6.11**) and found that there was almost no weight loss; there is also no yarn breakage after rubbing the laminated fabric 1000 times (50 per min) with 9 kPa load, which means the laminated fabric has very good abrasion resistant property.

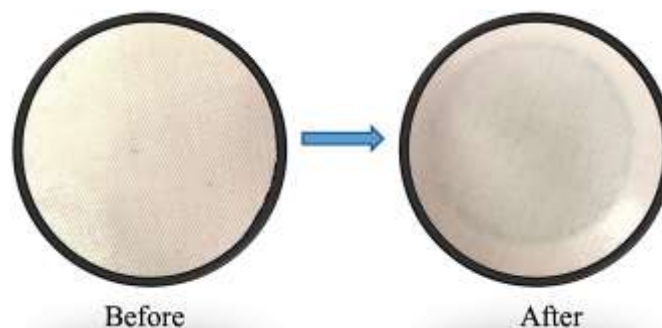


**Figure 6.11.** Abrasion resistant property of laminated fabric.

**Figure 6.12** is showing the fabricated membrane fabric and laminated fabric. The membrane was laminated with fabric by hot press at 150°C.

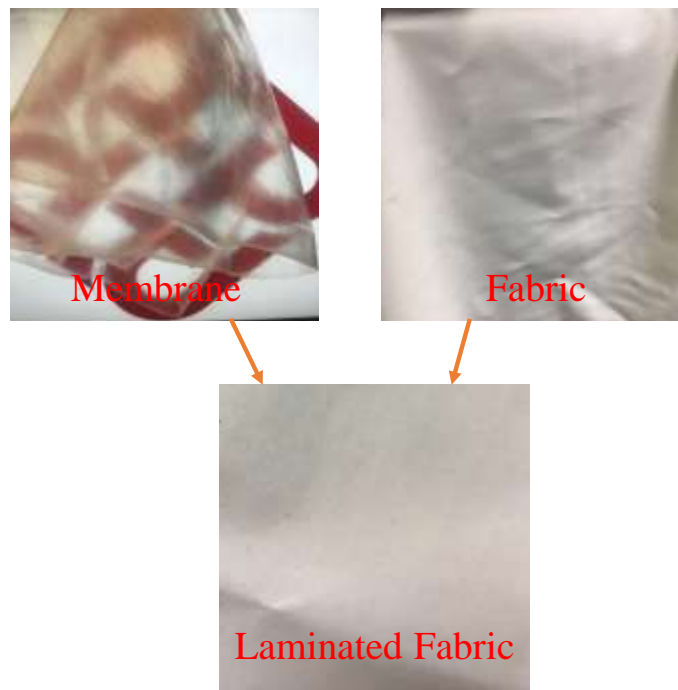


**Figure 6.12.** Fabricated membrane, fabric and prepared laminated fabric.

## 6.7. Summery

The particulate leaching method fabricates a highly porous polyurethane membrane. The used silica particles are rapidly water soluble, which saves time compared with the salt leaching method. The mechanical properties of the porous

membrane depend primarily on the added percentage of silica particles. PU and PPU1 have improved mechanical properties compared to PPU2. However, PPU2 has a better transmission of water vapor compared with PPU1 and PU. All of these membranes have good water resistance properties. Such highly porous, water vapor transmittable, water droplet resistant and mechanically strong polymeric membranes can be used on laminated textile areas.

Published work “Jahid, M. A., et al., Novel approach of making porous polyurethane membrane and its properties for apparel application. J. Appl. Polym. Sci., 2019.137: 48566”.

## Reference

1. Hou, Q., et al., Porous polymeric structures for tissue engineering prepared by a coagulation, compression moulding and salt leaching technique. *Biomaterials*, 2003. 24: p. 1937-1947.
2. Ye, Q., et al., The formation of regular porous polyurethane membrane via phase separation induced by water droplets from ultrasonic atomizer, *Mat. Let.*, 2013. 100: p. 23-25.
3. Reignier, J., et al., Preparation of interconnected poly(3-caprolactone) porous scaffolds by a combination of polymer and salt particulate leaching. *Polymer*, 2006. 47: p. 4703-4717.
4. Iannace, S., et al., Preparation and Characterization of Polyurethane Porous Membranes by Particulate-leaching Method, *Cell Polym.*, 2001. 20: p. 321-338.
5. Janik, H., and Marzec, M., A review: Fabrication of porous polyurethane scaffolds, *Mate. Sci. Engi. C*, 2015. 48: p. 586-591.
6. Turken, T., et al., Reinforced thin film composite nanofiltration membranes: Fabrication, characterization and pilot testing. *J. Appl. Polym. Sci.* 2019.136: p.48001.
7. Sheridam, M. H., et al., Bioabsorbable polymer scaffolds for tissue engineering capable of sustained growth factor delivery, *J. Cont. Rele.*, 2000. 64: p. 91-102.
8. Heijkants, R. G. J. C., et al., Preparation of a polyurethane scaffold for tissue engineering made by a combination of salt leaching and freeze-drying of dioxane. *J. Mater. Sci.*, 2006. 41: p. 2423-2428.
9. Termonia, Y., et al., Fundamentals of polymer coagulation, *J. Polym. Sci. B Polym. Phys.*, 1995. 33: p. 279-288.
10. Rowlands, A. S., et al., Cooper-white, Polyurethane/poly(lactic-coglycolic) acid composite scaffolds fabricated by thermally induced phase separation, *Biomaterials*, 2007. 28: p. 2109-2121.
11. Thomson, R. C., et al., Polymer scaffold processing, *Principal of Tissue Engineering*, Academic Press, San Diego, 2000. P. 251-262.
12. Kim, H. J., et al., Gas foaming fabrication of porous biphasic calcium phosphate for bone regeneration, *Tissue. Eng. Regen. Med.*, 2012. 9: p. 63-68.
13. Stucki, M., et al., Thermoresponsive Microspheres as Smart Pore Plugs: Self-Venting Clothing Membranes for Smart Outdoor Textiles. *Macromol. Mater. Eng.* 2018. 303: p. 1700562.
14. Kim, J. and Hollinger, J. O., Recombinant human bone morphogenetic protein-2 released from polyurethane-based scaffolds promotes early osteogenic differentiation of human mesenchymal stem cells, *Biomed. Mater.*, 2012. 7: p. 045008.
15. Quirk, R. A., Supercritical fluid technologies and tissue engineering scaffolds, *Curr. Opin. Solid. State Mater. Sci.*, 2004. 8: p. 313-321.
16. Cheng, D., et al., Surface Characterization of Polyelectrolyte/Silver Nanocomposite Film. *Polym. Polym. Com.*, 2017. 25: p. 635-642.
17. Bijan, N. N., et al., Porous starch/cellulose nanofibers composite prepared by saltleaching technique for tissue engineering. *Carbohy. Polym.*, 2014. 108: p. 232-238.
18. Maria, F. J. S., Polymer nanofilms with enhanced microporosity by interfacial polymerization. *Nat. Mate.*, 2016. 15: p. 760-769.

19. Jahid, M A., et al., Fabric Coated with Shape Memory Polyurethane and Its Properties. *Polymers*, 2018. 10: p. 681.
20. Mondal, S. and Hu, J. L., Water vapor permeability of cotton fabrics coated with shape memory polyurethane. *Carbo. Polym.*, 2007. 67: p. 282–287.
21. M. A. Jahid, M. A., et al., *Smart Textile Coatings and Laminates*, Chap6, 2018. p. 155-173.
22. Hu, J L., A review of stimuli-responsive polymers for smart textile applications. *Smart. Mater. Struct.*, 2012. 21: 23.
23. Mondal S. and Hu, J. L., Segmented shape memory polyurethane and its water vapor transport properties. *Desig. Mono. and polym.*, 2006. 9: p. 527–550.
24. Hu, J. L., et al., Self-adaptive water vapor permeability and its hydrogen bonding switches of bio-inspired polymer thin films. *Mate. Chem. Fron.*, 2017. 1: p. 2027- 2030.
25. Meng, Q. H. and Hu, J. L., A temperature-regulating fiber made of PEG-based smart copolymer. *Sol. Ener. Mate. and Sol. Cel.*, 2008, 92 : p. 1245-1252.
26. Xianyuan, G., et al., Electrospun polyurethane microporous membranes for waterproof and breathable application: the effects of solvent properties on membrane performance. *Polym. Bull.*, 2018. 75: p. 3539-3553.
27. Bertuzzi, M. A., et al., Physicochemical characterization of starch based films. *J Food Eng.*, 2007. 82: p.17-25.
28. Thakur, S., et al., Mechanically strong shape memory polyurethane for water vapour permeable Membranes. *Polym. Int.*, 2018. 67: p. 1386-1392.
29. Zlatanovic, A., Effect of Structure on Properties of Polyols and Polyurethanes Based on Different Vegetable Oils. *J. Polym. Sci. B Polym. Phys.*, 2004. 42: p. 809–819.
30. Morishige, K., et al., Effect of Pore Shape on Freezing and Melting Temperatures of Water. *J. Phys. Chem. C.*, 2010. 114: p.4028-4035.
31. Ali, P. I., et al., Enhancement of CO<sub>2</sub> capture by polyethylene glycol-based polyurethane membranes. *G. Behnam, J. of Mem. Sci.*, 2017. 542 : p. 143-149.
32. Zheng, Y; et al., Biocompatible shape-memory poly(vinyl chloride) with a tunable switching temperature via a plasticization effect. *J. Appl. Polym. Sci.* 2019, 47992, 1.
33. Lomax, G. R., Breathable polyurethane membranes for textile and related industries. *J. Mater. Chem.*, 2007. 17: p. 2775–2784.
34. Jin, S., et al., Preparation of breathable and superhydrophobic polyurethane electrospun webs with silica nanoparticles. *Text. Res. J.*, 2019. 86: p. 1816-1827.
35. Kopitar, D., et al., Influence of nonwoven fabric pore sizes on water vapor resistance, *Text. Res. J.*, 2018. 88: p. 1402-1412.

# Chapter7. Temperature sensitive gating textile

## 7.1. Introduction

Climate change is making the world warmer day-by-day, which is one of the fundamental challenges for human civilization now to keep the global warming below a rise of 2°C, deployment of negative emissions technologies (NETs) is required to keep the global temperature in the range [1, 2]. Additionally, improving energy efficiency and reducing energy consumption can also be considered to keep the global temperature in the range, approximately, 12.3% of total U.S. energy consumptions are residential and commercial energy consumptions and mostly used for space cooling and heating. By minimizing the demand for space cooling and heating (indoor temperature), will have huge influence on global energy consumptions [3-5]. This hot environment also can have a huge negative impact on human body, like dehydration, heat stroke, elevated heart rate, etc. [6]. To avoid such heat related illness and reducing energy consumptions for regulating indoor temperature, personal cooling mechanism in a textile could play an important role in controlling the body temperature during extreme weather.

Personal cooling and heating technologies in a textile have attracted huge attention because of their ability to provide thermal comfort by locally controlling the

temperature of a person in an energy saving way [7-9]. The incorporating of personal cooling mechanism in a wearable textile has been regarded as one of the great strategies to bring personal cooling technologies into regular wearable textiles [10]. Cooling functions in wearable textiles can provide the wearer thermal comfort during hot weather by controlling the wearer's microclimate, resulting minimizing the cost for cooling the whole building [10, 11]. The idea of 'personal thermal management' can be very effective alternative, the objective of this idea to provide thermal comfort (heating or cooling) to a human body and its surroundings instead of heating and cooling the whole building. Because the thermal mass of a human body is much smaller compared with the whole building, in this way, personal thermal management would be very energy efficient [12, 13, 8]. To make thermo-regulating wearable textile, considerable amount of efforts has been given to produce personal cooling and heating textile, Hu Jinlian and co-worker reported polyurethane film to make highly water vapor transmittable textile [14, 15], Gang chen and co-worker reported a infrared-transparent visible-opaque fabric (ITVOF) that provides passive cooling via the transmission of thermal radiation emitted by the human body directly to the environment [16]. Yi cui and co-worker reported radiative cooling textile using mid-infrared transparent nanoporous polyethylene [8], YuHuang Wang and co-worker reported dynamic gating of infrared radiation in a textile by using triacetate-cellulose bimorph fibers with a thin layer of carbon

nanotubes[17]. Furthermore, there are several materials has been reported to make microclimate controlled textile, phase change materials[18], shape memory polyurethane[19,20], air-cooled textiles[21], graphene to E-textile, liquid cooling textiles [23] and so on. Recently, liquid crystal elastomer fibers also been reported to make smart textile [24]. Liquid crystal elastomers are a class of materials can be used for actuators [25], artificial muscle [26], soft robots [27], and sensors [28]. Liquid crystal elastomers have the ability to reversible shape changes (nematic state to isotropic state) in response to external stimulus [29], such as heat [30, 31], light [32, 33], magnetic field [34] and electric field [35]. Recently, a two-step a thiol-acrylate Michel addition and photopolymerization techniques was developed [36], where they demonstrate the fabricated LCE can be actuated immediately after fabrication upon heating above transition temperature.

There are various techniques are being used to make polymer fiber, like melt spinning [37], electro spinning[38], solution spinning[39], and direct ink writing (DIW) [24]. Melt spinning is one of the most economical and easy process to make polymer fiber due to polymer can melted easily and spinning rate vary high compare with other fiber spinning method[37], this technique is very extensively used make polymer fiber for textile application, the challenges of this technique is to make small scale production, like few grams. Electro spinning is also a widely used to technique to make fiber for textile application, which use high electric



voltage to make fibers, the challenges of this technique is to maintain uniform diameter of fiber and collecting individual fiber. Recently, LCE fiber was fabricated through direct ink writing by 3D printing technology [24], through this technique highly viscous liquid can be extruded because it can maintain very high pressure. In this chapter, the LCEs was synthesized and the filaments and 2cm (diameter) radial shaped film was fabricated by using 3D printing technology in order to make dynamic gating in a textile as a function of temperature. The aim of this study is to fabricate liquid crystal elastomers with tunable (physical and molecular) properties where 3D printing technology will be used to make filaments and films, filaments will be used to make waving fabric and films will be incorporated in textile in order to get open/close functions in the textile as a function of temperature. **Figure 7.1 (A, B)** is showing the way human body got heated and how core temperature gets increased along with exercise time, where **Figure 7.1 (C, D)** is showing the open/close (woven structure which is closing as a function of temperature where film is opening with increased temperature) in a textile.

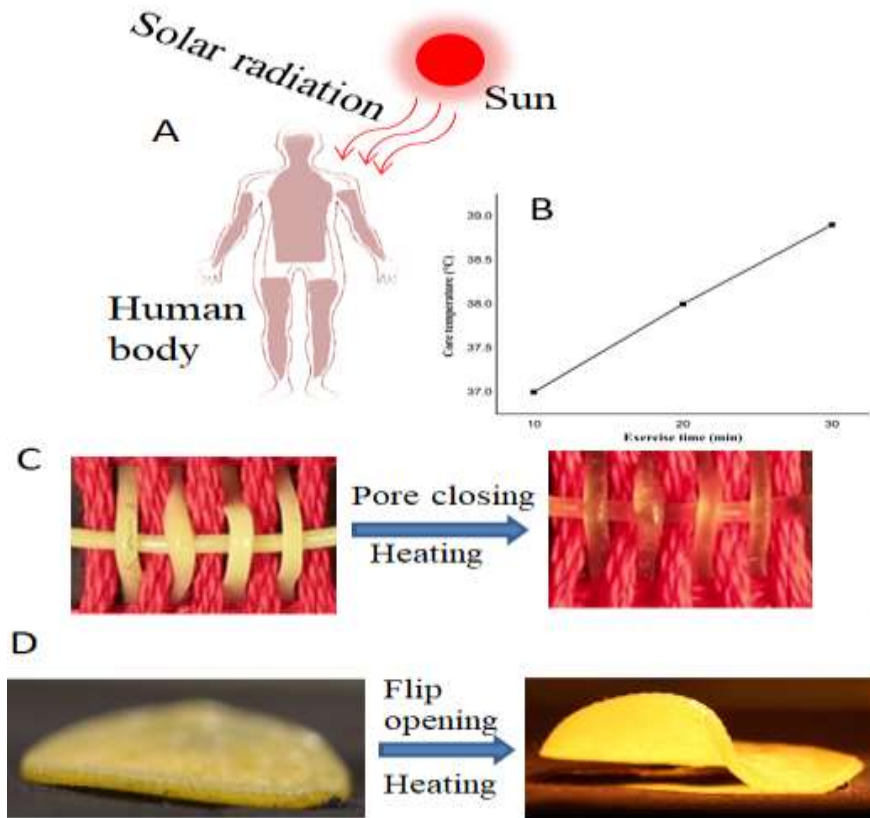


**Figure 7.1.** Mechanism of body heating and open/close in a textile as function of temperature.

## 7.2. Results and discussion

### 7.2.1. Molecular mechanism of LCEs

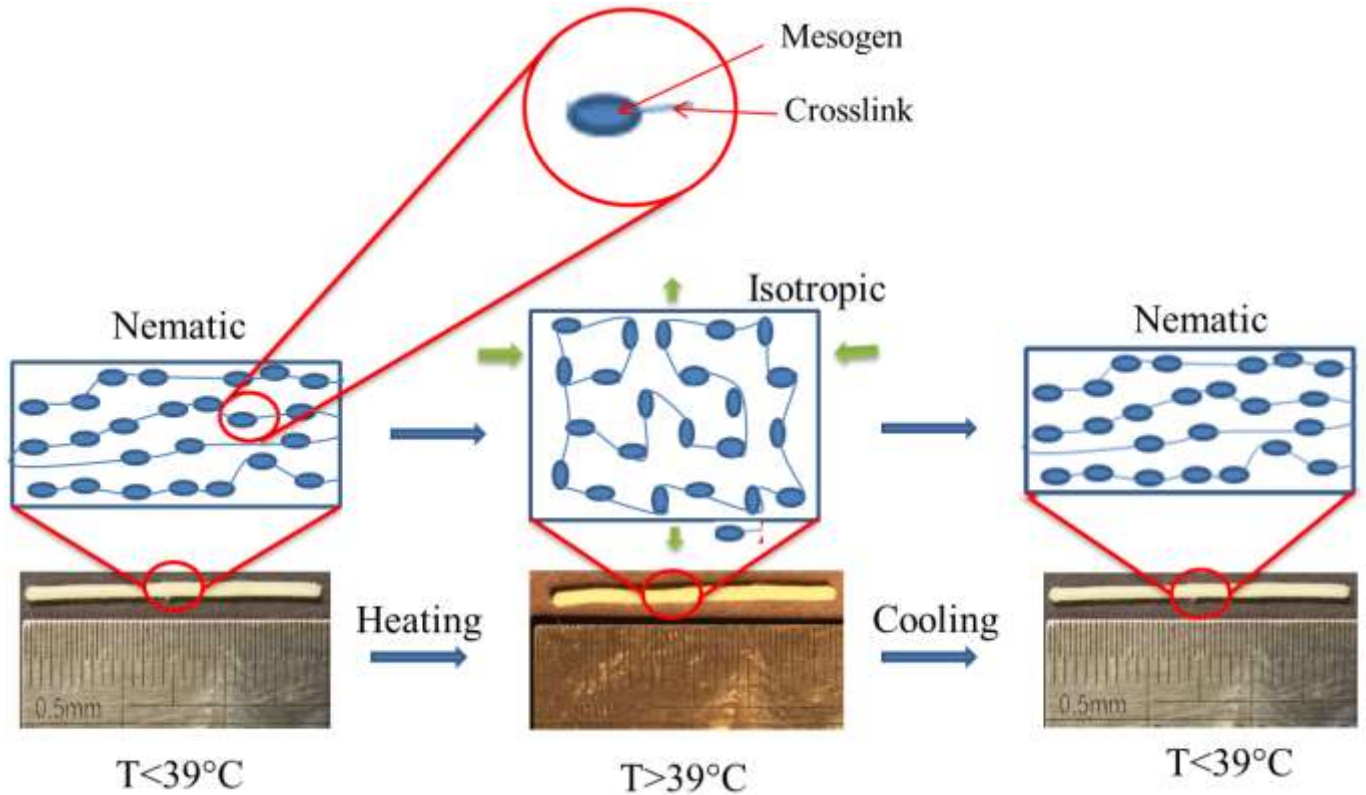


**Figure 7.2.** Molecular mechanism of liquid crystal elastomers.

Liquid crystal elastomers (LCEs) are a class of functional materials using the interactions between the polymers and liquid crystals, the polymerization of monomers that exhibits liquid crystalline phase into a polymer network [39]. LCEs are mechanically programmable soft material which can undergo reversible shape changes upon heating. In this study, we showed a route to synthesis LCEs for 3D printing for apparel applications, which can change shape as a function of temperature (**figure 7.2**). The thermo-mechanical property and process ability of

the synthesized materials can be controlled, and the actuation temperature of LECs also can be controlled. The fabricated 3D printed filaments shrink above transition temperature. The 3D printed filaments were then used to make woven textile to see the actuation behavior in the textile. The details of the actuation behaviors will be discussed below.

### **7.2.2. Pores are closing as a function of temperature**

The controllable actuation temperatures of 3D printed filaments were used to make plain woven (1\*1) fabric. The fabricated weaved fabric was able close its pores as a function of temperature (**figure 7.3 (A)**), and pore closing temperature can be tuned by controlling the molecular weight of mesogens and percentage of mesogens. As we can see from the **figure 7.3 (B)**, the pores are closing along with temperature, pore size (approximate 1100 $\mu$ m) of both RM82/RM257 (80:20) and RM82/RM257 (60:40) are similar at room temperature (25°C), and pores are closed down to 180  $\mu$ m at temperature 65°C and returning back to its original position at room temperature. As we can see that, RM82/RM257 (60:40) has better pores closing ability at different temperature level compare with RM82/RM257 (80:20). **Figure 7.3 (C)** is showing the contraction of filaments along with thickness expansion, which prove the pores closing ability of the fabric. This kind

pore closing/opening textile can be used to block sunlight from our skin or window cover to block sunlight.

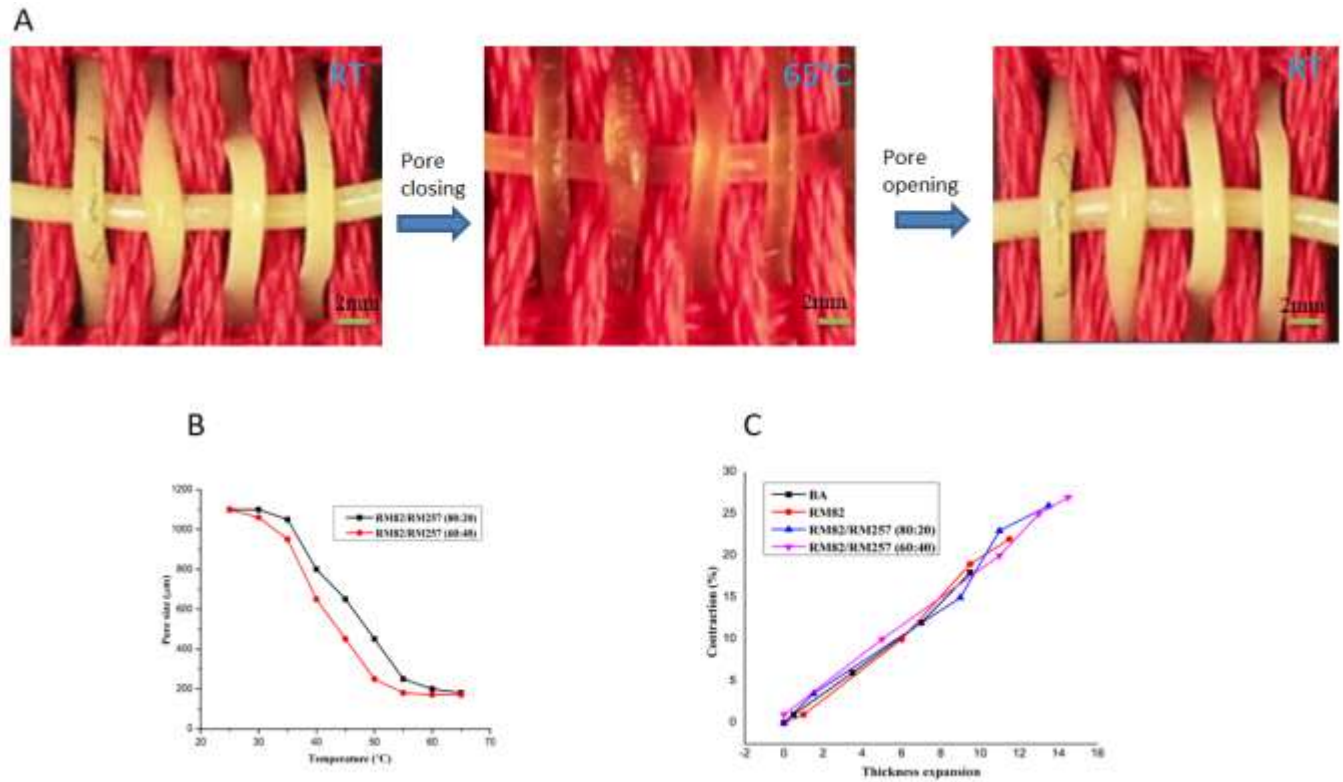


**Figure 7.3.** A) Open/close mechanism in weaved fabric, B) Pore actuation as a function of temperature and C) Contraction of filaments along with thickness changes.

### **7.2.3. Contraction of single filament**

Contraction of filaments as a function of temperature showing the synthesized materials can be contracted when temperature applied. **Figure 7.3** is showing the contraction ability of filaments as a function of temperature. As we can see that BA contracted less compare with others and it's also need relatively high temperature to be contracted. RM82/RM257 (60:40) has contacted maximum and comparatively low temperature because of higher RM257 concentration in the mixture. RM82/RM257 (80:20) has better contracted compare with RM82 because of RM257 concentration in the mixture. We can say that, RM 257 has influence on contraction percentage and contracted temperature.

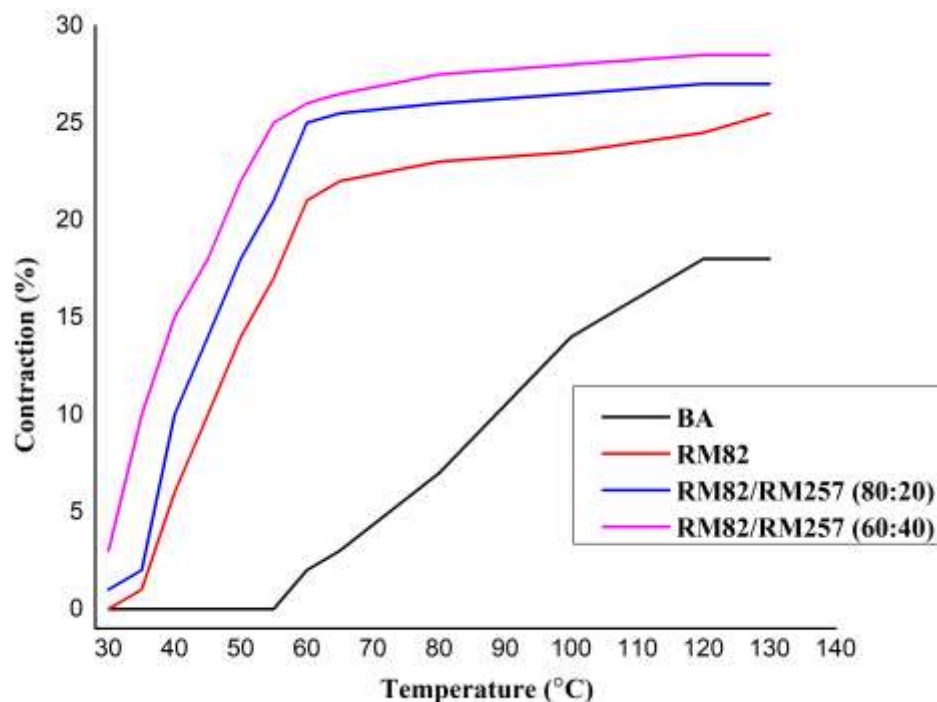


**Figure 7.3.** Contraction of filaments as a function of temperature.

#### 7.2.4. DSC of Liquid crystal elastomers

The transition temperature is very important for responsive apparel application.

Our synthesized liquid crystal elastomers (LCEs) have near body or skin temperature transition temperature, which is very useful for apparel applications.

**Figure 7.4**, RM82/RM257 (60:40) (32°C) has significantly lower transition temperature compare BA (108°C) because of overall weight fraction of mesogen within the materials. RM82/RM257 (80:20) has lower transition temperature compare with RM82 because of the presence of RM257 in the solution.

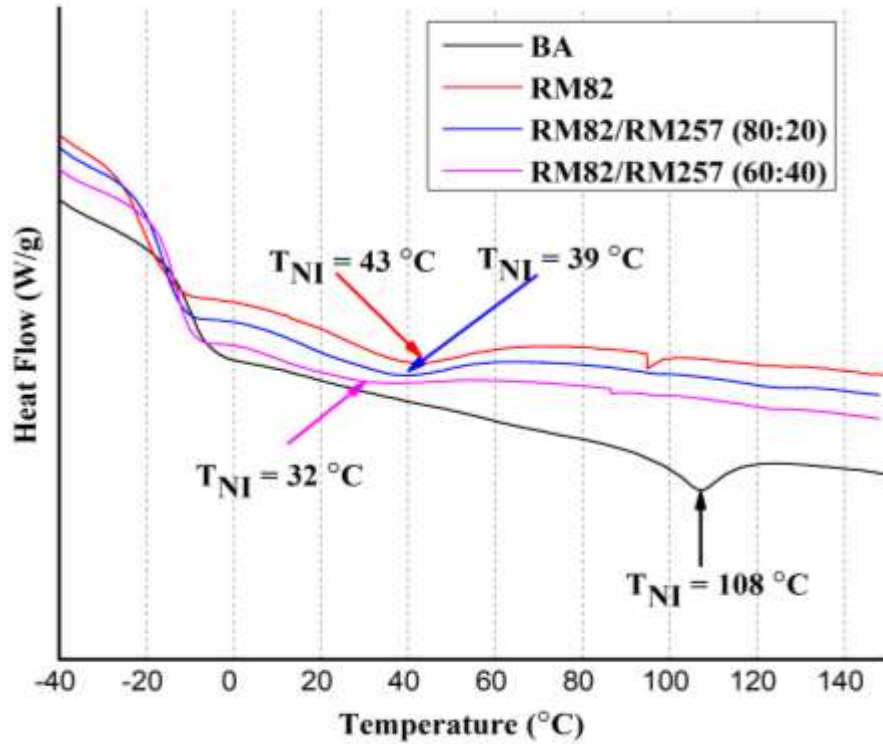


**Figure 7.4.** DSC of LCEs.

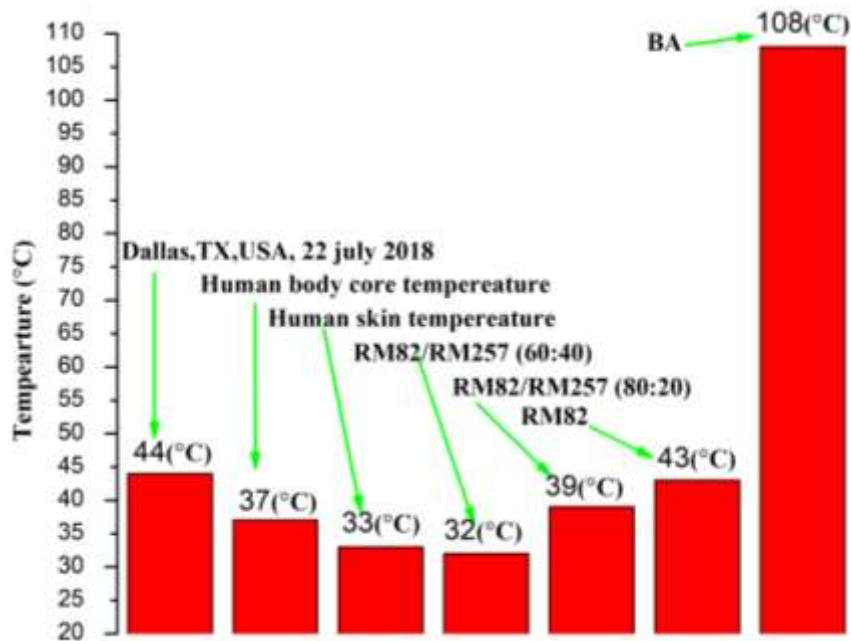


**Figure 7.5.** Transition temperatures of LCEs.



The transition temperature of liquid crystal elastomers has very interesting transition temperature which would be very useful for textile applications. As we see from the **Figure 7.5**, the temperature of dallas, TX, USA on 22 July 2018, human body core temperature, human skin temperature, RM82/RM257 (60:40), RM82/RM257 (80:20), RM82 and BA is 44°C, 37 °C,33 °C,32 °C,39 °C,43 °C and 108 °C, respectively. The transition temperature of RM82/RM257 (60:40) shows that it can sense when the skin temperature increases, where RM82/RM257 (80:20) shows that it will actuate when the core temperature increases. This interesting transition temperature of LCEs will be used to make temperature sensitive gating textile.

### **7.2.5. Mechanical property of filaments**

Mechanical property of LCEs is very important for application point of view. As we can see from the **figure 7.6** that are better stress (9.3MPa) compare with those others due to the butayle amine presence in polymer, where strain is above 400%. More stress require to break RM82 (3.34MPa) compare to RM82/RM257 (80:20) (1.15MPa), RM82/RM257 (60:40) (0.632MPa), but the strain of RM82/RM257 (80:20) and RM82/RM257 (60:40) is much better compare with RM82. Which proves that the presence of RM257 weaken the filaments but increase the strain.

This kind of LCEs can use for apparel applications due to good mechanical property.

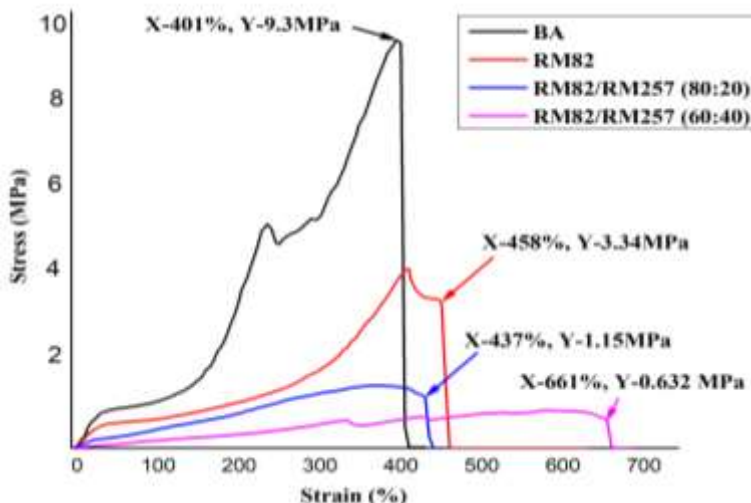


**Figure 7.6.** Mechanical properties of LCEs.

### 7.2.6. Flip opening/closing in a textile as a function of temperature

Liquid crystal elastomers are mechanically active which can maintain rapid, reversibly shape change without mechanical bias or external forces, these reversible shape change happen as a function of temperature. Three dimensional printed radial shaped films were used to make to be incorporated into textile for making open/close functions in textile. As we can see **figure 7.7 (A)**, radial shaped films can bend up to  $64^{\circ} \pm 2^{\circ}$  with  $65^{\circ}\text{C}$  temperature. **Figure 7.7(B)** is showing the bending angle of films at different temperature level. RM82/RM257 (80:20) and

RM82/RM257 (60:40) has quite similar bending angle and actuation temperature level. **Figure 7.7(B)** is showing the bending height of films at different temperature level.

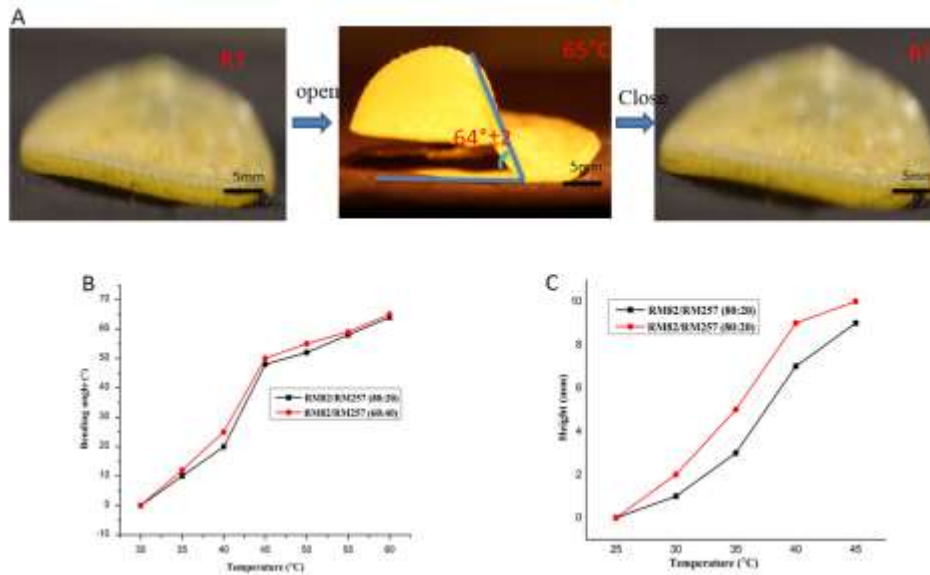


**Figure 7.7.** A) Flip open/close mechanism in weaved fabric, B) Bending angle of flip as a function of temperature and C) bending height of flip as a function of temperature.

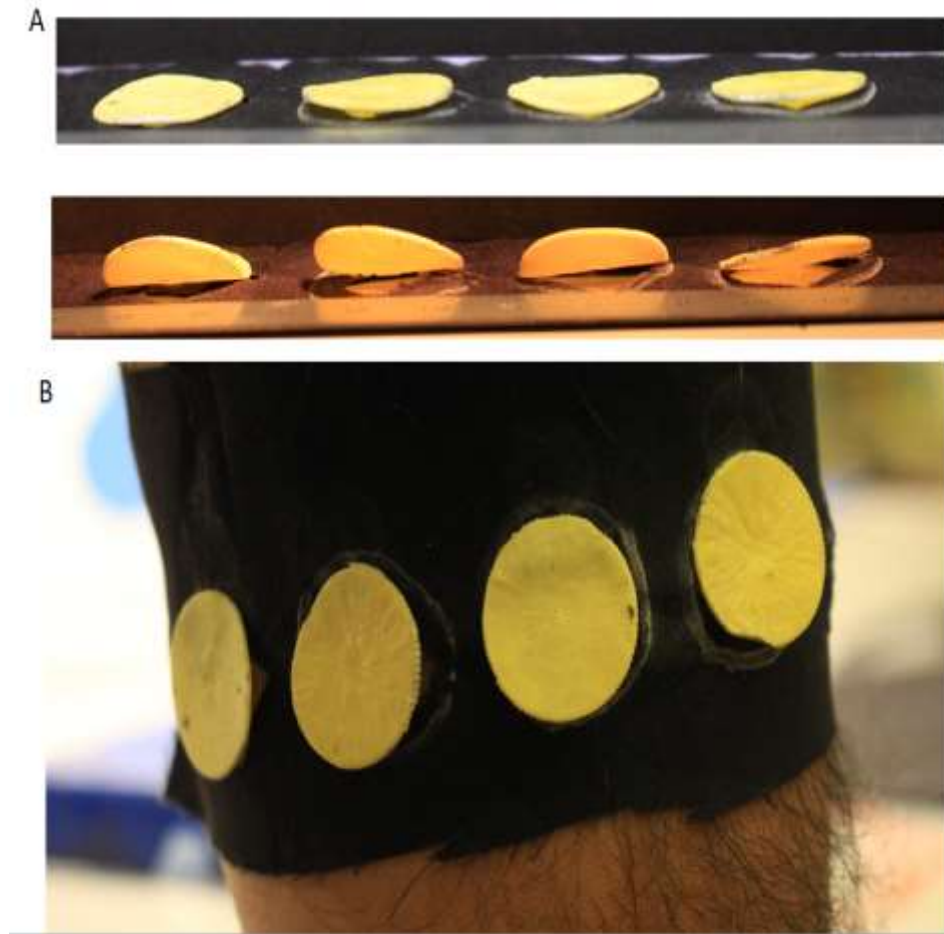


**Figure 7.8.** Flip open/close in woven fabric as a function of temperature. A) Flip closed (above)/opened (below) when temperature applied, B) Radial shaped 3D printed films can be incorporated into textile and be used as clothing.

**Figure 7.8** is showing the flip opening when temperature applied after incorporating into textile. We have cut the 2cm (diameter) area of fabric then fix the radial shaped films by using glue. **Figure 7.8A** (above), films is not open at room temperature; **Figure 7.8A** (below) is showing the films are open at 55°C temperature which will help the human body to cool down when temperature is

higher, means it will help the ventilation process of human body. **Figure 7.8B**, the film incorporated fabric was worn in hand to see the user ability of this textile. This kind of flip opening/closing in a textile can be used when surrounding temperature get increased or during sports activity, high activity level when body temperature get increased.

### **7.3. Summary**

In this study, I studied a class of liquid crystal elastomers (LCEs) that can be used to make filaments and can be 3D printed into complex geometries; the thermo-mechanical properties of the synthesized materials (e.g., shape changing temperature and elongation) can be controlled. Then, this filament was used to make woven to the actuation in the structure, also used to make complex 3D printed radial shaped film to be incorporated into textile to make temperature sensitive gating textile. This control allows for printing of LCEs with ultra-low actuation temperatures. This class of 3D-printed LCEs can be used to make filaments and films for smart temperature responsive gating textile or window textile applications.

## Reference

1. Glen, P.P., et al., The challenge to keep global warming below 2°C. *Nature Clim. Change*, 2013. 3: p. 4-6.
2. Pete, S., et al., Biophysical and economic limits to negative CO<sub>2</sub> emissions. *Nature Clim. Change*, 2016. 6: p. 42-50.
3. U.S. Energy Information Administration, *Annual Energy Outlook 2015 with Projections to 2040* (U.S. Energy Information Administration, 2015).
4. Bryant, T., et al., *Medium Term Energy Efficiency Market Report 2015* (International Energy Agency, 2015).
5. Raman, A. P., et al., Passive radiative cooling below ambient air temperature under direct sunlight. *Nature*, 2014. 515. P. 540–544.
6. Maxwell, F., et al., The relationship between outdoor thermal conditions and acute injury in an aluminum smelter. *Inter. J. Ind. Ergono.*, 2005. 35: p. 47–55.
7. Law, T. *The Future of Thermal Comfort in an Energy-Constrained World*; Springer International Publishing; Heidelberg, 2013. p. 1–4.
8. Hsu, P.C., et al., Radiative Human Body Cooling by Nanoporous Polyethylene Textile. *Science*, 2016, 353. P. 1019–1023.
9. Yang, A., et al., Thermal Management in Nanofiber-Based Face Mask. *Nano Lett.*, 2017. 17: p. 3506–3510.
10. Hu, J., et al., A Review of Stimuli- Responsive Polymers for Smart Textile Applications. *Smart Mater.Struct.*, 2012. 21: p. 053001.
11. Catrysse, P. B., et al., Photonic Structure Textile Design for Localized Thermal Cooling Based on a Fiber Blending Scheme. *ACS Photonics*, 2016. 3: p. 2420–2426.
12. Tingting, G., et al., Three-Dimensional Printed Thermal Regulation Textiles. *ACS Nano*, 2017. 11: p. 11513-11520.
13. T. Law, *the Future of Thermal Comfort in an Energy-Constrained World*. Springer Theses (Springer International Publishing, 2013).
14. Jahid, M. A., et al., Fabric Coated with Shape Memory Polyurethane and Its Properties. *Polymers*, 2018. 10: p. 681.
15. Thakur, S., et al., Mechanically strong shape memory polyurethane for water vapour permeable membranes. *Polym. Inter.*, 2018. 67: p. 1386-1392.
16. Jonathan, K. T.; Xiaopeng, H.; Svetlana, V. B.; James, L.; Yanfei, X.; Gang, C. Infrared-Transparent Visible-Opaque Fabrics for Wearable Personal Thermal Management. *ACS Photo.*, 2015. 2: p. 769–778.
17. Xu A., et al., Infrared-Transparent Visible-Opaque Fabrics for Wearable Personal Thermal Management. *ACS Photonics*, 2015. 2: p. 769–778.
18. Gao, C., et al., Personal Cooling with Phase Change Materials to Improve Thermal Comfort from a Heat Wave Perspective. *Indoor Air*, 2012. 22: p. 523–530.
19. Hu, J. L., et al., Recent advances in shape–memory polymers: Structure, mechanism, functionality, modeling and applications. *Prog. in Poly. Sci.*, 2012. 37: p. 1720– 1763.
20. Jahid M. A., et al., Water vapor transmission and water resistant: opposite but May Coexist. *Materials Today: Proceedings*, 2019. 16. p. 1485–1490.
21. Yang, J. H., et al., Measurement of Airflow around the Human Body with Wide-Cover Type Personal Air- Conditioning with PIV. *Indoor Built Environ.*, 2009. 18: p. 301–312.

22. Nazmul K., et al., Scalable Production of Graphene-Based Wearable E-Textiles. *ACS Nano*, 2017. 11: p. 12266–12275.
23. Bartkowiak, G., Assessment of an Active Liquid Cooling Garment Intended for Use in a Hot Environment. *Appl. Ergon.*, 2017. 58: p. 182–189.
24. Devin, J. R., et al., Long Liquid Crystal Elastomer Fibers with Large Reversible Actuation Strains for Smart Textiles and Artificial Muscles. *ACS Appl. Mater. Interfaces*, 2019. 11: p. 19514–19521.
25. Mohand, O. S., et al., Molecularly-Engineered, 4D-Printed Liquid Crystal Elastomer Actuators. *Adv. Funct. Mater.*, 2019. 29: p. 1806412.
26. Thomsen, D. L., et al., Liquid Crystal Elastomers with Mechanical Properties of a Muscle. *Macromolecules*, 2001. 34: p.5868-5875.
27. Rich, S. I., et al., Untethered soft robotics. *Nat. Electron.*, 2018. 1: p.102-112.
28. Ohm, C., et al., Liquid crystalline elastomers as actuators and sensors. *Adv. Mater.*, 2010. 22: p.3366-3387.
29. Yuan, C., et al., 3D printed reversible shape changing soft actuators assisted by liquid crystal elastomers. *Soft Matter*, 2017. 13: p. 5558–5568.
30. Yakacki, C. M., et al., Tailorable and programmable liquid-crystalline elastomers using a two-stage thiol-acrylate reaction. *RSC Adv.*, 2015. 5: p. 18997–19001.
31. Cedric, P. A., et al., Four-dimensional Printing of Liquid Crystal Elastomers. *ACS Appl. Mater. Interfaces*, 2017. 9: p. 37332–37339.
32. Yu, Y., Photomechanics: Directed bending of a polymer film by light. *Nature*, 2003. 425: p. 145.
33. Lu, X., Liquid-Crystalline Dynamic Networks Doped with Gold Nanorods Showing Enhanced Photocontrol of Actuation. *Adv. Mater.*, 2018. 30: p. 1706597.
34. Kaiser, A., Magnetoactive liquid crystal elastomer nanocomposites. *J.Mater. Chem.*, 2009. 19: p. 538–543.
35. Brehmer, M., et al., Ferroelectric liquid-crystalline elastomers. *Macromol. Chem. Phys.*, 1994. 195: p. 1891–1904.
36. Yakacki, C. M., et al., Tailorable and programmable liquid-crystalline elastomers using a two-stage thiol-acrylate reaction. *RSC Adv.*, 2015. 5: p. 18997–19001.
37. Ramazan Asmatulu and Waseem S. Khan, Introduction to electrospun nanofibers, *Micro and Nano Technologies*, 2019: P. 1-15.
38. Lee, K., et al., Stress-strain behavior of the electrospun thermoplastic polyurethane elastomer fiber mats. *Macromol. Res.*, 2005. 13: p. 441–445.
39. Ruvini S. K., et al., Liquid Crystal Elastomer Actuators: Synthesis, Alignment, and Applications. *J. of Polym. Sci, P. B: Polym. Phy.*, 2017. 55: p. 395–411.

# **Chapter 8. Conclusion & suggestions for future work.**

In this chapter, the summary of the major findings, significances, limitations, as well as the recommendations for future study will be presented.

## **8.1. Conclusion**

In this study, a series of polyurethane/polyurethane composite membrane was prepared, and a time saving particulate leaching reported was reported to make porous membrane, and different types synthesized polyurethane was used make coated fabric and its properties was investigated. finally, liquid crystal elastomers was synthesized to make temperature responsive gating textile. With all careful consideration and optimal combination, a systematic study was carried out on the synthesized polymers to make responsive textile. The major conclusions are summarized as follows-

1. The developed composite membranes can be used to regulate human body temperature through a cooling mechanism (evaporation of perspiration, air convection and emission of heat radiation directly into the environment). The fabricated polyurethane/silica aerogel composite membranes showed super evaporative and radiative effects and also can facilitate the convection process of the human body. The material possessed robust mechanical properties for



the longevity of the material, high water evaporative ability and air permeability to provide comfort to the wearer.

2. The porous membrane was prepared by particulate leaching technique, using quick water-soluble silica particles. A crucial discovery during this work was to reduce the particulate leaching time to 5min. To make a porous structure the particles were leached out from the PU matrix over five minutes through sonication. An investigation was conducted into the surface morphology of the porous PU (PPU) membrane using a scanning electron microscopy (SEM). The microporous average diameter was approximately  $2\mu\text{m}$ . the fabricated membranes has better water vapor transmission along with water droplet resisting ability. The effects of different silica particle percentage ratios also were investigated. Such a highly porous promising PU membrane may have a use in laminated textile and tissue engineering.
  
3. The coated cotton fabrics could provide thermal insulation with lower permeability at low temperature or low relative humidity (RH), and high permeability at room temperature or above, or high relative humidity with its water-resistance property. The proposed coated textiles have a water-resistant property with good water vapor transmitting ability. In order to provide

thermo-physiological comfort to the wearer, textile materials should have some functional property like water-resistance or water vapor transmission (WVT), so that perspiration can evaporate and be transmitted from the body surface to the environment even in extreme weather conditions that require wind and rain proof.

4. The synthesized low-temperature liquid crystal elastomers (LCEs) have been used to make woven textile, where pores are closing at low temperature (approximate 39°C). Radial shaped three dimensional printed films were incorporated into textile to see its open/close behaviour as a function of temperature (approximate 39°C). This temperature responsive gating behaviour of LCEs textiles would provide thermal comfort to the human body. LCEs filaments also show very good mechanical properties compare with traditional LCEs (Acrylate amine). These open/close mechanism in the textiles would help the human body to release its heat to the environment by convection, radiation and evaporation of perspiration to the environment, this mechanism of LCEs textiles would help human body to keep its core and skin temperature constant even at hot weather or high activity time.

These results indicate that the polyurethane/polyurethane composites, porous membranes, LCEs have great potential in thermo-regulating textile

applications, would help the heat exchange process of human body with its environment through textiles. In addition, this work also indicated that polyurethane/polyurethane composites, porous membranes can be used to laminate/coat onto the textile for functional property like water vapor transmission, rain drop resistant and so on. Furthermore, study also showed that, LCEs can be used to temperature sensitive gating textiles. These developed polymers/polymer composites has huge potential in thermo-regulating textile.

## **8.2. Suggestions for future work**

Despite of the contributions stated above, it is not possible to cover everything in this present work. There are still some works needs to be focused on in the near future. The limitations of the current work and suggestions for future works are listed below:

1. In this study we made evaporative, radiative, convective textile. To enhance the water vapor transmission and other properties of the polyurethane and composite membrane, different soft and hard segment rations of polyurethane can be synthesized, also need to work with to improve the mechanical property when the soft segment is higher. Furthermore, different

size of silica aerogel particles can be tried to see the effect of particle size on water vapor transmission and other properties.

2. In this study, time saving method of making porous membrane has been discovered by using particulate leaching technique, but mechanical property was slightly decreased of porous membranes. In the future, need to work with to improve the mechanical property of the porous membrane by keeping the improved water vapour transmission and water resistant property. Furthermore, need to work with different silica particle size to see the effect of particle size on the porous membrane.
3. To make coated fabric, need to work with other easy techniques to make coated fabric, also need to work to improve the water vapour transmission and water resistant property of the coated fabric. Furthermore, need to work with different thickness of coated materials on the fabric surface.
4. Temperature responsive woven fabric has also been fabricated in this study; needs to work with to improve the mechanical properties of the low temperature liquid crystal elastomers. Furthermore, other fabric related performance tests need to be done to see how well the liquid crystal elastomers as textile materials.

